On the neurobiology of apathy and depression in cerebral small vessel disease

Jonathan Tay

Clare Hall

October 2019

This dissertation is submitted for the degree of Doctor of Philosophy.

Declaration

This thesis is the result of my own work and includes nothing which is the outcome of work done in collaboration except as declared in the Preface and specified in the text. It is not substantially the same as any that I have submitted, or, is being concurrently submitted for a degree or diploma or other qualification at the University of Cambridge or any other University or similar institution except as declared in the Preface and specified in the text. I further state that no substantial part of my thesis has already been submitted, or, is being concurrently submitted for any such degree, diploma or other qualification at the University of Cambridge or any other University or similar institution except as declared in the Preface and specified in the text. It does not exceed the prescribed word limit for the relevant Degree Committee.

On the neurobiology of apathy and depression in cerebral small vessel disease

Jonathan Tay

Abstract

Cerebral small vessel disease (SVD) is a cerebrovascular pathology that affects the small vessels of the brain, resulting in heterogeneous brain tissue changes. These can lead to neuropsychiatric symptoms such as apathy, a loss of motivation, and depression, which is characterised by low mood and a loss of pleasure. Apathy and depression are both prevalent symptoms in SVD, but an understanding of the relationship between underlying disease processes and the expression of these neuropsychiatric symptoms remains poor.

This thesis uses magnetic resonance imaging techniques to examine the neurobiological basis of apathy and depression in SVD. We show that apathy is related to focal grey matter damage and distributed white matter microstructural change. These microstructural changes underlie large-scale white matter network disruption, which is related to apathy, but not depression. We then show that depression, as a construct, can be dissociated into distinct symptoms which are associated with overlapping and distinct areas of cortical atrophy over time. This suggests that depression as a general syndrome may be characterised by atrophy in core structures, while different symptoms are associated with atrophy in more specialised areas. Consistent with these patterns of overarching tissue damage, we find that apathy, but not depression, predicts conversion to dementia in patients with SVD.

Our findings suggest that different types of SVD-related pathology lead to apathy and depression. Diffuse white matter damage may lead to widespread network disruption, resulting in apathy and cognitive impairment. In contrast, depressive symptoms are associated with focal patterns of grey matter atrophy over time. This highlights the importance of differentiating neuropsychiatric symptoms, and paves the way for targeted treatment approaches.

Dedication

To my family, especially Andrew Tay, who always told me to think for myself, and my parents, who are eternally patient, understanding, and loving.

To all the lovely people who I have worked with both here in Cambridge and at Radboud University, without whom this PhD would not exist. The consistent and deliberate use of "we" and "our" in this thesis, rather than "I" or "my", acknowledges this fact.

To my friends back in Canada, here in the UK, and around the world - for believing in me when I did not have the strength to believe in myself.

To Kimberly Anderson, my rock.

To Isaac Newton, the giant whose shoulders I will always remain in the shadow of.

Preface

The work described in this thesis has been conducted primarily at the University of Cambridge. The data used in this thesis was previously collected by others under the guidance of Professor Frank-Erik de Leeuw (Radboud University) and Professor Hugh Markus (University of Cambridge). I have personally designed the experiments, analysed the imaging data, and conducted the statistical analyses in the chapters described herein.

Parts of this thesis have been published, or are under review, in peer-reviewed journals (Tay *et al.*, 2019, 2020*a*, *b*):

Tay J, Tuladhar AM, Hollocks MJ, Brookes RL, Tozer DJ, Barrick TR, Husain M, de Leeuw FE, Markus HS. Apathy is associated with large-scale white matter network disruption in small vessel disease. *Neurology*. 2019 Mar 12;92(11):e1157-67.

Tay J, Lisiecka-Ford DM, Hollocks MJ, Tuladhar AM, Barrick TR, Forster A, O'Sullivan MJ, Husain M, de Leeuw FE, Morris RG, Markus HS. Network neuroscience of apathy in cerebrovascular disease. *Progress in Neurobiology*. 2020 Mar 6:101785.

Tay J, Morris RG, Tuladhar AM, Husain M, de Leeuw FE, Markus HS. Apathy, but not depression, predicts all-cause dementia in cerebral small vessel disease. Journal of Neurology, Neurosurgery & Psychiatry. 2020 Sep 1;91(9):953-9.

Tay J, Morris RG, Markus HS. Under review. Apathy after stroke: diagnosis, mechanisms, consequences, and treatment.

Contents

Chapter 1: Introduction

1.1. Apathy

"Desire, wish, will, are states of mind which everyone knows, and which no definition can make plainer."

William James, *The Principles of Psychology*, Chapter 26

Motivation is one of the key fixtures of mental life, and plays a role in every volitional action. All goals in life, whether big – such as attempting to write a PhD thesis – or small – such as preparing a meal – require some degree of physical or cognitive effort. The success or failure of these goal-directed behaviours depends on how hard we try, if we try at all. Motivation is therefore a crucial element to our normal lives.

Apathy can be defined as a loss of motivation that manifests as a reduction in goal-directed behaviour (GDB) (Marin, 1991; Levy and Dubois, 2006). This reduction is defined in relation to a patient's previous level of functioning, in order to account for the interindividual, environmental, and sociocultural factors that may influence normative functioning. Other terms used to describe apathy include abulia, akinetic mutism, and athymhormia (Levy and Dubois, 2006).

Apathy is the most common behavioural symptom of Alzheimer's disease (Zhao *et al.*, 2016) and Huntington's disease (Craufurd *et al.*, 2001), and is a prominent symptom in stroke (van Dalen *et al.*, 2013), vascular dementia (Staekenborg *et al.*, 2010), traumatic brain injury (Starkstein and Pahissa, 2014), Parkinson's disease (den Brok *et al.*, 2015), and multiple sclerosis (Figved *et al.*, 2005). Apathy is also one of the diagnostic criteria for the behavioural variant of frontotemporal dementia (Piguet *et al.*, 2011), and is the most prevalent negative symptom of schizophrenia (Fervaha *et al.*, 2015). Some degree of apathy also exists in healthy individuals (Ang *et al.*, 2017), and although no authoritative studies have been conducted, it is estimated that over 10 million people in the United States suffer from some degree of apathy (Chase, 2011).

Apathy is both prevalent and problematic. Research across neurological disorders has shown that apathy is consistently associated with negative outcomes, such as reduced patient functioning, poorer response to treatment, and increased caregiver distress (van Reekum *et al.*, 2005). Apathy may have far-reaching societal implications as well, as motivation affects education, employment, and civic engagement (Vansteenkiste *et al.*, 2005).

1.2. Definitions of apathy: from ancient Greece to the present day

Apathy is etymologically derived from the Greek *apatheia* (i.e., a-pathos), meaning a lack of passion. Motivational deficits may have been described in medical texts as early as Hippocrates' *On the Sacred Disease*, where apathy figures into the description of the four humours: "Those who are mad through phlegm are quiet, and neither shout nor make a disturbance." (Marin, 1991). The condition was also recognised by the 19th century neurologist Edouard Brissaud (1852-1909), a pupil of Jean-Martin Charcot (1825-93), who described "absolute apathy" as a state of "mixed indifference and lack of reaction to external as well as internal events" (Prange *et al.*, 2018).

Although apathy has been recognised as an important symptom for millenia, clinical recognition or scientific interest in the condition did not begin until the early 1990s, when Robert Marin defined apathy as a "lack of motivation" (Marin, 1991). This definition of apathy is the source from which all modern definitions are derived. Importantly, a loss of motivation should not be attributable to intellectual impairment, emotional distress, or a state of diminished consciousness (Marin, 1991).

For Marin, this was a key point that distinguished apathy as a *symptom* from apathy as a *syndrome*. If diminished motivation was attributable to another cause, then apathy was merely symptomatic of a different syndrome. For instance, a patient with severe dementia, lacking the cognitive capacity to form plans such as going shopping, would not be considered to have syndromic apathy. Similarly, an individual with major depression, if too dysphoric to bring themselves to do anything, would have symptomatic apathy, but not syndromic apathy.

Syndromic apathy is a broader construct than symptomatic apathy, and features complex behavioural, cognitive, and emotional concomitants. These distinctions are psychological in nature, but all share a common behavioural manifestation, which is a quantitative reduction of goal-directed, or purposeful, behaviour. It is important to note that this definition is relativistic in nature: a reduction in behaviour must be contextualised by a patient's previous level of functioning, as well as by their socio-cultural norms. The behavioural, cognitive, and emotional features of apathy described by Marin are important to current understanding of the syndrome. These can be conceptualised as "subtypes" of apathy.

Behavioural apathy, synonymous with ‘athymhormia’ or ‘auto-activation deficit’, is the most severe form of apathy, manifesting as an inability to initiate self-generated actions without external prompting. ‘Self-generated’ or ‘self-initiated’ actions are a set of spontaneous behaviours that occur without an external stimulus, in contrast to externally-

triggered, reflexive actions (Passingham *et al.*, 2010). Accordingly, patients of this type lack initiative, remaining sedentary. This state can temporarily be reversed, albeit by external, rather than internal, prompting.

Cognitive apathy, which has also been called cognitive inertia, manifests as a lack of interest in learning new things or engaging in new experiences, which can lead to reduced performance on tasks that assess planning, rule-finding, and set-shifting, which are crucial executive processes for the generation and elaboration of complex behaviours. These deficits may be related to the intrinsic costs of "cognitive control", a theoretical construct explains difficulties associated with engaging and sustaining cognitively demanding tasks (Miller and Cohen, 2001). Although speculative, it has been suggested that cognitive control is "costly" due to resource bottlenecks in mental representational capacity, a natural limitation of the executive neural network that supports information processing (Shenhav *et al.*, 2017). If this proposition is true, then it is possible that cognitive apathy is a manifestation of reduced or slower information processing capacity following executive network damage (1.9.2). Overcoming processing bottlenecks may therefore require cognitive resources that have been limited due to network damage, leading to an increase in perceived effort costs associated with engaging in behaviours requiring cognitive control. This may manifest as cognitive apathy, leading to the host of deficits described earlier.

Finally, emotional apathy manifests as a decreased ability to associate emotion with behaviour. It is also associated with an indifference to both positive and negative stimuli. This indifference, particularly with regard to positive stimuli, is similar to some symptoms, such as loss of pleasure, in major depressive disorder, which will be discussed later (1.5).

We now return to the example of an unmotivated depressed individual. As previously mentioned, if a loss of GDB is attributable to dysphoria, then this individual's apathy can be considered a symptom of their depression. On the other hand, reductions in GDB that are characterised by the behavioural, cognitive, or emotional deficits that have been highlighted may point towards syndromic apathy. This type of apathy may not respond to treatments in the same manner as symptomatic apathy, which could be ameliorated by first treating the individual's dysphoria.

1.3. Diagnostic criteria for apathy

These three apathy subtypes have been incorporated into many diagnostic criteria for apathy. Diagnosis is conventionally performed using specific criteria that are assessed by clinical interview or behavioural observation (Marin, 1991). The most widely adopted standard,

developed through expert consensus, is characterised by four key criteria (Robert *et al.*, 2009). A recently published revision of these criteria is adapted here with permission (Robert *et al.*, 2018):

CRITERION A: A quantitative reduction of goal-directed activity either in behavioral, cognitive, emotional or social dimensions in comparison to the patient's previous level of functioning in these areas. These changes may be reported by the patient themselves or by observation of others.

CRITERION B: The presence of at least 2 of the 3 following dimensions for a period of at least four weeks and present most of the time:

B1. BEHAVIOUR & COGNITION

Loss of, or diminished, goal-directed behaviour or cognitive activity as evidenced by at least one of the following:
General level of activity: The patient has a reduced level of activity either at home or work, makes less effort to initiate or accomplish tasks spontaneously, or needs to be prompted to perform them.
Persistence of activity: They are less persistent in maintaining an activity or conversation, finding solutions to problems or thinking of alternative ways to accomplish them if they become difficult.
Making choices: They have less interest or take longer to make choices when different alternatives exist.
Interest in external issue: They have less interest in or reacts less to news, either good or bad, or has less interest in doing new things.
Personal wellbeing: They are less interested in their own health and wellbeing or personal image.

B2. EMOTION

Loss of, or diminished, emotion as evidenced by at least one of the following:
Spontaneous emotions: The patient shows less spontaneous (self-generated) emotions regarding their own affairs, or appears less interested in events that should matter to them or to people that they know well.
Emotional reactions to environment: They express less emotional reaction in response to positive or negative events in their environment that affect them or people they know well.
Impact on others: They are less concerned about the impact of their actions or feelings on the people around them.
Empathy: They show less empathy to the emotions or feelings of others.
Verbal or physical expressions: They show less verbal or physical reactions that reveal their emotional states.

B3. SOCIAL INTERACTION

Loss of, or diminished engagement in social interaction as evidenced by at least one of the following:
Spontaneous social initiative: The patient takes less initiative in spontaneously proposing social or leisure activities to family or others.
Environmentally stimulated social interaction: They participate less, or are less comfortable or more indifferent to social or leisure activities suggested by people around them.
Relationship with family members: They show less interest in family members.
Verbal interaction: They are less likely to initiate a conversation, or withdraws soon from it
Homebound: They prefer to stay at home more frequently or longer than usual and shows less interest in getting out to meet people.

CRITERION C: These symptoms (A - B) cause clinically significant impairment in personal, social, occupational, or other important areas of functioning.

CRITERION D: The symptoms (A - B) are not exclusively explained or due to physical disabilities, to motor disabilities, to a diminished level of consciousness, to the direct physiological effects of a substance, or to major changes in the patient's environment.

For a diagnosis of apathy, a patient should meet all four criteria. It should be noted that this differs slightly from the originally proposed criteria, as this revised version combines cognitive and behavioural symptoms whilst adding social symptoms (Robert *et al.*, 2009, 2018). Although the validity of these criteria has not been formally tested, the original version has been validated in patients with a range of neurological disorders, including those with cerebrovascular damage, with good inter-rater reliability (Mulin *et al.*, 2011).

Another method for assessing and diagnosing apathy is using clinical questionnaires that quantitatively grade the presence and severity of apathetic symptoms. Many of these measures use a semi-structured interview format, although some, such as the Apathy Evaluation Scale (AES), have additional self-report and informant-report measures (Marin *et al.*, 1991). These can be less thorough than structured clinical examinations, but have rapid administration times and require less expertise, which is useful in research studies and clinical screening (Cummings *et al.*, 2015).

Following clinical assessment, a patient can be formally diagnosed with apathy using the International Classification of Diseases 10 - Clinical Modification (ICD-10-CM) criteria, which lists “demoralization and apathy” under code R45.3. Unfortunately, no corresponding diagnosis exists for apathy in the Diagnostic and Statistical Manual of Mental Disorders, fifth edition (DSM-5), which integrates apathy into descriptions of other disorders, such as mood and neurocognitive disorders, rather than having the syndrome as its own diagnostic entity (American Psychiatric Association, 2013). Although DSM-5 recognizes apathy as playing a significant role in a variety of disorders, a unique diagnostic code may aid in the diagnosis and subsequent treatment of this syndrome.

1.4. Depression

"Frequently I fall into a mood of complete listlessness and indifference; nothing gives me great pleasure."

Wolfgang Amadeus Mozart

Depression is the leading cause of disability worldwide (World Health Organization, 2017) with a lifetime prevalence of 10% to 15% (Lépine and Briley, 2011). It is unsurprising, given these figures, that depression has emerged as one of the most important diseases to recognise and manage in general clinical practice (Paykel and Priest, 1992). Unfortunately, this has led to apathy being overlooked, both clinically and empirically, due to having similar behavioural

manifestations - and sometimes diagnostic criteria - with depression, which are now discussed.

Although depression is a heterogeneous disease with numerous symptoms and subtypes, we primarily focus on the "classical" picture of depression, which would be consistent with major depressive disorder. Major depressive disorder, as defined in DSM-5, is a syndrome characterised by the presence of at least five out of the following nine symptoms in the past two weeks:

1. Depressed mood
2. Loss of interest or pleasure (anhedonia)
3. Change in weight or appetite
4. Insomnia or hypersomnia
5. Psychomotor agitation or retardation
6. Loss of energy (anergia) or fatigue
7. Feelings of worthlessness or guilt
8. Impaired concentration or indecisiveness
9. Thoughts of death, suicidal ideation, or suicide attempt,

with depressed mood and anhedonia being cardinal symptoms (American Psychiatric Association, 2013). The term "depression", used henceforth, will generally refer to this general syndrome.

1.5. Differentiating between apathy and depression

From the diagnostic criteria presented alone, it should be apparent that apathy and depression are distinct clinical syndromes. Defining apathy as a construct that was to some extent orthogonal to depression was one of the primary goals of Marin's (1991) formal definition of the term. Indeed, modern definitions of apathy do not generally include or emphasise the negative emotionality or somatic disturbances that may be symptomatic of major depression (e.g., Robert *et al.*, 2018).

One important point of potential overlap between apathy and depression may be in the symptom of anhedonia. Anhedonia, as defined in DSM-5, can include deficits in the capacity to feel pleasure and take interest in things, manifesting as a hyposensitivity towards rewarding or positive stimuli (American Psychiatric Association, 2013). Anhedonia can relate to the *liking* of a stimulus, which is the visceral experience of pleasure associated with consuming a stimulus, or the *wanting* of a stimulus, which is the pleasure associated with the

anticipation of a future stimulus (Treadway and Zald, 2011). These are very closely related topics, as the liking of a stimulus will influence future wanting of it, but not completely synonymous. This anticipatory component of anhedonia may involve several motivational components that overlap with apathy, and in this regard anhedonic symptoms of depression may appear behaviourally similar to apathy. These behavioural similarities may have similar underlying neurobiological processes, such as those that guide value-based decision-making (Husain and Roiser, 2018).

Anhedonia is, by definition, symptomatic of depression, and it is easy to see how this can precede, or be synonymous with, symptomatic apathy in these cases (Section 1.2). Motivational deficits in depressed individuals with anhedonia may well be driven by a reduction or loss of pleasure or interest in stimuli. If this is the case, then anhedonia and apathy may be different manifestations of the same underlying neurobiological changes that affect emotional processing, cognition, and behaviour in major depression. Despite this, there are some subtle points that may distinguish symptomatic apathy and anhedonia in this case. Individuals with depression and anhedonia may show a hypersensitivity towards punishing stimuli (Chiu and Deldin, 2007), whilst those with apathy would show a reduction in motivation towards both rewarding and punishing stimuli.

Other symptoms of depression such as low energy or anergia may appear *behaviourally* similar to apathy despite being fundamentally different. For instance, low energy may result in an individual not being able to physically complete GDBs. This is not apathy, however, as there is no actual reduction in motivation.

1.6. Apathy and depression in cerebrovascular disease

Having now discussed the differences between apathy and depression generally, we now explore this topic in more detail in cerebrovascular disease, which will be the primary focus of this thesis. Cerebrovascular disease, used herein, primarily refers to large vessel stroke and cerebral small vessel disease (SVD).

Strokes can be classified as ischaemic or haemorrhagic. Ischaemic strokes are caused by an obstruction of blood flow, whilst haemorrhagic strokes are caused by bleeding. Large vessel strokes, by definition, affect the major arteries of the brain, such as the anterior, middle, and posterior cerebral arteries.

Conversely, SVD affects the small vessels of the brain, leading to heterogeneous parenchymal changes. Some of the radiologically visible markers of SVD include lacunar infarcts, which are punctate infarcts typically affecting subcortical grey matter and white

matter structures, and white matter hyperintensities (WMH), which appear as diffuse areas of high intensity signal in the white matter on T2-weighted MRI. Pathological processes related to SVD are a major cause of disability and age-related cognitive decline (Pantoni, 2010).

Apathy and depression have been identified as consequences of stroke and SVD. Both syndromes present in approximately one out of three patients following ischaemic or haemorrhagic stroke, and preliminary evidence suggests they are highly prevalent in SVD. Despite this prevalence, however, apathy and depression are only modestly correlated (~10-20%) (Brodaty *et al.*, 2005; Caeiro *et al.*, 2006; Santa *et al.*, 2008; Mayo *et al.*, 2009), although others report no overlap (Marin *et al.*, 1991). Furthermore, reported estimates of point prevalence suggest that comorbid apathy and depression occur in only a minority of patients. For instance, a study in patients with acute stroke found that 22% of patients were apathetic, but not depressed, whilst 7% of patients were depressed, but not apathetic (Withall *et al.*, 2011). Only 4% of patients were both apathetic and depressed, with the remaining sample not fitting criteria for apathy or depression (Withall *et al.*, 2011). It should be noted that many of these studies assess and diagnose apathy and depression using clinical scales rather than through a structured physician interview. One criterion often used in the development of apathy scales is a lack of correlation with depression scales (e.g., Marin *et al.*, 1991; Ang *et al.*, 2017), which may explain the low levels of overlap.

Apathy and depression also have distinct effects on outcome measures such as functional independence and quality of life in patients with stroke (Hama *et al.*, 2007*a*; Matsuzaki *et al.*, 2015) and SVD (Hollocks *et al.*, 2015). Furthermore, apathy appears to be more strongly related to neurocognitive abilities in both stroke patients (Fishman *et al.*, 2018*a, b*) and SVD (Lohner *et al.*, 2017), and consistent with this, symptoms of apathy, but not depression, predict conversion to dementia (van Dalen *et al.*, 2018*a*). This may be driven by differential associations between apathy, depression, and white matter damage, which have been explored in SVD (Hollocks *et al.*, 2015; Le Heron *et al.*, 2018*b*).

These results suggest that apathy and depression are distinct entities in cerebrovascular disease. If they were equivocal constructs, then one would expect to see higher rates of correlation and comorbidity than what is actually seen. Moreover, one would expect more substantial overlap in terms of effects on functional outcome and relationships with cognition.

Before proceeding further, we briefly discuss the topic of fatigue. Post-stroke fatigue may be a potential comorbidity with post-stroke apathy and depression. Fatigue, which can be defined as a feeling of weariness or lack of energy, is a frequent complaint after stroke,

with a recent systematic review suggesting it occurs in 50% of cases (Cumming *et al.*, 2016). This presents a potentially complicated topic, as the symptoms of fatigue may appear *behaviourally* similar to the symptoms of apathy. Despite this, preliminary research suggests that apathy and fatigue are not correlated, do not interact over time (Douven *et al.*, 2017*b*). Although this research requires replication, it does suggest that motivational deficits are independent of subjective feelings of low energy.

1.7. Consequences of apathy on functional outcomes

Apathy has been associated with a variety of physical deficits in stroke, and patients with apathy have a greater number of somatic comorbidities (Sagen *et al.*, 2010). These include basic motor skills, such as disturbances in sitting balance (Hama *et al.*, 2007*b*) and gait (Moretti *et al.*, 2015), but also extend to basic activities of daily living (ADLs), such as eating and dressing (Brodaty *et al.*, 2005; Santa *et al.*, 2008; Mayo *et al.*, 2009; Caeiro *et al.*, 2013; Tang *et al.*, 2014; van Almenkerk *et al.*, 2015; Mihalov *et al.*, 2016). Longitudinal studies on functional outcomes also suggest that apathy impairs recovery of physical functions after stroke (Hama *et al.*, 2007*a*; Santa *et al.*, 2008; Mikami *et al.*, 2013*b*; Harris *et al.*, 2014; Matsuzaki *et al.*, 2015).

The reasons why apathy is associated with such deficits is still unknown. It is possible that reductions in basic ADLs could be a manifestation of the behavioural apathy subtype, which is characterised by a reduction in self-initiated actions. These motivational deficits may also impair physical rehabilitation by reducing willingness to engage in physiotherapy programs, for instance. Furthermore, apathy could precede sedentary behaviour, which may explain why apathy has been associated with an increased risk of future cardiovascular events (Eurelings *et al.*, 2018). This would not explain deficits in neurological functions such as sitting balance or gait however, which may be more reflective of damage to white matter tracts underlying apathy and motor control (Hollocks *et al.*, 2015; Moretti *et al.*, 2015; Le Heron *et al.*, 2018*b*).

Apathy is also associated with impaired cognitive functioning. Apathetic patients scored ~2–3 points lower on the Mini-Mental State Examination (MMSE), a measure of general cognitive impairment (van Dalen *et al.*, 2013). Analyses of specific cognitive domains have reported that apathy in stroke is associated with impaired verbal learning and short- and long-term verbal recall (Fishman *et al.*, 2018*b*), verbal fluency (Okada *et al.*, 1997; Yamagata *et al.*, 2004), semantic fluency (Fishman *et al.*, 2018*a*), abstract reasoning (Caeiro *et al.*, 2013), and attention and concentration (Brodaty *et al.*, 2005).

The cognitive disturbances that accompany apathy also have functional consequences. Patients with apathy show impairment on instrumental ADLs (Zawacki *et al.*, 2002; Brodaty *et al.*, 2005, 2013; Reyes *et al.*, 2009; Castellanos-Pinedo *et al.*, 2011), which are tasks that require planning, such as shopping and housekeeping. Furthermore, apathy is associated with worse scores on dementia scales (Onoda *et al.*, 2011), and a higher risk of incident dementia (van Dalen *et al.*, 2018*a*, *b*). It is possible that apathy may be symptomatic of prodromal vascular dementia (van Dalen *et al.*, 2018*a*), indicating disrupted white matter connectivity which has also been shown to underlie vascular dementia caused by small vessel disease (Lawrence *et al.*, 2018*b*). Apathy may therefore be used as a behavioural marker for patients at-risk for cognitive impairment and dementia.

Although apathy can co-occur with some level of depression, it may also cause later depression. Longitudinal studies report that apathy is associated with increased depression at follow-up (Withall *et al.*, 2011), and apathetic stroke patients have an almost twofold risk of concurrent depression (van Dalen *et al.*, 2013). Furthermore, apathy, independently of depression, is a predictor of suicidal ideation three months after stroke (Tang *et al.*, 2015). These results suggest that apathy may not only occur in tandem with depression, but also contribute to it. Indeed, some authors have pointed out that there are similarities between the constructs of apathy and anhedonia, a common feature of major depression which can be associated with reduced motivation to seek pleasure (Husain and Roiser, 2018).

The relationship between apathy and other psychiatric disturbances has been far less studied. Limited evidence suggests that apathy is associated with anxiety in the post-acute (Mihalov *et al.*, 2016), but not acute (Starkstein *et al.*, 1993), phase of stroke. This anxiety may stem from apathetic patients becoming more aware of general deficits they suffer from after stroke or the anxiety provoking consequences of inactivity. Recent longitudinal work on personality traits and post-stroke symptoms suggest that higher extraversion predicted lower apathy scores, in contrast to higher neuroticism, which was predictive of more severe depression (Douven *et al.*, 2018*b*). There is no evidence as of yet to support a relationship between apathy and psychotic symptoms (Reyes *et al.*, 2009). Apathetic patients with Cerebral Autosomal Dominant Arteriopathy with Subcortical Infarcts and Leukoencephalopathy (CADASIL), a monogenic form of SVD, have a greater frequency of psychiatric symptoms such as irritability/lability, agitation/aggression, disinhibition and euphoria, as well as somatic symptoms such as disturbed sleep and appetite (Reyes *et al.*, 2009). Whether these symptoms show a similar etiology to apathy is still unknown.

1.8. Treatments for apathy

Despite its importance, there is a lack of high-quality treatment studies for apathy in cerebrovascular disease, precluding the recommendation of pharmacological agents for treating it in clinical practice. We were able to identify three double-blind placebo-controlled trials. Two trials have evaluated the efficacy of nefiracetam, which enhances monoaminergic, cholinergic and GABAergic signalling, in the treatment of post-stroke apathy. The first, conducted to treat post-stroke depression, examined apathy diagnosed using the Starkstein Apathy Scale (SAS) (Table 1) in a subset of 70 patients, and found that 900 mg/day of nefiracetam reduced apathy after one month of treatment (Robinson *et al.*, 2009). The second study treated apathy, also measured with the SAS, as a primary outcome measure under the same dose of nefiracetam, and found a small, but non-significant effect after three months of treatment (Starkstein *et al.*, 2016). This null result should be interpreted with caution, however, given the small sample size and limited power to detect a clinically-relevant effect. Future studies are needed to assess the efficacy of nefiracetam in treating post-stroke apathy.

The other trial for treating apathy was conducted using escitalopram, a selective serotonin reuptake inhibitor. In this study, 98 stroke patients who were apathy-free were administered 5 or 10 mg/day escitalopram or placebo. After one year, the escitalopram group had lower risk of developing apathy compared to the placebo group (Mikami *et al.*, 2013*a*). Although this suggests that escitalopram may prevent the onset of apathetic symptoms after stroke, there is no data on whether escitalopram improves symptoms in patients already diagnosed with apathy.

An open-label trial examined the acetylcholinesterase inhibitors galantamine and donepezil in treating apathy in cognitively impaired stroke patients (Whyte *et al.*, 2008). Thirteen stroke patients were administered 12 mg/day galantamine, and 13 patients were administered 10 mg/day donepezil. Although the whole group showed a trend to improving apathy over three months, this was not significant, but again, the study may have been underpowered. The rest of the pharmacological trials to treat post-stroke apathy are in case reports and case series, which report effects for bromocriptine (Catsman-Berrevoets and Harskamp, 1988; Barrett, 1991; Parks *et al.*, 1992; Marin *et al.*, 1995; Powell *et al.*, 1996), methylphenidate (Marin *et al.*, 1995; Watanabe *et al.*, 1995; Spiegel and Chatterjee, 2014), ropinirole (Kohno *et al.*, 2010; Adam *et al.*, 2013), levodopa (Adam *et al.*, 2013), zolpidem (Mathieu *et al.*, 2011; Autret *et al.*, 2013), selegiline (Marin *et al.*, 1995), and olanzapine (Spiegel and Chatterjee, 2014). There is a great need for well-conducted randomised

controlled trials to determine whether any of these treatments are successful in treating apathy in post-stroke patients or individuals with SVD.

There have been only a few attempts to evaluate behavioural interventions for stroke-related apathy. Problem-solving therapy, during which a patient selects a problem and then goes through a process to arrive at a course of action, reduces the risk of developing apathy over one year compared to placebo, but not as much as escitalopram (Mikami *et al.*, 2013*a*). Strategy training, during which patients learn to address activity goals by using self-derived strategies, improved apathy compared to a control condition at three months, and it remained improved, but not significantly so, at six months (Skidmore *et al.*, 2015). A group-based intervention that included exercise and other project-based activities showed improvement of apathy over the course of one year, but these changes were deemed not clinically meaningful (Mayo *et al.*, 2015).

1.9. The standard model of the neurobiological basis of apathy

It is clear that apathy is a prevalent and debilitating syndrome in cerebrovascular disease. It affects important patient functional outcomes such as quality of life, activities of daily living, and recovery of function after stroke. This makes accurate diagnosis and treatment of apathy essential. It is likely that understanding the underlying neurobiology of apathy in cerebrovascular disease may make these problems more tractable.

The most influential neurobiological framework for investigating apathy has been proposed by Levy and Dubois (2006), who theorised that that the symptoms of apathy can be conceptualized as 'emotional-affective', 'cognitive', and/or 'auto-activation' deficits. The proposed mechanisms underlying apathy related to impaired emotional-affective processing are an inability to: associate emotion or affect with behaviour, to accurately decode the affective context that guides behavior, and to evaluate the consequences of actions in terms of positive or negative outcomes. Apathy associated with impaired cognitive processing is characterised by an impairment in the elaboration of plans of actions, such as rule-finding, set-shifting, maintenance of goals and subgoals, and strategies to retrieve information. Finally, apathy associated with impaired auto-activation processing is attributed to difficulties in self-activating thoughts or behaviours.

It has been proposed that these symptoms arise spontaneously as a consequence of focal damage or disruption to territories within the basal ganglia and prefrontal cortex (PFC), which may constitute a core subcortical-cortical circuit underlying GDB. Importantly, this theoretical delineation of apathy subtypes is *mechanistic* in nature, as opposed to the *clinical*

subtypes highlighted earlier (Section 1.3) (Robert *et al.*, 2018). This framework has guided much apathy research over the past decade, and has been incorporated into proposed diagnostic criteria and several clinical scales (Radakovic *et al.*, 2015; Robert *et al.*, 2018).

Unfortunately, empirical evidence that supports the three separate dissociable constructs proposed by Levy and Dubois (2006) remains scarce. This is especially true regarding apathy in cerebrovascular disease. If apathy is the product of lesions to specific regions of the basal ganglia or PFC, then one would expect a clear relationship between stroke location and the presentation of apathy symptoms. This, however, has proven not to be the case, as lesions are distributed heterogeneously in patients with apathy (Tang *et al.*, 2013; Yang *et al.*, 2015*b*; Sagnier *et al.*, 2019). Furthermore, meta-analytic evidence suggests that there is no clear relationship between lesion location and the development of post-stroke apathy (van Dalen *et al.*, 2013; Douven *et al.*, 2017*a*).

Other findings also appear anomalous, or difficult to explain, when viewed through this framework. For instance, some patients who are apathy-free during the acute phase of stroke develop it one year later, whilst other patients with apathy in the acute phase recover after one year (Withall *et al.*, 2011; Caeiro *et al.*, 2013). If apathy develops spontaneously after a focal basal ganglia or PFC lesion, then why would apathy present up to a year later? Conversely, what mechanisms lead to some patients with apathy recovering normal function? These questions make it clear that a classical lesion-deficit model of apathy is unable to explain the full clinical phenotype of the syndrome in cerebrovascular disease.

1.10. A network model linking cerebrovascular pathology and apathy

We propose that apathy might potentially be better understood as a syndrome caused by damage to large-scale brain networks supporting GDB. This connectionist model is based on the tenets of graph theory and network analysis (Bullmore and Sporns, 2009), which have recently been able to explain and synthesize an impressive array of neuroscientific data (e.g., Schindlbeck and Eidelberg, 2018). This section will begin with a brief overview of network neuroscience (Section 1.10.1), followed by a proposal of the network mechanisms underlying apathy (Section 1.10.2). Evidence to support the hypothesis that apathy is a syndrome of network disruption is then reviewed in stroke (Section 1.10.3) and SVD (Section 1.10.4).

1.10.1. Fundamentals of network neuroscience

The study of brain networks has been made increasingly more tractable with the application of graph theory. A graph has two fundamental elements: nodes and their connecting edges. In

the context of macroscopic whole-brain networks, nodes are typically defined using a parcellation that divides the brain using predefined criteria, such as on the basis of sulci and gyri (e.g., Desikan *et al.*, 2006) or cyto- and myelo-architecture (e.g., Eickhoff *et al.*, 2005), whilst edges are defined based on the context of the study. For example, studies on structural connectivity can define an edge as the probability that two regions are connected by a white matter tract. Studies of functional connectivity can define an edge as the correlation between the time series of two regions as an edge (Bullmore and Sporns, 2009).

This graph-based representation of the brain can then be quantitatively analyzed to make inferences based on network topology. Two fundamental network measures are degree and efficiency (Figure 1). The degree of a node is simply the number of connections it has to other nodes (Figure 1a). High-degree nodes are known as network hubs, which are core elements of large-scale brain networks (van den Heuvel and Sporns, 2013). Due to a large number of connections with other nodes, hubs participate in a diverse set of cognitive functions (Bassett *et al.*, 2009), albeit at an increased metabolic cost (Collin *et al.*, 2013). Hubs can be contrasted with low-degree peripheral nodes, which tend to show more local and specialized patterns of connectivity. A more comprehensive discussion of hubs can be found elsewhere (van den Heuvel and Sporns, 2013).

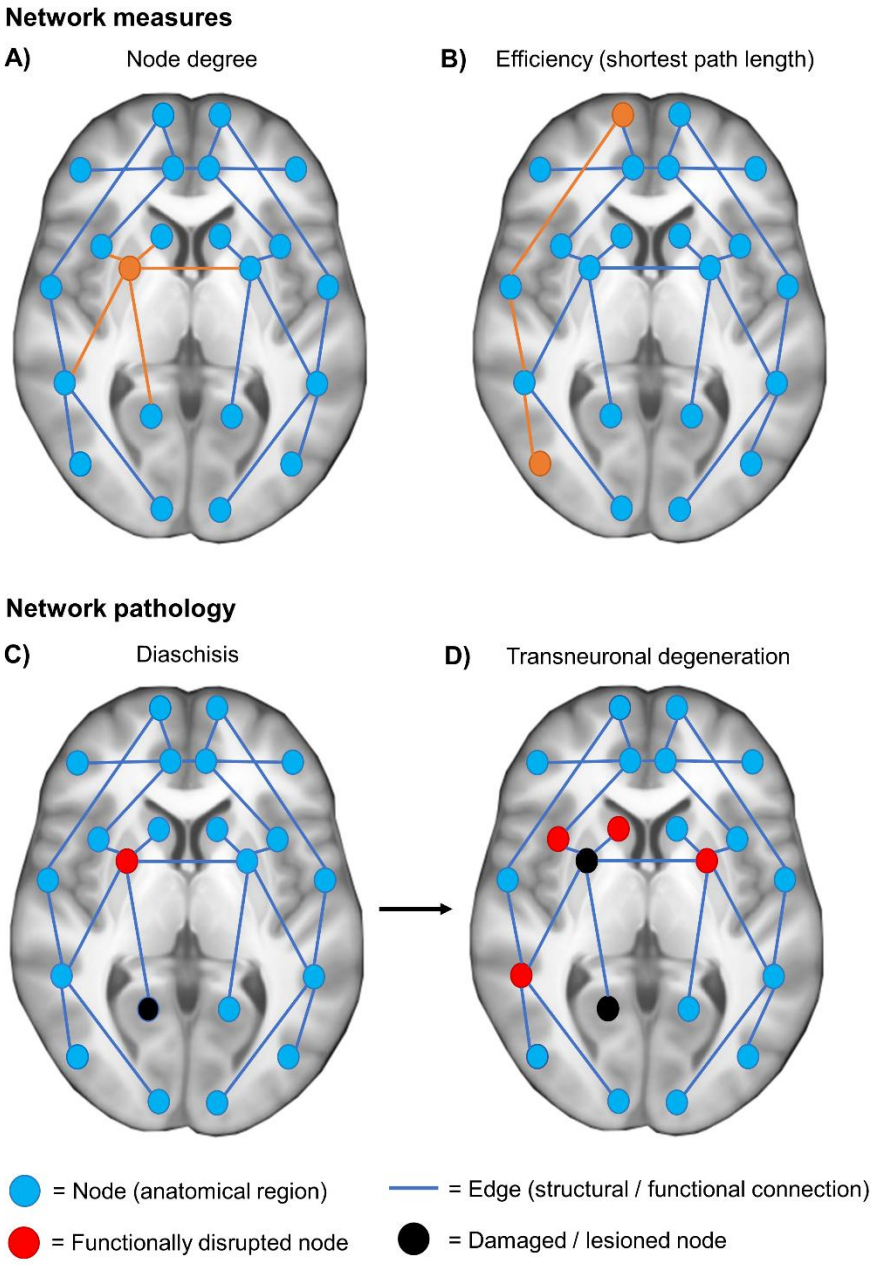

Figure 1. Network measures and pathology. **A)** The degree of a node is a measure of how many connections it has; **B)** The shortest path between two nodes is a measure of efficiency; **C)** Diaschisis is a functional deficit in a region that is remote from a damaged node; **D)** Transneuronal degeneration involves the physical breakdown of nodes, which propagates from connections to already damaged nodes.

Another important network measure is efficiency, which measures the ease of information transfer in a network (Latora and Marchiori, 2001). The shortest path length between two nodes minimizes the number of edges traversed between the two (Figure 1b). The average inverse shortest path length between all nodes in a network is its global efficiency, and is a measure of overall integration in a network. The local efficiency of a node is the global efficiency of a subgraph composed of all first-degree neighbors of that node. The average local efficiency across all nodes is a measure of segregation and specialization. More rigorous mathematical definitions of these concepts can be found elsewhere (Watts and Strogatz, 1998; Latora and Marchiori, 2001). Global and local efficiency are susceptible to neuropathology (Rubinov and Sporns, 2010).

The effects of brain pathology can be described using network models (Fornito *et al.*, 2015). Direct damage to network hubs, such as through focal ischaemia or haemorrhage, could lead to apathy. However, cerebrovascular disease may also lead to remote changes that result in apathy. These remote changes can be modeled as network pathologies, of which two are discussed: diaschisis and transneuronal degeneration. Diaschisis refers to a functional deficit in a region that is connected to a focally damaged area (Figure 1c), which is mediated by a reduction or interruption in the connectivity between the two regions (Carrera and Tononi, 2014). This can be operationalized as reduced glucose metabolism or regional cerebral blood flow (rCBF) in the area of diaschisis, under the assumption that neurovascular coupling (functional hyperemia) is preserved in this region (Baron *et al.*, 1984). Although these functional deficits were once thought to be temporary and reversible, this notion has been challenged by recent evidence suggesting that morphological changes may occur in remote regions directly connected to an infarct (Duering *et al.*, 2015). These changes are also seen in young stroke patients (Schaapsmeerders *et al.*, 2016), suggesting that they are related to stroke and not a different neurodegenerative pathology. Secondary morphological damage is consistent with transneuronal degeneration (Figure 1d), a process by which damage to distant nodes propagates through structural or functional connections (Fornito *et al.*, 2015).

1.10.2. Candidate network mechanisms underlying apathy

These network measures allow us to reconceptualize the neurobiological basis of apathy. We propose that the hub nodes of GDB-related networks correspond to the structures found to be associated with apathy across neurological diseases. These include the anterior cingulate cortex (ACC), medial orbitofrontal cortex (OFC), ventral striatum, medial thalamus, and ventral tegmental area (Kos *et al.*, 2016; Le Heron *et al.*, 2018*a*). These structures play

important roles in the cognitive processes that guide effort-based decision-making in healthy individuals (Le Heron *et al.*, 2018*a*), so it is reasonable to suppose that they form a foundation for motivation-related brain networks in humans. Damage to these putative network hubs - such as through focal ischaemic or haemorrhagic stroke - can lead to immediate failure of GDB-related cognitive functions, which would then manifest as apathy. This view effectively subsumes the classical lesion-based view of apathy (Levy and Dubois, 2006).

In contrast to hub node damage, peripheral node damage may result in diaschisis or transneuronal degeneration. Based on the connectivity profile of the damaged node, these pathologies can lead to apathy by spreading to a remote hub node, or through progressive damage over time to GDB-related subnetworks. The former case can be illustrated by a hypothetical patient with a focal supplementary motor area (SMA) infarct. SMA shares direct white matter connections with the ACC, a hub node, in the form of branching U-fibers from the corticospinal tract (Nachev *et al.*, 2008; Vergani *et al.*, 2014). These structural connections form the basis of functional interactions between these areas. One relevant GDB-related function is the formation of intentions to move, which is characterized by ramping activity of neural populations in SMA, followed by corresponding increases in neural activity in ACC (Fried *et al.*, 2011). This may reflect the formation of motor execution plans or an attempt for ACC to integrate the information to the rest of the network. In either case, SMA damage may lead to reduced functioning in connected ACC neurons, which have been deprived of a direct input (diaschisis). Over time, poor axonal nutrient transport and mitochondrial dysfunction lead to the anterograde degeneration of axons (Coleman, 2005) in cingulate motor fibers and then within the ACC itself (transneuronal degeneration). In both cases, according to the model we propose here, apathy is the result.

To illustrate how progressive damage to subnetworks might lead to apathy, the parietal-premotor network may be used as an example. This network consists primarily of the premotor and posterior parietal cortices, which form a relatively closed loop underlying movement intention and inhibition independently of motor execution (Desmurget and Sirigu, 2009). Partial damage or disconnection of the structures within this loop, whilst not directly leading to apathy, may impair the synchronous timing of neural signals necessary for movement. This decreased network efficiency makes complex movements more difficult to execute, leading to perceived task-related effort costs appearing greater (Zénon *et al.*, 2015), as the network needs to work harder (i.e., expend more energy) to achieve normal levels of functioning (Ginsberg *et al.*, 1989). The result is postulated to lead to an overall decrease of

GDB which might not be severe enough to meet criteria for an apathetic state. Over time, diaschisis and transneuronal degeneration occur within this network, leading to greater efficiency deficits that manifest as increasing apathy. The function of these structures and circuits has been simplified here for the purposes of illustrating how damage to non-hub nodes may lead to apathy.

The subsequent subsections will review evidence that suggests that apathy can be modeled as a network pathology in stroke and SVD. Prior to this, however, we clarify the neuroanatomical terminology used in these sections, as well as the studies included in the scope of the discussion. Although GDB may have a firm basis in specific brain regions and connections, very few studies have examined apathy using this level of granularity. This may be a consequence of small sample sizes in most studies, which limits the number of patients with isolated infarcts in each area. Our description of research on a per-study basis will therefore reflect the terminology used by the authors as closely as possible, since extrapolation to more specific structures is not possible. Additionally, any research that assesses the relationship between apathy and stroke using very broad neuroanatomical divisions (e.g., left/right hemisphere, anterior/posterior, etc.) will not be discussed, as these are too nonspecific to aid a mechanistic understanding of apathy.

1.10.3. Apathy in stroke

Apathy, in the acute and early subacute phase of stroke, may be the product of functional changes to nodes that are either part of or distant from the initial infarct. This is supported by a study of apathy and N-acetylaspartate (NAA) in first-time ischaemic stroke patients (Glodzik-Sobanska *et al.*, 2005). NAA is a nervous system-specific metabolite that may reflect myelin lipid turnover and mitochondrial energy production in humans, and can be interpreted as a marker for overall neuronal health (Moffett *et al.*, 2007). Remarkably, the authors found that patients with apathy had reductions in prefrontal NAA levels despite all participants having lesions *outside* the frontal lobes, which was apparent an average of nine days post-stroke (Glodzik-Sobanska *et al.*, 2005). In a similar vein, an electroencephalography study of patients with subcortical stroke showed that apathy was associated with decreased P3 amplitude and reduced P3 latency over frontal sites (Yamagata *et al.*, 2004). The P3 is an event-related potential evoked by novel stimuli (Friedman *et al.*, 2001), and the P3 changes documented by the authors may be consistent with decreased network efficiency in distant regions.

Studies of apathy and rCBF show converging results. rCBF is a measure of the brain's haemodynamic response, which is spatially and temporally coupled to changes in local field potentials elicited by synaptic activity (Shibasaki, 2008). As a result of this neurovascular coupling, a change in rCBF can be interpreted as a change in regional neural activity (Raichle and Mintun, 2006). Apathy has been associated with reduced prefrontal rCBF in patients with subcortical stroke, as well as cerebellar and thalamic infarcts (Okada *et al.*, 1997; de Oliveira Lanna *et al.*, 2012; Demirtas-Tatlidede *et al.*, 2013), suggesting functional changes in neural populations distant to the acute infarct. Moreover, apathetic patients showed lower rCBF in the basal ganglia compared to non-apathetic patients one month after stroke (Onoda *et al.*, 2011). These functional changes may persist for several years, as demonstrated by a case study of a patient with severe apathy who showed aberrant functional connectivity, assessed using resting-state functional MRI, in ACC despite a lack of lesions in that area (Siegel *et al.*, 2014). Functional connectivity deficits and apathy levels remained stable after three years (Siegel *et al.*, 2014). These findings further support the notion that apathy may occur as a syndrome of functional diaschisis in patients with stroke. That said, more longitudinal research is required to examine whether functional changes really lead to apathy.

Structural changes may later follow these functional changes. One study, which assessed ischaemic stroke patients during the subacute phase of stroke (10-28 days) and six months after the event, found that increasing apathy was associated with delayed atrophy in the posterior cingulate cortex (Matsuoka *et al.*, 2015). This atrophy may be the product of anterograde transneuronal degeneration (Fornito *et al.*, 2015), which can occur between 18-54 months post-stroke (Duering *et al.*, 2015). This secondary neurodegeneration is studied primarily using diffusion tensor imaging (DTI), an MRI technique used to measure molecular diffusion in biological tissue. Due to the hindered nature of water diffusion in tissues with complex architecture, such as those with coherent myelin fiber orientations, DTI measures such as fractional anisotropy (FA) can be used to infer the microstructural properties of underlying white matter (Basser and Pierpaoli, 1996). DTI data can also be used for tractography, which attempts to reconstruct three-dimensional white matter pathways through a continuous diffusion vector field (e.g., Mori *et al.*, 1999).

Evidence to support transneuronal degeneration as a network mechanism underlying apathy comes from two case studies of post-stroke patients with apathy with left or right caudate lesions (Jang and Kwon, 2018; Jang *et al.*, 2019). In both cases, diffusion tractography was used to reconstruct white matter pathways originating from the infarct. Both patients showed reduced caudate-prefrontal connectivity, suggesting that secondary

neurodegeneration resulting in cortical disconnection was a factor underlying apathy. This is further evidenced by associations between apathy and lesions to the internal capsule (Tatemichi *et al.*, 1992; Starkstein *et al.*, 1993), as well as reduced FA in the genu of the corpus callosum, anterior corona radiata, and white matter of the inferior frontal gyrus (Yang *et al.*, 2015*b*).

These white matter changes are likely to have direct consequences on whole-brain network connectivity. One study that explored tractography-derived white matter networks in ischaemic stroke patients showed that apathy was associated with decreased degree in 24 nodes across the cerebral cortex (Yang *et al.*, 2015*a*). This included changes to the bilateral inferior frontal gyrus *pars orbitalis*, bilateral posterior cingulum, left SMA, and right putamen and thalamus. Other nodes correlated with apathy were found in the occipital, temporal, and parietal lobes, as well as the insula. These changes in nodal degree were paralleled by decreased global and local efficiency in the nodes of the apathy-related subnetwork. Notably, DTI data was acquired within seven days of stroke onset, whilst assessments of apathy were conducted one month post-stroke. We can therefore conclude that early changes in the connectivity between these regions may predict the onset of apathy one month later. Whether these network changes result in apathy contemporaneously remains unexplored.

This is not to suggest that apathy, during the acute and post-acute phases of stroke, is *only* a product of diaschisis and transneuronal degeneration. Focal lesions to GDB-related hub nodes may lead to immediate network failure and apathy. For instance, apathy is a prominent feature of many patients with isolated ACC (Kumral *et al.*, 2019), thalamic (Ghika-Schmid and Bogousslavsky, 2000), and striatal infarcts (Bhatia and Marsden, 1994). Similarly, reward sensitivity deficits, which are associated with apathy in chronic stroke patients, can be mapped to lesions in structures that include the ventral basal ganglia, thalamus, and PFC (Adam *et al.*, 2013; Rochat *et al.*, 2013). These demonstrate that hub node lesions can affect networks at large, without spreading to connected nodes.

These results suggest that post-stroke apathy can result from two different types of damage. One is driven by an acute lesion to a hub node, which causes immediate network failure and apathy. The other is driven by an acute lesion to a peripheral node, which, if connected to a hub node, can lead to a decrease in functioning of that hub node. Over time, these functional changes may lead to structural changes, such as cortical atrophy due to a loss of synaptic input. Our model therefore suggests that connectomal diaschisis, later followed by transneuronal degeneration, may be a mechanism underlying post-stroke apathy in cases

where the initial infarct occurs in a non-hub node. These connectivity changes could result in decreased global and local efficiency due to disconnection or disruption of the white matter networks underlying GDB.

This view of the pathogenesis of post-stroke apathy allows us to explain two major inconsistencies in the current literature. One is the lack of association between apathy and lesion location. As previously discussed, lesion location alone cannot adequately capture distant structural or functional changes that may lead to apathy. This may be why pairwise comparisons of lesion location in stroke patients with apathy against those without apathy yield negative results, whilst studies examining all patients with apathy find common structural and functional changes (e.g., Okada *et al.*, 1997; Yang *et al.*, 2015*b*).

The second inconsistency concerns the trajectory of post-stroke apathy. Some patients without apathy in the acute phase develop it up to one year later, whilst some patients with apathy in the acute phase are apathy-free later (Withall *et al.*, 2011; Caeiro *et al.*, 2013). Some of this may well be attributable to measurement error, as a diagnosis of apathy is usually made using cut scores on clinical scales. However, a potential neurobiological explanation for this crossover effect may be individual changes in functional network dynamics. In the former scenario, later-onset apathy may be the result of time-dependent post-stroke transneuronal degeneration, as previously described. Indeed, overall levels of apathy tend to increase in stroke patients over five years, although this may be due to subsequent cerebrovascular incidents (Brodaty *et al.*, 2013).

In the latter case, remitting apathy may be the result of functional network reorganization, a notable phenomenon studied most extensively in the context of motor recovery after stroke (Grefkes and Fink, 2014). This entails an initial disruption of functional network connectivity following stroke, which is then followed by a gradual restoration of interhemispheric functional connectivity over several months in individuals who recover function (van Meer *et al.*, 2010). Evidence to support this functional network recovery in stroke patients with apathy comes from case studies using brain stimulation. Repetitive transcranial magnetic stimulation (rTMS) coils induce magnetic fields that lead to the depolarization of superficial cortical axons, inducing activity in potentially disrupted networks (Lefaucheur *et al.*, 2014). This form of stimulation, applied in certain cortical areas, may lead to a recovery of function over many sessions.

Such a recovery has been demonstrated in a sample of 13 chronic stroke patients who received high-frequency rTMS over the ACC and medial PFC, two putative hub nodes (Sasaki *et al.*, 2017). After five days of treatment, individuals in the rTMS group showed an

improvement in apathy symptoms. In contrast, apathy scores in individuals assigned to the sham condition remained static. A case study suggests that these rTMS-based decreases in post-stroke apathy are associated with improved interhemispheric activity (Mitaki *et al.*, 2016), suggesting a direct parallel with the mechanisms underlying motor recovery after stroke. This functional network recovery may be the result of vicariation, when neighboring tissues take on functions related to damaged tissue (Dancause, 2006). It has been suggested that structures that show similar connectivity profiles to the damaged tissues may be more likely to adopt these functions (Silasi and Murphy, 2014). Thus, an accurate understanding of the structural network basis of GDB may open up new targets for rTMS-based recovery in patients with post-stroke apathy.

1.10.4. Apathy in cerebral small vessel disease

Cerebral SVD is a term used to describe the pathologies that affect the small vessels of the brain, which include the small arteries, arterioles, and venules (Pantoni, 2010). SVD is the leading vascular cause of dementia (Pantoni, 2010). Most SVD is sporadic and related to age and vascular risk factors such as hypertension, but a minority of cases are caused by monogenic disorders, such as CADASIL (Pantoni, 2010). SVD-related pathology leads to heterogeneous changes in brain parenchyma, and can manifest radiologically as lacunes, WMH, or microbleeds, among others (Wardlaw *et al.*, 2013). These may occur in tandem with microstructural changes in major white matter tracts, leading to cognitive deficits that some have suggested to be the result of a disconnection syndrome (O'Sullivan *et al.*, 2005; Lawrence *et al.*, 2013).

Mounting evidence suggests that white matter changes may underlie apathy in SVD. Apathy has been associated with reduced FA in major white matter tracts such as the anterior cingulum and corpus callosum in patients with sporadic SVD (Hollocks *et al.*, 2015) (Figure 2a). FA reductions in these same tracts were found to be associated with apathy in CADASIL (Le Heron *et al.*, 2018*b*) (Figure 2b), an early-onset model of SVD free of age-related neurodegeneration (Chabriat *et al.*, 2009). In accordance with these changes, apathy has been found to be associated with disruption to large-scale white matter networks in SVD (Figure 2c).

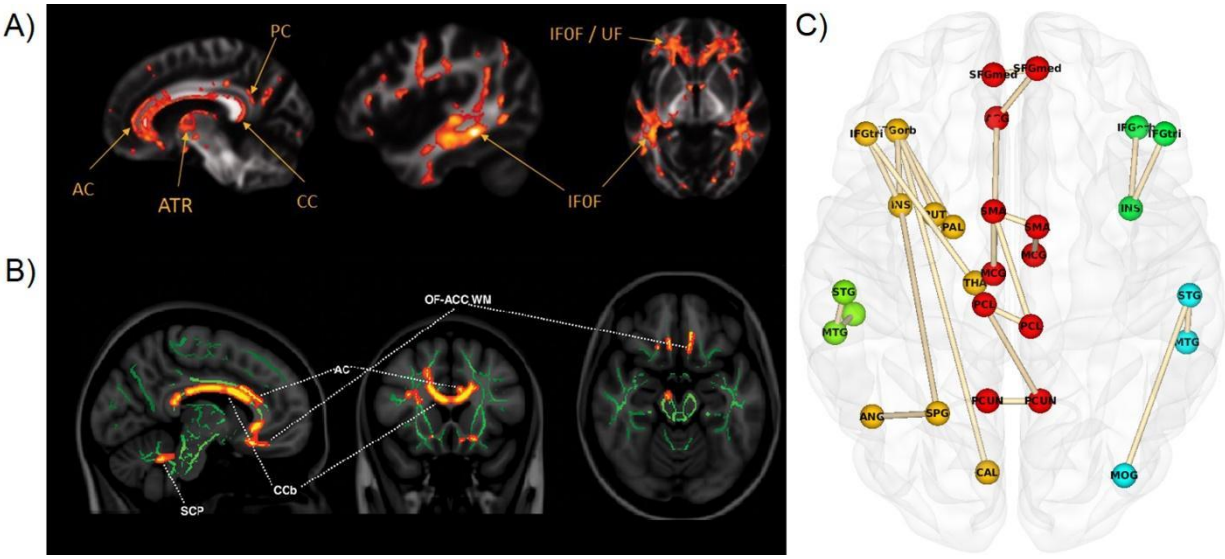

Figure 2. White matter network damage associated with apathy in cerebral small vessel disease (SVD). **A)** Reduced white matter fractional anisotropy (FA) associated with apathy in sporadic SVD; **B)** Reduced FA associated with apathy in CADASIL, a genetic form of SVD; **C)** Reductions in white matter network connectivity associated with apathy in sporadic SVD. Apathy is associated with a distributed pattern of white matter damage across the cortex, implicating several subnetworks in the pathogenesis of apathy. White matter damage related to apathy is consistent in sporadic and genetic SVD, suggesting a common basis. Adapted from Hollocks et al. (2015), Le Heron, Manohar, et al. (2018), and Tay et al. (2019) with permission. AC = anterior cingulum; PC = posterior cingulum; CC = corpus callosum; CCb = body of the corpus callosum; ATR = anterior thalamic radiation; IFOF = inferior fronto-occipital fasciculus; UF = uncinate fasciculus; SCP = superior cerebellar peduncle; OF-ACC WM = orbitofrontal-anterior cingulate cortex white matter.

Lacunar infarcts, whilst an important marker of SVD, have indirectly been covered in Section 2.3, as these tend to be sources of subcortical infarcts (Wardlaw *et al.*, 2013). Although lacunes have different etiologies than large artery infarcts, which arise from the occlusion of larger cerebral arteries and often involve the cortex, both types of stroke tend to result in similar pathophysiological cascades, and thus similar patterns of network damage (Duering *et al.*, 2015). The relationship between apathy and other radiological markers of SVD such as microbleeds, cortical microinfarcts, and enlarged perivascular spaces has yet to be explored.

WMH appear as areas of high signal intensity on T2-weighted MRI, and may reflect areas of ischaemic demyelination and axonal loss resulting from chronic hypoperfusion (Fazekas *et al.*, 1993; Fernando *et al.*, 2006). These lead to changes in the underlying white matter architecture of the affected tissue and surrounding areas, corresponding to decreased FA and NAA in proximal normal-appearing white matter (Firbank *et al.*, 2003; van Leijsen *et al.*, 2018). Tract-specific WMH progression is also related to incident cortical atrophy in the regions connected by that tract (Lambert *et al.*, 2016). This suggests that WMH-related network damage can be characterized by transneuronal degeneration, which originates in hypoperfused white matter and progresses down tracts. This then leads to atrophy in connected regions due to the progressive disruption of synaptic inputs.

WMH have been correlated with higher apathy levels in population-based cohort studies (Yao *et al.*, 2009; Grool *et al.*, 2014; Li *et al.*, 2016), and Alzheimer's disease patients with WMH have higher levels of apathy compared to patients without WMH (Starkstein *et al.*, 1997). These are paralleled by lower rCBF in basal ganglia, thalamus, and frontal lobes (Starkstein *et al.*, 1997), suggesting that WMH lead to functional disruption of GDB-related hub nodes, which may impact network efficiency. Although these results are cross-sectional, they suggest that WMH are related to apathy through the disruption of network efficiency. This, coupled with progressive neurodegeneration and consequent cortical thinning, may be a factor underlying apathy in SVD. The consequences of this chronic ischaemia, together with the earlier mentioned effect of acute infarcts, suggests a potential cascade linking ischaemia to apathy (Figure 3).

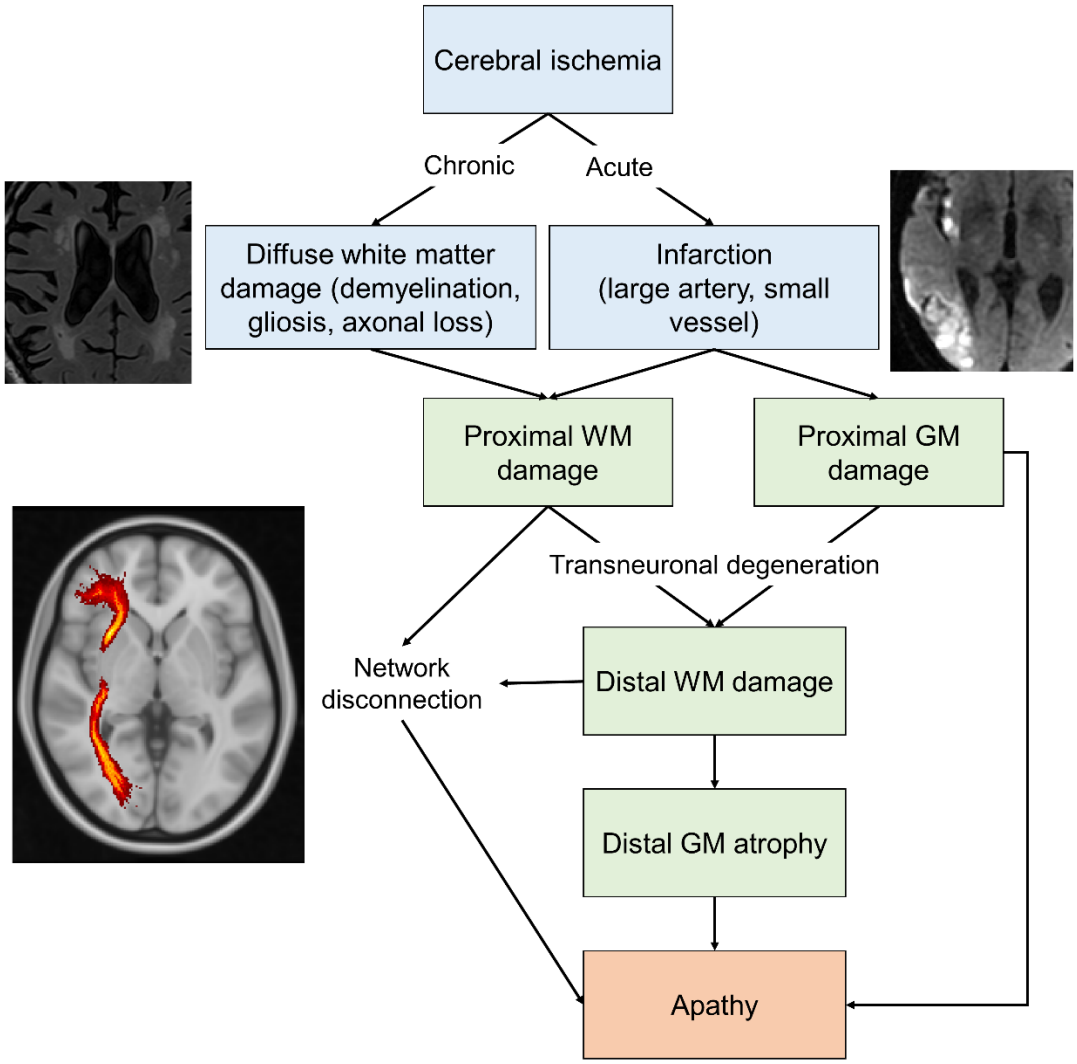

Figure 3. Hypothesized mechanisms linking ischemic pathology to apathy. Chronic and acute ischemia may lead to different types of tissue damage. Specific types of lesions that lead to damage in strategic grey matter structures or white matter tracts, such as those related to hub nodes, may immediately lead to apathy. Over time, secondary neurodegeneration propagates from lesioned tissue to connected areas, leading to network disconnection and apathy.

1.11. Neurobiological overlap between apathy and depression

Due to the possible neurobiological overlap between apathy and anhedonia (Husain and Roiser, 2018), it is possible that some candidate neurobiological mechanisms underlying apathy may also be related to this particular symptom of depression. Given that previous work has been unable to find associations between depression and white matter damage after controlling for apathy (Hollocks *et al.*, 2015), it is possible that neurobiological overlap may be restricted to grey matter changes. Indeed, functional evidence from individuals with major depression and anhedonia suggests that anhedonia is associated with changes in ventromedial prefrontal cortex, amygdala, and ventral striatum (Keedwell *et al.*, 2005). If these regional changes are coupled with focal grey matter damage in patients with cerebrovascular disease, then it is possible that the hub nodes that underlie apathy, particularly in the ventromedial prefrontal cortex and ventral striatum (1.10.2), may also partially underlie anhedonic symptoms of depression.

1.12. Hypotheses to be tested

The following chapters in this thesis will explicitly test the core predictions of the network model we have proposed. The majority of these will be tested in a single population of SVD participants, which is described in detail (Chapter 2). First, we examine the grey matter and white matter correlates of apathy and depression using voxel-based methodologies, as these may underlie network changes (Chapter 3). Based on previous work, we expect that apathy is associated with focal grey matter damage, particularly in the ACC and ventral striatum (Le Heron *et al.*, 2018*a*), as well as diffuse white matter damage (Hollocks *et al.*, 2015). In contrast, we expect that depression will not be associated with white matter damage (Hollocks *et al.*, 2015), but may be associated with grey matter changes in the prefrontal cortex and ventral striatum (Keedwell *et al.*, 2005).

We then investigate the relationship between apathy and white matter network damage (Chapter 4). Given the association between apathy and diffuse white matter damage (Hollocks *et al.*, 2015), we expect apathy to be associated with large-scale damage to white matter networks. We predict that fronto-striatal subnetworks may be damaged, as these connect hub nodes that may be important for motivation (1.10.2), as well as extensive damage to peripheral connections and subnetworks.

To further probe focal changes that may be associated with the neurobiology of depression, we then investigate longitudinal patterns of grey matter atrophy associated with

anhedonic, mood, and somatic symptoms of depression (Chapter 5). As mentioned earlier, we expect anhedonia to be associated with atrophy in areas similar to those associated with apathy in voxel-based analyses (Section 1.10; Chapter 3). In contrast, we predict that mood and somatic symptoms may be related to other morphometric changes associated with depression, such as hippocampal and amygdalar atrophy (Ashtari *et al.*, 1999).

Finally, we investigate associations between apathy, depression, and conversion to dementia, an important outcome variable in SVD. Given the degree to which apathy seems to be associated with white matter damage, as well as previous research, we predicted that apathy, but not depression, would be associated increased dementia risk in participants with SVD (Lohner *et al.*, 2017; van Dalen *et al.*, 2018*b*).

Chapter 2: The Radboud University Nijmegen Diffusion tensor and Magnetic resonance Cohort (RUN DMC)

2.1. Introduction

The primary cohort used to investigate the questions raised previously (Chapter 1) was the Radboud University Nijmegen Diffusion tensor and Magnetic resonance Cohort (RUN DMC). The RUN DMC study is a prospective cohort study designed to investigate the causes and consequences of cerebral small vessel disease (SVD) using magnetic resonance imaging (MRI). As the RUN DMC cohort is investigated in all subsequent experimental chapters, basic sample characteristics are summarised here.

2.2. Methods

2.2.1. Study population

In 2006, consecutive individuals referred to the Department of Neurology at Radboud University between October 2002 and November 2006 were selected for possible participation. Inclusion criteria were: (1) age between 50 and 85 years old; and (2) evidence of cerebral SVD on neuroimaging, defined as white matter hyperintensities (WMH) or lacunar infarcts of vascular origin (Wardlaw *et al.*, 2013). Individuals who were eligible because of a clinical lacunar stroke syndrome (Bamford *et al.*, 1991) were included > 6 months after the event to minimise the effect of the acute infarct on outcomes.

Exclusion criteria included: (1) presence of dementia, assessed using DSM-IV-TR criteria (American Psychiatric Association, 2000); (2) presence of Parkinson's Disease or parkinsonism; (3) intracranial haemorrhage; (4) life expectancy < 6 months; (5) intracranial space-occupying lesion; (6) disease interfering with cognitive testing or follow-up, including psychiatric diseases such as bipolar disorder and schizophrenia; (7) current or recent use of acetylcholinesterase inhibitors, neuroleptic agents, levodopa or dopamine agonists or antagonists; (8) WMH of non-vascular origin, such as multiple sclerosis; (9) prominent visual or hearing impairment; (10) language barrier; or (11) MRI contraindications or known claustrophobia.

The study was approved by the Medical Review Ethics Committee region Arnhem-Nijmegen (van Norden *et al.*, 2011). All participants provided written informed consent according to the Declaration of Helsinki. One thousand and four individuals were invited by

letter. Of these, 727 were deemed eligible after contact by phone, and 525 agreed to participate. Twenty-two of these individuals were found to meet exclusion criteria upon visiting the research center. This left 503 participants for the baseline assessment.

Of the 503 participants recruited to the baseline in 2006, 398 were able to attend follow-up in 2011. Reasons for missing the assessment included death (n = 49), illness (n = 19), relocation (n = 5), lack of time (n = 30), or lost to follow-up (n = 2). Subsets of these 398 individuals at 2011 will be investigated in subsequent chapters as assessments of apathy began at this timepoint.

2.2.2. Measures

Basic demographic (age, sex, education) and information on vascular risk factors, including hypertension, hypercholesterolemia, diabetes, and body mass index (BMI), were collected.

Apathy was assessed using the clinician-rated Apathy Evaluation Scale (AES), a validated measure of apathy in stroke (Marin *et al.*, 1991). The AES has 18 items which are graded on a Likert scale of 1-4. Items 6, 10, and 11 are negatively-worded, and must be reverse-coded prior to scoring the scale. Total scores range from 18-72, with higher scores indicating greater apathy. The AES was administered at the 2011 assessment, precluding an analysis of apathy at baseline in 2006.

Depression was assessed using the Center for Epidemiologic Studies Depression Scale (CESD), a well-validated tool for screening depressive symptoms that has previously been used in SVD (Radloff, 1977; Prins *et al.*, 2005). The CESD is a 20-item self-report measure, with responses ranging from 0-3. Items 4, 8, 12, and 16 are reverse-coded. Total scores can range from 0-60, with higher scores indicating more depression.

Cognitive impairment was assessed using the Mini Mental State Examination (MMSE) (Folstein *et al.*, 1975). The MMSE is a 30-item test that assesses orientation to time and place, verbal learning, attention and mental arithmetic, verbal recall, language, and visual perception. These scores are then added to provide an aggregate measure of general cognitive function, which is sensitive to cognitive impairment (Tombaugh and McIntyre, 1992).

2.2.3. MRI acquisition protocols

MR images were acquired on a Siemens Magnetom Avanto Tim 1.5 Tesla MRI scanner (Erlangen, Germany). The protocol included a T1-weighted (T1w) three-dimensional magnetization-prepared rapid gradient echo (MPRAGE) image (repetition time (TR) = 2250 ms, echo time (TE) = 2.95 ms, inversion time (TI) = 850 ms, flip angle = 15°, voxel size =

1.0 mm x 1.0 mm x 1.0 mm), an axial fluid-attenuated inversion recovery (FLAIR) sequence (TR = 14240 ms, TE = 89 ms, TI = 2200 ms, voxel size = 1.2 mm x 1.0 mm x 2.5 mm, interslice gap = 0.5 mm), and a diffusion-weighted imaging (DWI) sequence (TR = 10200 ms, TE = 95 ms, voxel size = 2.5 mm x 2.5 mm x 2.5 mm; 7 scans with b = 0 s/mm², 61 scans with b = 900 s/mm²).

2.2.4. White matter hyperintensity ratings

WMH were defined as areas of hyperintense signal on FLAIR images without corresponding cerebrospinal fluid-like hypointense areas on the T1w image. Gliosis surrounding lacunar and territorial infarcts were not considered to be WMH (Hervé *et al.*, 2005). WMH were segmented on the FLAIR images using a semiautomatic method (Ghafoorian *et al.*, 2016), and were visually inspected for errors.

2.2.5. Lacunar infarct rating

Lacunes were defined as hypointense areas > 2 mm and < 15 mm on FLAIR and T1w images, ruling out perivascular spaces (< 2 mm, except around the anterior commissure, where perivascular spaces can be large) and infraputaminal pseudolacunes (Hervé *et al.*, 2005). Lacunes were counted by two trained raters blind to the clinical data, and inter-rater reliability assessed using κ (Cohen, 1960). Reliability was excellent, κ = 0.95 (van Uden *et al.*, 2015).

2.2.6. Brain volumetry

Brain volumes were calculated using tools in FSL 6.0.1 (Smith *et al.*, 2004). T1w images were processed using SIENAX (Smith *et al.*, 2002). SIENAX first extracts brain and skull images from the T1w image using BET (Smith, 2002). Brain extracted images are then registered to the MNI152 standard brain using an affine transformation calculated using FLIRT (Jenkinson and Smith, 2001; Jenkinson *et al.*, 2002). The calculated transformation is also applied to the skull image to determine a scaling factor to correct for differences in head size relative to the MNI152 brain. Scaling factors > 1 indicate a skull smaller than the MNI152 template, factors < 1 indicate a larger skull. Finally, FIRST is used to calculate total brain volume (BV) (Zhang *et al.*, 2001). Raw BV and WMH volumes were normalised for differences in skull size by multiplying them by the previously calculated scaling factor, creating nBV and nWMH, respectively.

2.2.4. Statistical analysis

Continuous variables were summarised using means and standard deviations (SD), whilst binary and ordinal variables were summarised using counts and percentages. Pearson product-moment correlation coefficients were calculated between pairs of continuous variables to determine the degree of association between both variables. Given the exploratory nature of these analyses, only raw (uncorrected) P values are presented.

All tests were two-tailed, with $\alpha = 0.05$. All statistical analyses were conducted using R 3.6.2 (R Core Team, 2019).

2.3. Results

Descriptive statistics for the 398 participants in 2011 are shown in Table 1. The mean age of participants in 2011 was nearly 70, whilst 57% of the sample was male. Average MMSE scores revealed that the population suffered from minimal levels of cognitive impairment. The majority of the population was hypertensive, had under 1 lacune, and had modest levels of WMH. Apathy and depression scores were mildly elevated (Figure 1).

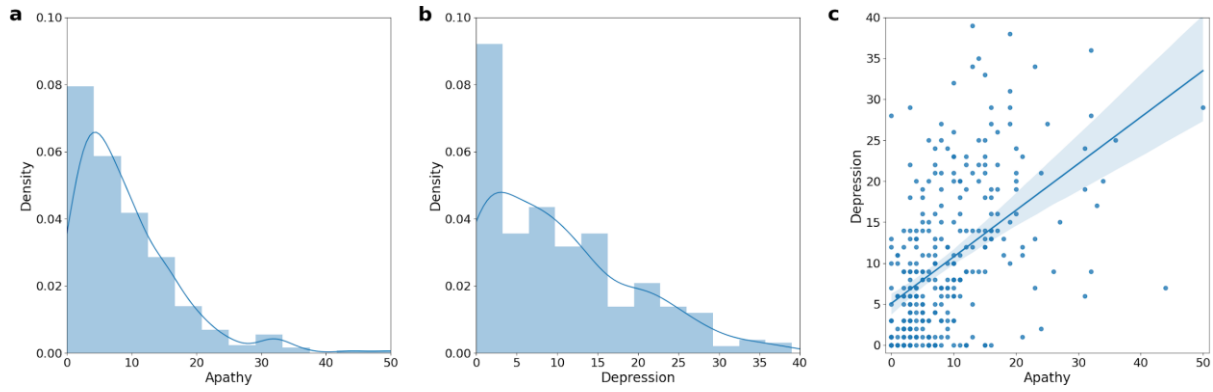

Figure 1. Apathy and depression in RUN DMC. **a,** Distribution of apathy scores. **b,** Distribution of depression scores. **c,** Scatterplot of apathy and depression scores.

Table 1. Descriptive statistics for RUN DMC at 2011 (n = 398).

	Mean (SD) or N (%)
Age, years	69.9 (8.5)
Sex, male	227 (57.0)
Education, years	11.0 (3.4)[1]
MMSE, score	27.8 (2.8)
AES, score	27.7 (8.2)[2]
CESD, score	10.5 (8.8)[3]
nBV, mm^3	1442855.3 (87549.0)[4]
nWMH, mm^3	12055.5 (17357.2)[4]
Lacunes, count	0.7 (1.5)[4]
Microbleeds, count	0.8 (3.7)[4]
Hypertension, presence	322 (80.9)[5]
Diabetes, presence	59 (14.8)[6]
Hypercholesterolemia, presence	201 (50.5)[6]
BMI, mm/kg^2	27.6 (5.4)[7]
Smoking, presence	
Never	117 (29.4)
Ex	231 (58.0)
Current	50 (12.6)

Note. MMSE = Mini-Mental State Examination, AES = Apathy Evaluation Scale, CESD = Center for Epidemiologic Studies Depression Scale, nBV = Brain volume, normalised, nWMH = White matter hyperintensity volume, normalised, BMI = body mass index. Superscripts denote *n* missing cases: [1] = 1, [2] = 34, [3] = 19, [4] = 39, [5] = 2, [6] = 18, [7] = 14.

Pearson correlations are shown in Table 2. Apathy and depression were highly correlated. Apathy also showed strong correlations with MMSE score, age, brain volumes, and radiological markers of SVD. Depression, by contrast, showed a more mixed pattern of correlations, with statistically significant relationships showing weaker coefficients compared to apathy overall. For instance, AES-MMSE r = -0.42, P < 0.001, whilst CESD-MMSE r = -0.14, P = 0.005.

Table 2. Pearson product-moment correlation matrix for continuous variables of interest.

	AES	CESD	MMSE	Age	nBV	nWMH	Lacunes
AES							
CESD	0.50 (<0.001)						
MMSE	-0.42 (<0.001)	-0.14 (0.005)					
Age	0.28 (<0.001)	0.09 (0.084)	-0.36 (<0.001)				
nBV	-0.31 (<0.001)	-0.13 (0.015)	0.27 (<0.001)	-0.57 (<0.001)			
nWMH	0.29 (<0.001)	0.16 (0.002)	-0.28 (<0.001)	0.41 (<0.001)	-0.28 (<0.001)		
Lacunes	0.23 (<0.001)	0.09 (0.081)	-0.18 (<0.001)	0.15 (0.005)	-0.23 (<0.001)	0.53 (<0.001)	

Note. Degrees of freedom for each cell are calculated on a pairwise basis due to missing data.

P values are uncorrected for multiple comparisons.

2.4. Discussion

Basic characteristics of the RUN DMC study, a large prospective cohort of SVD patients, were described. The population consisted of older individuals with a minor degree of cognitive impairment. On average, these individuals suffered from a higher burden of vascular risk factors compared to the general population, with correspondingly higher rates of SVD-related brain pathology such as WMH and atrophy (Shen *et al.*, 2020). Importantly, elevated levels of apathy and depression were found in the population, although mean scores were not at clinically significant cutoffs (Radloff, 1977; Andersson *et al.*, 1999).

Correlation analyses revealed that apathy and depression were highly related. Despite this, apathy and depression showed different patterns of correlations with other variables. Apathy was highly correlated with age, MMSE score, and SVD-related neuroimaging variables. In contrast, depression was unrelated to age and lacunar infarct count, and only modestly associated with MMSE score and nBV. That apathy and depression were highly related, but showed dissociable patterns of correlations with other variables, reinforces the notion that the two constructs are related but genuinely distinct entities.

Chapter 3: Grey and white matter correlates of apathy

3.1. Introduction

Apathy in cerebral small vessel disease (SVD) may be a syndrome of network disconnection. Prior to investigating networks directly, however, it would be beneficial to localise the underlying grey matter and white matter changes that may be associated with apathy and depression, as these may have consequences on whole-brain network structure and function.

To investigate these changes, we used voxel-based statistical techniques to analyse structural MRI images. This included voxel-based morphometry (VBM), which is traditionally used to analyse grey matter changes on T1w images, and a voxel-based implementation of tract-based spatial statistics (TBSS), which analyses white matter microstructural change on diffusion-weighted imaging (DWI) sequences.

Based on research across neurological disorders, we expected to find apathy associated with grey matter damage primarily in the anterior cingulate cortex (ACC) and nucleus accumbens (Le Heron *et al.*, 2018*a*). We also hypothesised that apathy would be associated with diffuse white matter damage given previous findings in another cohort of symptomatic SVD patients (Hollocks *et al.*, 2015). We also expect that depression will not be associated with white matter damage (Hollocks *et al.*, 2015), but may be associated with grey matter changes in the prefrontal cortex and ventral striatum (Keedwell *et al.*, 2005).

3.2. Methods

3.2.1. Study population, measures, and MRI acquisition parameters

The sample investigated was a subset of participants with neuroimaging data from the Radboud University Nijmegen Diffusion tensor and Magnetic resonance imaging Cohort (RUN DMC) study described previously (Chapter 2). The apathy and depression measures used included the Apathy Evaluation Scale (AES) and Center for Epidemiologic Studies Depression Scale (CESD) whilst cognition was assessed using the Mini Mental State Examination (MMSE) (2.2.2). The MRI sequences used included T1-weighted (T1w) and diffusion-weighted imaging (DWI) scans (2.2.3).

Although the AES was administered at both 2011 and 2015, different raters administered the scale at each timepoint. As a consequence, participant differences in apathy may have been attributable to either time or to a change in raters, making an analysis of

population-level changes in apathy difficult to interpret. Exploratory analyses revealed that the 2015 scores were indeed left-shifted compared to the 2011 scores, with 2015 scores showing an overall floor effect. Although this could be interpreted as apathy scores decreasing over time in SVD patients, an equally valid interpretation could be that the 2015 rater simply saw patients as less apathetic than the rater at 2011. In order to avoid this potential rater bias, we forego an analysis of longitudinal apathy scores, opting instead to focus only on the cross-sectional 2011 apathy and depression scores (as the 2011 visit has the larger sample size).

Of the 398 participants included at the 2011 timepoint, 87 were excluded due to missing MRI or clinical data (Table 1 in 2.3), leaving a total of 311 participants with complete data for the analysis.

3.2.2. Imaging analysis pipeline overview

The present work has two primary neuroimaging analyses: one, a VBM analysis to investigate grey matter changes, and two, a TBSS-style analysis to investigate white matter microstructural changes. VBM is performed on T1w images, while TBSS is performed on DWI images. Both of these require pre-processing of their respective images. Important common steps for both are registrations to standard space and deriving masks of the appropriate tissue type, which are crucial to localising effects across participants and restricting analyses to anatomically appropriate regions.

To this end, the FreeSurfer suite was first used to process T1w images, as this includes skull stripping, which is important for alignment, and the delineation of brain tissue into different classes. At this point, the T1w images are suitable for the VBM pipeline. The DWI images require additional pre-processing and tensor fitting prior to registration and TBSS. These are described in more detail below.

3.2.3.1. FreeSurfer analysis

For VBM, estimates of each participant's grey matter are needed. These were obtained using the automated FreeSurfer pipeline. Prior to analysis with FreeSurfer, all T1w volumes underwent bias field correction using the N4 algorithm (Tustison *et al.*, 2010), as implemented in the ANTs software suite (http://stnava.github.io/ANTs/). In brief, MRI images are corrupted by a low frequency intensity nonuniformity, which results in similar tissue types having different voxel intensities across the brain (Tustison *et al.*, 2010). Bias field correction involves the iterative estimation and correction of the bias field by modeling

several b-splines (Riesenfeld, 1973). The N4 correction has been shown to outperform the traditional N3 correction (Sled *et al.*, 1998; Tustison *et al.*, 2010), which is the default bias field correction method employed in FreeSurfer.

The N4 corrected T1w images were then processed by FreeSurfer 6.0 (http://surfer.nmr.mgh.harvard.edu/), a fully automated processing pipeline for anatomical images. It includes brain tissue extraction (Ségonne *et al.*, 2004), nonlinear registration to MNI 305 space (Evans *et al.*, 1993), volumetric segmentation of the subcortical white matter and deep grey matter structures (Fischl *et al.*, 2002, 2004*a*), further intensity normalization using the N3 algorithm (Sled *et al.*, 1998), tessellation of the grey and white matter boundaries, automatic topological defect correction (Fischl *et al.*, 2001; Ségonne *et al.*, 2007), and surface deformation along intensity gradients to determine the white-grey and grey-cerebrospinal fluid (CSF) boundaries, under the assumption that areas with the sharpest change in intensities define transitions between tissue classes (Dale and Sereno, 1993; Dale *et al.*, 1999; Fischl and Dale, 2000). The white and grey matter surfaces are then inflated (Fischl and Dale, 2000), then registered to a spherical atlas based on cortical folding patterns (Fischl *et al.*, 1999). Using this spherical atlas, the cerebral cortex is then parcellated into sulcal- and gyral-based regions of interest (Fischl *et al.*, 2004*b*; Desikan *et al.*, 2006). Cortical thickness is then calculated as the closest distance from the grey-white boundary to the grey-CSF boundary at each vertex on the tessellated surfaces (Fischl and Dale, 2000). FreeSurfer is a widely-used software suite that has been extensively validated in comparisons against manual measurements (Kuperberg *et al.*, 2003; Salat *et al.*, 2004) and histological analysis (Rosas *et al.*, 2002).

FreeSurfer was used to process all T1w images at 2011. This yielded a hard segmentation of grey matter tissue for all participants.

3.2.3.2. Diffusion-weighted image preprocessing

For TBSS, diffusion tensor-derived images are needed. This section describes the pre-processing of the raw DWI images for this. Due to the fast acquisition times of EPI sequences, DW images suffer from low signal-to-noise and are highly susceptible to bulk motion, necessitating a degree of post-processing. The first step in the DWI preprocessing pipeline was denoising the raw diffusion data using a local principal component analysis (PCA) filter (Manjón *et al.*, 2013). In brief, this approach takes a 3D patch of voxels in the DW image, then uses PCA to decompose the signal into local principal components. Smaller

components, which are thought to reflect noise, are shrunk. The signal is then reconstructed, yielding an image with reduced noise.

Next, eddy currents were corrected using the eddy tool in FSL (fsl.fmrib.ox.ac.uk/fsl/). Eddy currents are generated when rapidly changing magnetic fields induce opposing currents in nearby gradient coils, leading to spatial stretching and shearing (https://fsl.fmrib.ox.ac.uk/fsl/fslwiki/FDT/UserGuide). These are corrected by registering each volume in the DW time-series to a reference image, which was the first b = 0 mm/s^2 volume (henceforth, the *b0* volume).

Finally, bulk motion artifacts were corrected prior to tensor fitting. Common motion artifacts include head rotation and cardiac pulsation, which can lead to signal dropout and bias the final analysis (Norris, 2001). The PATCH algorithm was used to estimate and correct the effects of head movement and cardiac motion (Zwiers, 2010) (github.com/marcelzwiers/didi).

Geometric distortions were unwarped by normalising the DWI images to the T1w images in the phase-encoding direction (Kybic *et al.*, 2000; Andersson *et al.*, 2001) using the Unwarp toolbox in SPM12 (fil.ion.ucl.ac.uk/spm/toolbox/unwarp/). Finally, non-brain tissue was removed by generating a binary brain mask using BET (Smith, 2002) in FSL. BET was iterated several times using the -R flag, yielding a robust estimate of brain tissue.

3.2.3.3. Diffusion tensor imaging

The diffusion tensor is a robust and widely-used method for modeling DWI data (Assaf and Pasternak, 2008). A diffusion tensor, *D*, is a 3 x 3 symmetric matrix that describes diffusion along the *x*, *y*, and *z* axes:

$$D = \begin{bmatrix} D_{xx} & D_{xy} & D_{xz} \\ D_{yx} & D_{yy} & D_{yz} \\ D_{zx} & D_{zy} & D_{zz} \end{bmatrix}.$$

D has six independent components that can be estimated from the DWI data using linear regression techniques (Basser *et al.*, 1994*a*). Since *D* is a symmetric and positive-definite matrix, it can be expressed as

$$D = V \Lambda V^T,$$

where *V* is a matrix with columns defining the orthogonal eigenvectors v_1, v_2, and v_3 of *D*, and Λ is a diagonal matrix of associated eigenvalues $\lambda_1 \geq \lambda_2 \geq \lambda_3$. This means that *D* can be represented geometrically as an ellipsoid, with axes defined by the eigenvectors and the magnitude along each axis determined by the eigenvalues. The shape of the tensor can therefore be used to infer the underlying tissue architecture of each voxel. For instance, CSF

has an isotropic (spherical) diffusion profile, with $\lambda_1 = \lambda_2 = \lambda_3$, while WM has an anisotropic (elongated) diffusion profile, with $\lambda_1 > \lambda_2 = \lambda_3$ (Basser *et al.*, 1994*b*). At the current imaging resolution (2.5 mm isotropic), GM voxels express intermediate diffusion characteristics.

D was fit using ordinary least squares using FDT in FSL 6.0.1. This yielded an image with tensors fit at each voxel in the DWI data. Additionally, several rotationally invariant scalar diffusion metrics were calculated using the obtained eigenvalues (Basser and Pierpaoli, 1996). Mean diffusivity (MD) is simply the average rate of molecular diffusion:

$$MD = \frac{\lambda_1+\lambda_2+\lambda_3}{3} = \frac{D_{xx}+D_{yy}+D_{zz}}{3},$$

while fractional anisotropy (FA) is the directional coherence of diffusion:

$$FA = \sqrt{\frac{3}{2}}\sqrt{\frac{(\lambda_1-MD)^2+(\lambda_2-MD)^2+(\lambda_3-MD)^2}{\lambda_1^2+\lambda_2^2+\lambda_3^2}}.$$

These scalar diffusion indices have been used to make voxel-wise inferences of underlying WM microstructural integrity (Basser and Pierpaoli, 1996). Damage to WM microstructure is reflected by increased MD and decreased FA.

3.2.3.4. Image registration

Image registration is the process by which two images are aligned using geometric transformations. Each transformation is associated with a degree of freedom permitting some change in the original image. Typically, the minimum number of degrees of freedom for a three-dimensional image would be 3, corresponding to translation across the x, y, and z axes. Another 3 degrees of freedom could be added to adjust the roll, pitch, and yaw of the image. These translations and rotations are known as rigid body transformations, as the position of the object changes, but not the size or shape. Transformations with $6 <$ degrees of freedom ≤ 12 are known as affine transformations, as these will change size and shape. These degrees of freedom permit extra changes such as scale, stretch, and skew along the xy, xz, and yz axes.

Both rigid body and affine transformations are known as linear transformations, as all points in an image can be linearly mapped from one area to another using a single function. This is not the case with nonlinear transformations, which can use thousands of degrees of freedom to deform the original image. This allows for more precise image alignment, such as changing the shape of one brain to match another. This type of transformation is nonlinear because each point in an image may be mapped to another using an arbitrary function. These point-wise functions yield an inhomogeneous warp field, with each point in that field corresponding to a unique input deformation function.

In MR image analysis, image points typically correspond to individual voxels in an image. The calculation of a linear transformation yields a matrix, while a nonlinear transformation yields an image of a warp field. Both types of transformations can be applied to an original image to align it with a target image. The type of interpolation determines how this occurs. Nearest neighbour interpolation, which is the most frequently used type of interpolation in this work, preserves the original image intensity values throughout the transformation. All linear registrations described were calculated with FLIRT in FSL 6.0.1 (Jenkinson and Smith, 2001), whilst non-linear registrations were calculated using symmetric diffeomorphic transformations in the ANTs suite (Avants *et al.*, 2008).

3.2.3.5. Voxel-based morphometry

Our VBM protocol was adapted from a previously-published optimised protocol. First, a binary segmentation of the grey matter in each participant's brain was extracted from their respective FreeSurfer-processed T1w image and re-registered to native space. These grey matter segmentations were then registered to MNI space using a 12 degree affine transformation followed by a nonlinear symmetric diffeomorphic transformation. This brought each individual's grey matter segmentation into a common space with a generally consistent morphology. All images were then averaged to create a population-specific template image.

This template image was then used as a new target for registration. Individual grey matter segmentations in native space were then nonlinearly registered to this template image. Since this template image was built from the sample itself, interpolation errors should be reduced when compared to using a different template as a registration target (i.e., the MNI 152 image). These registered images were then corrected for local expansion or contraction by modulating them using the Jacobian determinant of the warp field generated from the nonlinear transformation, then smoothed using an isotropic Gaussian kernel with a $\sigma = 4$ mm.

3.2.3.6. Tract-based spatial statistics

Our TBSS protocol was adapted from a modified voxel-based protocol that empirically outperforms standard TBSS (Schwarz *et al.*, 2014). Brain-extracted FA images for each participant were first registered to the FMRIB 58 image in MNI space using a linear and nonlinear transformation. These registered FA images were then averaged to produce a population-specific template image. The template image was then used as a new target for registration, with each participant's FA image in native space being registered to this image.

3.2.4. General linear models and permutation testing

Voxel-wise statistical inference in VBM and TBSS was carried out using a general linear model (Friston *et al.*, 1994). The general linear model is a generalisation of ordinary least squares regression, which takes the form of

$$Y = X\beta + \epsilon,$$

where Y is a matrix of response variables with elements y_{ij}, with each column j corresponding to an edge and each row i to a participant. The matrix X is known as the design matrix, with elements, x_{ik}, corresponding to the value of the covariate, k, for each participant, i. β is a parameter matrix of coefficients, with $\beta = [\beta_1\ \beta_2\ \dots\ \beta_j]^T$, such that β_j corresponds to a column vector of parameters for edge j. ϵ is a matrix of normally distributed error terms. Importantly, this equation does not include a constant or intercept term. This may be explicitly added by adding a column of 1's to X. Alternatively, the need for an intercept term can be removed by mean correcting each column of X, thereby making the intercept equal to 0. We used the former method in our study.

Effects of interest are then assessed using a linear contrast vector, c, which specifies the weight given to β. For instance, a two-sample t-test, where β_1 was the mean for group 1 and β_2 was the mean for group 2, could be tested using $c = [1\ -1]$. On the other hand, in a linear regression, where β_1 corresponded to the effect of interest, β_2 corresponded to a covariate of no interest, and β_3 to an intercept term, testing for a positive regression slope would yield, $c = [1\ 0\ 0]$, and for a negative slope, $c = [-1\ 0\ 0]$.

Voxel-wise inference is carried out using permutation testing, which can compute P values corrected for familywise error rates. The basic assumption of a permutation test is that data points and their associated labels can be randomly rearranged under the null hypothesis without significantly changing the test statistic (Winkler *et al.*, 2014). In the case of a regression analysis, such as ours, the design matrix is partitioned into the effect of interest and nuisance regressors. The data are fit to these nuisance regressors, yielding nuisance-only residuals. These residuals are permuted, or shuffled, before adding the nuisance signal back in, creating an approximation of the data under the null hypothesis. This is then fit to the data to compute the test statistic. The process is then repeated thousands of times to generate a distribution of test statistics under the null hypothesis. If the test statistic associated with the effect of interest is significantly different from this empirical null distribution, then the null hypothesis can be rejected (Winkler *et al.*, 2014). Correction for multiple comparisons is done by recording the maximum value of the test statistic, as well as its empirical null

distribution, across all tested points in the brain. P-values corrected for familywise error can then be obtained as the proportion of the permuted test statistics that are greater than real test statistics for each test, yielding a single corrected P-value threshold. Importantly, permutation testing for the general linear model is nonparametric and performs well with heteroscedastic data (Winkler *et al.*, 2014), allowing us to analyse raw apathy and depression scores.

3.2.5. Statistical analyses

First, we assessed grey matter changes associated with apathy and depression using general linear models on the smoothed T1w images processed using the VBM pipeline (2.2.3.5). All design matrices included apathy and depression, as well as age, estimated total intracranial volume (TIV) from FreeSurfer (2.2.3.1), and an intercept. Age was included to control for age-related effects on grey matter such as incident neurodegeneration, whilst TIV was included to control for gross differences in head size (Buckner *et al.*, 2004).

For each model, either apathy or depression was treated as the primary effect of interest, with the other being treated as a covariate of no interest. This allowed us to examine grey matter correlates of apathy and depression whilst controlling for the other, alongside age and TIV. Due to the potential relevance of cognition on apathy and depression (1.2), additional models were run with MMSE score as an extra covariate alongside age and TIV.

Next, we examined white matter changes associated with apathy and depression using the TBSS-ready DWI images (2.2.3.6). Design matrices included apathy and depression, along with age and an intercept. TIV was omitted as a covariate in these analyses as it is not typically included in analyses of DWI data. As before, analyses examined correlates of apathy or depression whilst controlling for the other, and separate models including MMSE score were included to assess the effects of cognition.

Tests using the general linear model are one-sided (Friston *et al.*, 1994). Hence, separate contrast vectors were used to test both positive and negative correlations for apathy and depression, and statistical significance defined as $\alpha = 0.025$. Each analysis was conducted using 2000 permutations, and contiguous clusters of significant activation were formed using threshold-free cluster enhancement (TFCE). TFCE considers all cluster-forming thresholds, resulting in an image that summarises the evidence for a cluster at each voxel (Smith and Nichols, 2009). Our modified protocol allowed us to use 3D TFCE for TBSS data (Schwarz *et al.*, 2014), in contrast to the 2D-optimised TFCE for standard TBSS. All analyses were conducted using 'randomise' within FSL 6.0.1.

3.3. Results

3.3.1. Sample characteristics

Descriptive statistics for the sample are shown in Table 1.

Table 1. Descriptive statistics for the study population (n = 310).

Variable	RUN DMC
AES	27.3 (7.8)
CESD	10.3 (8.8)
MMSE	28.1 (2.2)
Age, years	68.9 (8.3)
Sex, female (%)	194 (58.6)
Education, years	11.2 (3.4)
WMH volume, mL	8.4 (12.2)
LI count	0.6 (1.5)

3.3.2. VBM analysis

VBM analysis revealed that apathy was negatively associated with 13 contiguous clusters of grey matter change after controlling for depression, age, and TIV (Table 2; Figure 1a). After adding in MMSE as a covariate, many of these clusters reduced in size, with some smaller ones disappearing completely (Table 3; Figure 1b). Grey matter changes occurred primarily in subcortical regions as well as the ventromedial prefrontal cortex. This included the bilateral subgenual cingulate and orbitofrontal cortices, as well as the right dorsal putamen and nucleus accumbens. Some laterality in results was also observed. Right hemisphere associations, aside from the aforementioned putamen and nucleus accumbens, also included the hippocampus and right lingual, parahippocampal, and middle temporal gyri. Left hemisphere associations included the insula, operculum, and angular gyrus.

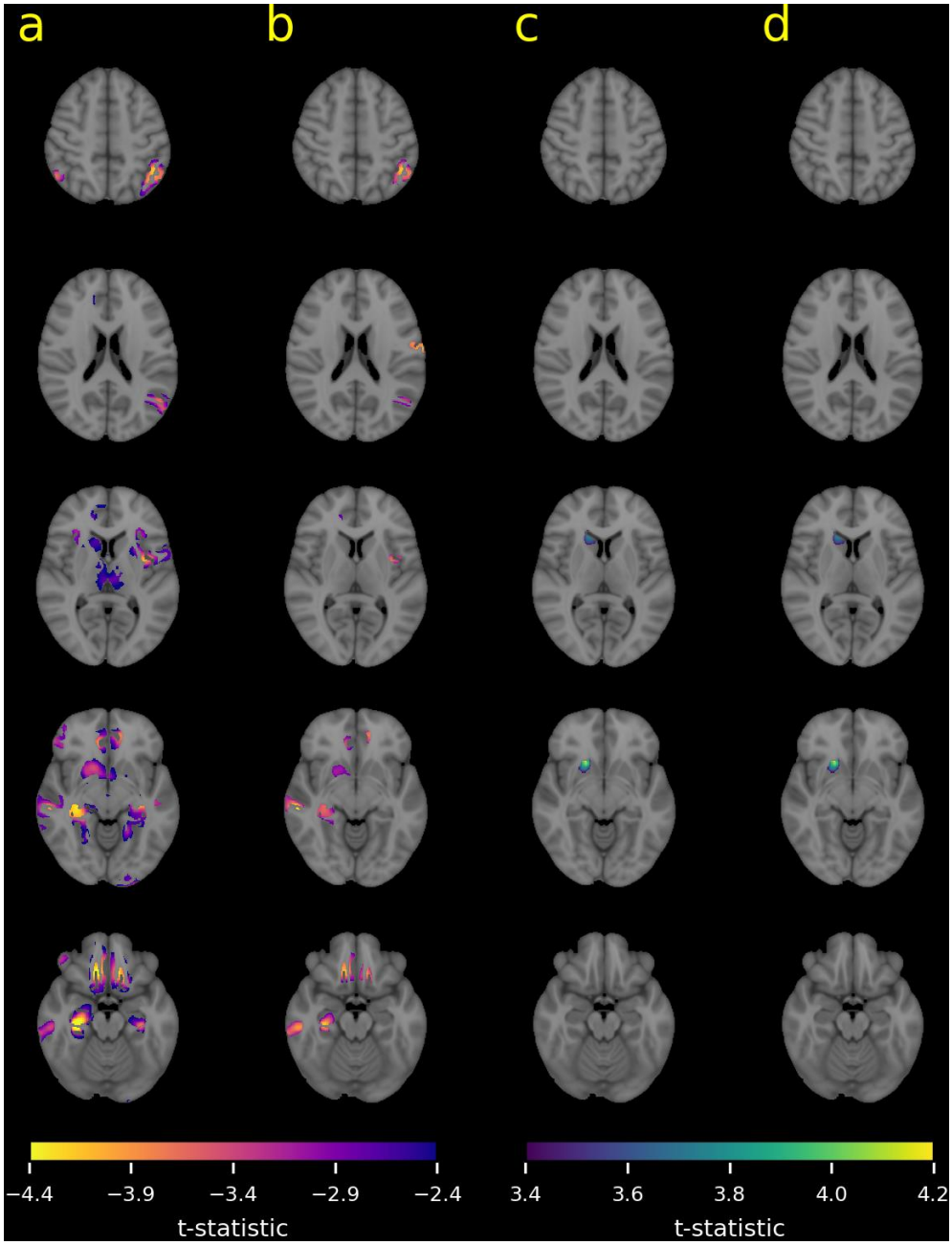

Figure 1. Grey matter correlates of apathy and depression. **a,** Clusters negatively correlated with apathy after controlling for depression, age, and total intracranial volume (TIV). **b,** Clusters negatively correlated with apathy after controlling for depression, age, cognition, and TIV. **c,** Clusters positively correlated with depression after controlling for apathy, age, and TIV. **d,** Clusters positively correlated with depression after controlling for apathy, age, cognition, and TIV.

Table 2. VBM clusters negatively correlated with apathy after controlling for depression, age, and TIV in MNI coordinates (mm).

Cluster	Voxels	t	$P_{corrected}$	X_{max}	Y_{max}	Z_{max}	X_{COG}	Y_{COG}	Z_{COG}
1	36488	5.24	<0.001	32	-25	-16	10.4	7.28	-10.5
2	8541	4.52	0.002	-43	-59	55	-46.5	-63.9	33.9
3	5241	4.43	0.002	-29	-23	-10	-26.1	-33.8	-9.78
4	4811	4.12	0.003	-34	1	9	-39.7	9.1	6.04
5	4299	4.03	0.006	61	-28	-7	58.9	-27.7	-9.64
6	2333	3.37	0.016	53	40	-9	42.4	37.8	-6.24
7	1262	3.08	0.019	-27	8	7	-24.3	8.47	1.41
8	1036	3.84	0.013	51	-55	53	47.7	-58.2	48.6
9	914	3.27	0.019	-19	-96	-3	-20.0	-99.0	-8.09
10	412	4.09	0.016	-50	-22	-3	-50.8	-22.8	-4.49
11	159	2.84	0.024	-13	-80	-14	-12.9	-78.7	-14.0
12	149	2.71	0.024	-12	-89	-13	-11.4	-91.5	-12.7
13	144	2.8	0.024	67	-48	-6	65.0	-46.8	-6.27

Note. VBM = voxel-based morphometry, COG = centre of gravity, TIV = total intracranial volume, MNI = Montreal Neurological Institute.

Table 3. VBM clusters negatively correlated with apathy after controlling for depression, MMSE, age, and TIV in MNI coordinates (mm).

Cluster	Voxels	t	$P_{corrected}$	X_{max}	Y_{max}	Z_{max}	X_{COG}	Y_{COG}	Z_{COG}
1	3935	4.27	0.003	10	26	-24	7.9	33.6	-19.0
2	3481	4.2	0.004	-45	-51	50	-47.8	-57.2	39.9
3	3186	4.32	0.004	32	-26	-15	30.1	-26.0	-12.6
4	2606	4.41	0.005	61	-27	-7	62.2	-26.4	-12.2
5	798	4.21	0.009	-9	31	-15	-8.96	36.3	-11.8
6	651	3.15	0.021	21	9	-9	17.5	10.1	-8.26
7	610	3.67	0.019	-34	0	7	-36.0	2.48	10.1
8	474	3.84	0.017	-53	1	2	-53.3	3.35	2.6
9	410	4.05	0.018	-65	-9	21	-61.2	-7.79	20.4
10	400	3.91	0.018	-11	27	-17	-11.7	25.2	-19.5

Note. VBM = voxel-based morphometry, COG = centre of gravity, MMSE = Mini-Mental State Examination, TIV = total intracranial volume, MNI = Montreal Neurological Institute.

In contrast, depression scores, after controlling for apathy, age, and TIV, were positively correlated with a single cluster of grey matter in the right caudate, dorsal putamen, and nucleus accumbens, (voxels = 2032, t = 4.16, $P_{corrected}$ = 0.008, X_{max} = 19, Y_{max} = 18, Z_{max} = -9; Figure 1c). This did not appreciably change after adding MMSE as a covariate, (voxels = 2025, t = 4.15, $P_{corrected}$ = 0.009, X_{max} = 19, Y_{max} = 18, Z_{max} = -9; Figure 1d).

3.3.3. TBSS analysis

TBSS analysis revealed that apathy, after controlling for depression and age was negatively associated with diffuse white matter damage throughout the cortex (Figure 2a). This was largely localised to a single cluster comprising 61740 voxels (Table 4). Adding MMSE score reduced the overall size of many clusters, and split the single large cluster into several smaller ones (Figure 2b, Table 5). The largest cluster identified showed peak t-values in the right splenium of the corpus callosum (forceps major), with a centre of gravity in the right anterior limb of the internal capsule. Other affected areas included the superior longitudinal fasciculi, inferior fronto-occipital fasciculi, forceps minor, external capsule, and corona radiata. In contrast, depression was neither positively or negatively associated with any white matter change regardless of the covariates included (Figure 2c,d).

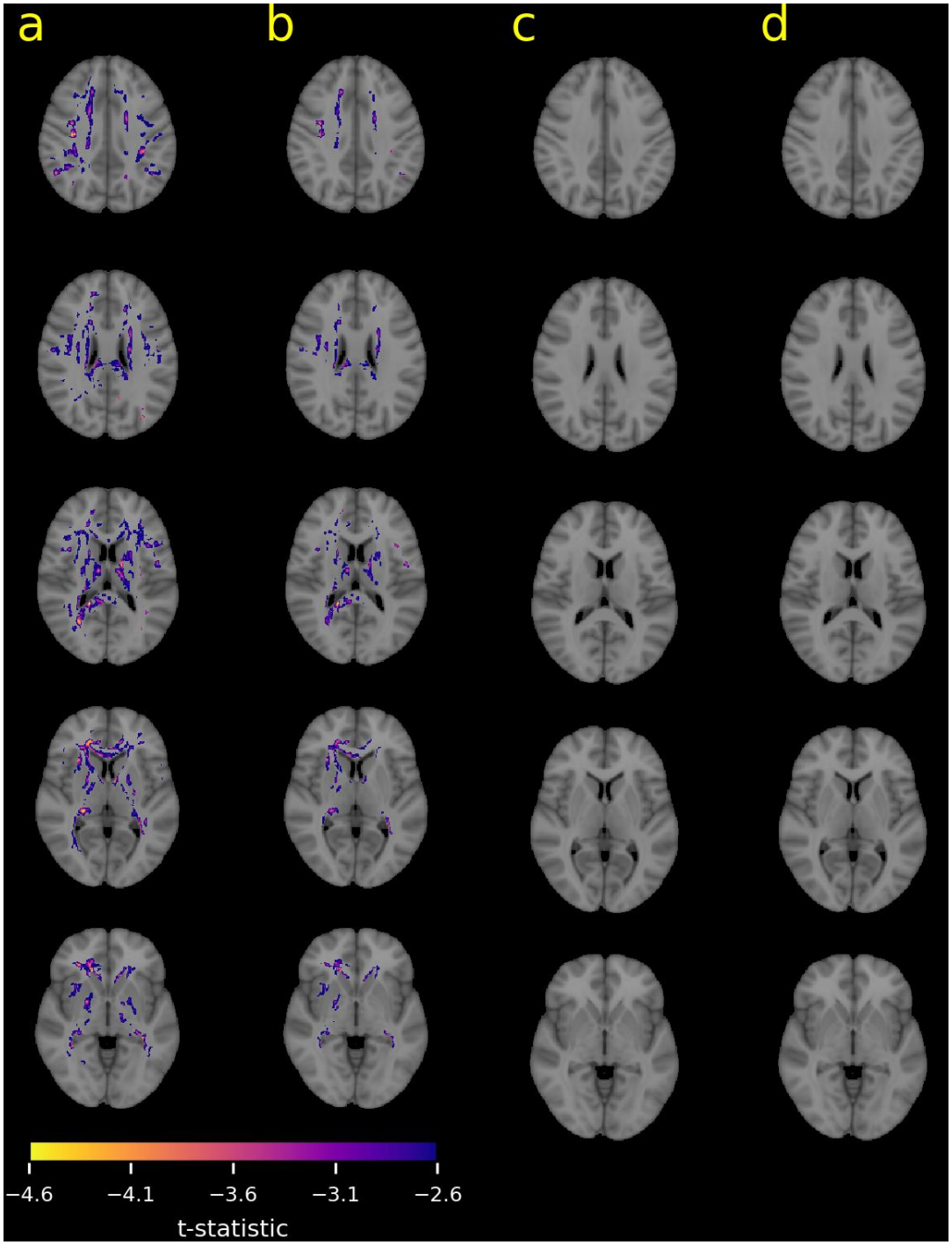

Figure 2. White matter correlates of apathy and depression. **a**, Clusters negatively correlated with apathy after controlling for depression and age. **b**, Clusters negatively correlated with apathy after controlling for depression, age, and cognition. **c**, Depression is not associated with any clusters after controlling for apathy and age. **d**, Depression is not associated with any clusters after controlling for apathy, age, and cognition.

Table 4. TBSS clusters negatively correlated with apathy after controlling for depression and age in MNI coordinates (mm).

Cluster	Voxels	t	$P_{corrected}$	X_{max}	Y_{max}	Z_{max}	X_{COG}	Y_{COG}	Z_{COG}
1	61740	5.29	0.001	34	10	18	4.55	-5.17	18.4
2	223	4.26	0.018	-32	-75	32	-33.5	-72.9	23.9
3	108	4.31	0.018	-37	-51	16	-36.8	-50.7	17.3

Note. TBSS = tract-based spatial statistics, COG = centre of gravity, MNI = Montreal Neurological Institute.

Table 5. TBSS clusters negatively correlated with apathy after controlling for depression, MMSE, and age in MNI coordinates (mm).

Cluster	Voxels	t	$P_{corrected}$	X_{max}	Y_{max}	Z_{max}	X_{COG}	Y_{COG}	Z_{COG}
1	20208	4.8	0.008	19	-44	14	13.9	-1.76	16.1
2	1078	4.11	0.016	-13	23	39	-14.3	26.5	28.7
3	558	4.59	0.015	-34	-35	0	-31.8	-39.3	1.63
4	344	4.08	0.017	28	-13	48	27.5	-18.0	47.4
5	229	3.94	0.02	-34	-41	33	-35.7	-47.2	32.1
6	169	5.08	0.015	-47	-5	17	-48.0	-4.66	15.1
7	167	4.8	0.016	-38	4	20	-38.9	0.861	20.5
8	104	3.87	0.02	-35	13	16	-37.4	13.3	15.3

Note. TBSS = tract-based spatial statistics, COG = centre of gravity, MMSE = Mini-Mental State Examination, MNI = Montreal Neurological Institute.

3.4. Discussion

We set out to examine the grey and white matter correlates of apathy in a large cohort of SVD patients. Using voxel-based methodology, we found that apathy was associated with focal grey matter damage, particularly in subcortical and frontal structures, as well as diffuse microstructural changes across the white matter of the cerebral cortex.

These patterns of brain tissue damage are remarkably consistent with neuroanatomical damage caused by SVD. Radiological markers of SVD such as lacunar infarcts are primarily

localised to subcortical structures such as the thalamus and basal ganglia (Wardlaw *et al.*, 2013), both of which were associated with apathy in this study. Furthermore, WMH, another radiological marker of SVD, may be a marker of microstructural tissue damage (Wardlaw *et al.*, 2019), which again was related to apathy in this study. This suggests that radiological markers of SVD may be an indicator of apathy.

Grey matter changes associated with apathy were found in the orbitofrontal cortex, subgenual ACC, thalamus, and ventral striatum, among others. These areas are notable because they converge with previous research examining the neural correlates of apathy across neurological diseases (Kos *et al.*, 2016), and may play important roles in decision-making and behavioural activation in healthy individuals (Le Heron *et al.*, 2018*a*). Our findings therefore support the notion that the fundamental neural substrates underlying apathy are similar across disorders, and that SVD-related grey matter changes that affect these regions are an important factor underlying apathy in these patients.

A large body of translational and transdiagnostic research suggests that these structures play important roles in nearly all aspects of behaviour. The ACC, in particular, has been conceptualised as a key hub underlying 'cognitive control', which is largely synonymous with 'executive function' (MacDonald *et al.*, 2000). These terms are quite broad, but generally refer to the cognitive processes that guide behaviour, which can include attentional control, response inhibition, and mental flexibility, among others (Miller, 2000). Unfortunately, this broad definition renders the specific role of the ACC in supporting goal-directed behaviour relatively opaque. Are these cognitive processes dissociable, and if so, which are related to motivation?

The specific role of the ACC in apathy remains a matter of debate, but one salient function of the ACC may be its role in reward-based decision-making (Silvetti *et al.*, 2014). ACC receives strong monosynaptic inputs from dopaminergic neurons in the ventral tegmental area, which may play a critical role in reward incentivisation and willingness to engage in effortful behaviours for reward (Chong *et al.*, 2015; Manohar *et al.*, 2015). Damage to ACC may result in reward insensitivity deficits, which may underlie apathy (Rochat *et al.*, 2013; Muhammed *et al.*, 2016).

The ventral striatum may share a similar role to ACC in generating motivated behaviour. This is because the ventral striatum includes the nucleus accumbens, a key component of corticostriatal reward circuitry (Haber, 2016). Dopaminergic neurons within the midbrain and nucleus accumbens play an essential role in encoding information about rewarding stimuli and behaviours, which may provide a putative substrate for reinforcement

learning (Glimcher, 2011). Damage to the ventral striatum may therefore impair an individual's ability to accurately assess the rewarding value of a stimuli, leading to certain goal-directed behaviours not appearing as worthwhile. This may impair motivation and consequently manifest as apathy.

The OFC, which was also found to be associated with apathy in our study, is also a key element of the brain's reward circuitry (Haber, 2016). Neurons in this area encode the subjective economic value of stimuli (Padoa-Schioppa and Assad, 2006), and by virtue of its inputs, may link sensory stimuli, such as food, to hedonic (pleasurable) experience (Kringelbach, 2005). Unsurprisingly, structural or functional changes to the OFC or ventral striatum have been documented as precursors to anhedonia (Der-Avakian and Markou, 2012). This loss of pleasure may also be symptomatic of apathy (Husain and Roiser, 2018), although this topic requires further investigation.

We also found that apathy was associated with thalamic damage, which is consistent with findings that apathy is a consequence of focal thalamic infarcts (Carrera and Bogousslavsky, 2006). The thalamus is similar to the ACC in that it is an important brain hub with connections to nearly all other parts of the cortex. The thalamus sends topographically organised projections to the striatum and the prefrontal cortex, and may be important for behaviours that integrate cognitive and emotional functions, such as goal-directed behaviours (Haber and Calzavara, 2009). If this is the case, then thalamic damage may not impair any one function related to motivation *per se*, but rather to the integration of those functions. This integrative failure may lead to an inability to form or execute goal-directed behaviours, manifesting as apathy.

Intriguingly, we also found that apathy was associated with focal hippocampal damage, suggesting that there is some relationship between apathy and long-term memory. This association is more plausible given that we controlled for age, which is associated with pathology such as hippocampal atrophy and memory decline (van Leijsen *et al.*, 2019). This is supported by our TBSS findings, which showed that apathy was associated with damage to the fornix, the major output tract of the hippocampus, a finding that converges with a previous study of apathy in an independent cohort of SVD patients (Hollocks *et al.*, 2015). A recently proposed theoretical framework suggests that apathy may in part be related to a failure to properly learn action-outcome contingencies from behaviour (Le Heron *et al.*, 2018*a*). In other words, individuals with apathy may not engage in rewarding behaviours simply because they do not learn which are worth performing. This may be related to reward-based learning as mentioned earlier. Unfortunately, direct evidence that supports this

assertion remains scarce, and our results should therefore be viewed as primarily correlational.

In contrast to the focal patterns of grey matter matter damage, apathy was found to be associated with widespread and diffuse white matter microstructural changes across the cortex. We found that nearly all white matter tracts were affected, including major commissural and association tracts. This is consistent with other studies of apathy in SVD (Hollocks *et al.*, 2015; Le Heron *et al.*, 2018*b*), as well as apathy in other neurological diseases such as Alzheimer's disease (Hahn *et al.*, 2013). This suggests that apathy in SVD may be a syndrome of white matter disconnection in addition to strategic grey matter damage, which is tested subsequently.

Chapter 4: Apathy is associated with disruption to large-scale white matter networks

4.1. Introduction

In the previous chapter, we found that apathy was associated with widespread white matter microstructural change, suggesting that apathy in SVD may be a syndrome of white matter network disconnection. This included damage to major commissural and association fibres, which form the basis of integrated neural circuits that underlie higher cortical functions (Schmahmann *et al.*, 2008). Similar white matter changes have been seen in other neurological conditions such as Alzheimer's disease (Kim *et al.*, 2011; Hahn *et al.*, 2013) and Parkinson's disease (Zhang *et al.*, 2018). Subtle differences in white matter microstructure may even be associated with symptoms of apathy in neurologically healthy individuals (Bonnelle *et al.*, 2015). These converging lines of evidence suggest that motivated behaviour is supported by the integrity of white matter pathways, and that apathy is a disconnection syndrome caused by damage to these pathways.

One potential limitation of previous research on the white matter correlates of apathy is that inferences have been made primarily on the basis of voxel-based morphometric techniques, such as tract-based spatial statistics (Smith *et al.*, 2006). This approach was also used to analyse apathy in the previous chapter. These methods are effective for probing the spatial distribution and extent of white matter damage, but cannot describe how connectivity and organisation of the underlying tracts are altered as a result. Elucidating the relationship between apathy and white matter topology is as important as understanding its microstructural correlates, as neural dynamics are governed by white matter architecture (Honey *et al.*, 2009). The topological properties of white matter networks can be quantitatively analysed using graph theoretical methods. This is done by describing the brain as a set of nodes (grey matter regions) that are connected by edges (white matter tracts), which can be mapped *in vivo* using diffusion tensor imaging and tractography (Hagmann *et al.*, 2008).

This graph-based representation of the brain has led to key insights into the functioning of the central nervous system (Bullmore and Sporns, 2009), and preliminary work suggests that structural network measures offer promising clinical biomarkers for cognitive decline and dementia (Lawrence *et al.*, 2014, 2018*b*). It is possible that graph

theoretical measures can also be applied to investigate the relationship between network disruption and apathy.

Here, we attempt to evaluate the hypothesis that apathy in SVD is a symptom of white matter network disruption. We also attempted to determine the specificity of these network changes by examining their associations with depression. To do so, we examined three inter-related questions. First, we investigated whether the relationship between key radiological markers of SVD and apathy is mediated by global network disruption, as has been suggested by our results in the previous chapter. Next, we attempt to determine the nature of apathy-associated network impairment by comparing various network metrics between groups of patients with apathy only, depression only, comorbid apathy and depression, and no apathy or depression. Finally, we attempt to determine where apathy-associated network disruption occurs by examining edge-wise relationships. Based on results presented in the previous chapter (3.3.3), we hypothesised that radiological markers of SVD would lead to apathy through network disruption, that patients with apathy would show reduced network metrics compared to depressed patients and controls, and that apathy would be associated with reduced connectivity in medial frontal and fronto-striatal structures.

4.2. Methods

4.2.1. Study population and measures

The study population was the Radboud University Nijmegen Diffusion tensor and Magnetic resonance imaging Cohort (RUN DMC) study which was described previously (Chapter 2). The apathy and depression measures used included the Apathy Evaluation Scale (AES) and Center for Epidemiologic Studies Depression Scale (CESD) whilst cognition was assessed using the Mini Mental State Examination (MMSE) (2.2.2). The MRI sequences used included T1-weighted (T1w) and diffusion-weighted imaging (DWI) scans (2.2.3). The data used is from the 2011 visit only (Section 3.2.1).

Of the 398 participants who attended follow-up in 2011, an additional 67 were excluded due to missing MRI data (n = 66) or failure of the tractography pipeline (n = 1), leaving 331 participants for the analysis.

4.2.2. Missing data

Some participants had missing scale data (AES, CESD, MMSE). Missing data is known to reduce statistical power, and so must be managed in some fashion. The most attractive of

these is the replacement of missing values (imputation), which allows one to leverage partially complete cases. Inference on imputed data is valid only if the missing data mechanism is ignorable, or in other words, if the data is missing completely at random (MCAR) (Rubin, 1976). In this case, there is no relationship between the observed or missing values, implying that the missing values are not conditional on another variable. This was tested using Little's MCAR test (Little, 1988*a*), which provides a test statistic indicating the deviation of the observed values to the maximum likelihood estimated population parameters. MCAR is established if the test does not yield a significant P value, as the null hypothesis is that the data is not missing in a systematic way. Little's test was not significant (χ^2= 15.018, P = 0.377), suggesting that the missing values in our data were MCAR.

Multiple imputation was carried out using the fully conditional specification (van Buuren *et al.*, 2006). In brief, a multivariate imputation model is specified on an individual variable basis. Imputations for each incomplete variable are drawn from a continuous probability distribution for that variable, which is conditional on the other variables in the data (van Buuren *et al.*, 2006). Practically, this can be broken down into six steps (Azur *et al.*, 2011):

1. All missing values are imputed using the mean as a placeholder value.
2. The placeholding values for one variable are set back to missing.
3. The observed values for the variable are regressed on all the other variables in the dataset.
4. The missing values are imputed with the predictions from the regression model.
5. Steps 2-4 are repeated for each variable with missing values.
6. Steps 2-4 are repeated for multiple cycles, with imputations being updated for each cycle.

The final imputations at the end of each sample are retained, yielding an imputed dataset.

Imputed values were generated using predictive mean matching, which draws imputed values from the observed values (Rubin, 1986; Little, 1988*b*), thus yielding "plausible" results. For example, AES totals are integer values. Predictive mean matching would impute missing AES values using observed integer scores, rather than using floating point numbers (which may be expected with imputation methods like linear regression).

Multiple imputation was implemented using the 'mice' package in R (van Buuren and Groothuis-Oudshoorn, 2010). Using the mice() function with a random number generator offset value of 1105, 100 imputations were carried out, generating 100 imputed datasets.

Then, for each missing cell in the final dataset, data was imputed using the most-frequently occurring value in the corresponding cell across the 100 complete datasets, yielding a final "likeliest" number.

4.2.3. MRI acquisition and analysis

4.2.3.1. MRI acquisition protocols

Images were acquired on a Siemens Magnetom Avanto Tim 1.5 Tesla MRI scanner (Erlangen, Germany). The protocol included a T1-weighted (T1w) three-dimensional magnetization-prepared rapid gradient echo (MPRAGE) image (repetition time (TR) = 2250 ms, echo time (TE) = 2.95 ms, inversion time (TI) = 850 ms, flip angle = 15°, voxel size = 1.0 mm x 1.0 mm x 1.0 mm), an axial fluid-attenuated inversion recovery (FLAIR) sequence (TR = 14240 ms, TE = 89 ms, TI = 2200 ms, voxel size = 1.2 mm x 1.0 mm x 2.5 mm, interslice gap = 0.5 mm), and a diffusion-weighted imaging (DWI) sequence (TR = 10200 ms, TE = 95 ms, voxel size = 2.5 mm x 2.5 mm x 2.5 mm; 7 scans with b = 0 s/mm², 61 scans with b = 900 s/mm²).

4.2.3.2. White matter hyperintensity ratings

WMH were defined as areas of hyperintense signal on FLAIR images without corresponding cerebrospinal fluid-like hypointense areas on the T1w image. Gliosis surrounding lacunar and territorial infarcts were not considered to be WMH (Hervé *et al.*, 2005). WMH were segmented on the FLAIR images using a semiautomatic method (Ghafoorian *et al.*, 2016), and were visually inspected for errors.

4.2.3.3. Lacunar infarct rating

LI were defined as hypointense areas > 2 mm and < 15 mm on FLAIR and T1w images, ruling out perivascular spaces (< 2 mm, except around the anterior commissure, where perivascular spaces can be large) and infraputaminal pseudolacunes (Hervé *et al.*, 2005). LI were counted by two trained raters blind to the clinical data, and inter-rater reliability assessed using κ (Cohen, 1960). Reliability was excellent, κ = 0.95 (van Uden *et al.*, 2015).

4.2.3.4. Brain volumetry

T1w images were processed using the 'segment' routine in SPM12 (fil.ion.ucl.ac.uk/spm/). Unified segmentation, as implemented in SPM12, alternates between three steps: image

registration, bias correction, and tissue classification. Tissue classification involves the assignment of each voxel in an image to a defined tissue class. For brain image analysis, these are usually grey matter (GM), white matter (WM), and cerebrospinal fluid (CSF). The probability of a voxel being drawn from a tissue class can be determined by its intensity and spatial distribution, which is conditional on a previously-defined population template (Ashburner and Friston, 2005). Finally, bias correction involves the correction of the bias field signal, which is caused by magnetic field inhomogeneities. This leads to a smooth, low frequency signal that corrupts MR images, resulting in the same tissue class having different intensities across the same image (Juntu *et al.*, 2005). Since these problems are interrelated, serial application of these steps can lead to the propagation of errors in downstream image processing steps. Unified segmentation attempts to solve these problems simultaneously using a single generative model, which estimates parameters by alternating between said steps (Ashburner and Friston, 2005).

Segmentation yields subject-specific tissue probability maps (TPMs), in which each voxel has been assigned a probability of belonging to a certain tissue class (Evans *et al.*, 1994). Only the first 3 TPMs were used, which correspond to GM, WM, and CSF, respectively. Volumes (in mm^3) for each tissue class were calculated as the sum of all voxels that have a probability > 0.5 on the corresponding TPM. Total brain volume (TBV) is the sum of the GM and WM volumes, while total intracranial volume (TIV) is the sum of the TBV and CSF volumes.

T1w and FLAIR images were co-registered using mutual information co-registration in SPM12. The resulting transformation was used to resample the WMH mask from the FLAIR image to the T1w image using cubic b-spline interpolation. WMH volume was then calculated as the number of the voxels under the intersection of the WMH mask and the thresholded WM TPM on the T1w image. This is then divided by the TIV to yield a proportional estimate of WMH volume (in mL), which is adjusted for individual differences in intracranial volume.

All segmentations and registrations were visually inspected for errors.

4.2.3.5. Diffusion tensor tractography

Prior to tractography, DWI images were preprocessed and the diffusion tensor fit as previously described (Section 2.2.3). Directional information within the diffusion tensor was also used to assess WM connectivity using tractography. Tractography methods attempt to reconstruct continuous WM fibre tracts (henceforth "streamlines"), under the assumption that

WM fibres are coaligned with the direction of diffusion in a WM voxel (Mori *et al.*, 1999). First, a continuous tensor field is created using the principal eigenvector of each voxel, defined as the eigenvector corresponding to the largest absolute eigenvalue (Basser *et al.*, 2000). Streamlines were initiated on an evenly-spaced 0.5 mm grid, then propagated in orthograde and retrograde directions by trilinear interpolation of the tensor field with a vector step length of 0.5 mm (Clark *et al.*, 2003). This sub-millimeter tracking (super-resolution) can reveal fibre tracts beyond the acquired imaging resolution (Calamante *et al.*, 2010). Streamlines were terminated in areas where FA ≤ 0.2, or the angle between consecutive vectors, $\theta > 45^{\circ}$ (Lawrence *et al.*, 2018*b*).

4.2.4. Graph theory and network analysis

In recent years, graph theory has emerged as the *de facto* standard for studying complex brain networks (Bullmore and Sporns, 2009). From a mathematical perspective, a graph, *G*, is a set of nodes, *N*, with a corresponding set of edges, *K*. An edge represents some relationship between any pair of nodes. *G* can therefore be represented using an *N* x *N* connectivity (or adjacency) matrix, where each entry a_{ij} is an element of *K*. Previous work using DWI to quantify brain networks has defined with *N* being defined as GM regions-of-interest (ROIs), and *K* being the number of reconstructed WM streamlines that connect them (Hagmann *et al.*, 2007). The resulting *G* can be interpreted as a whole-brain WM network, describing connectivity between all the structures in the brain. We adopt this convention here.

4.2.4.1. Network construction

Network nodes were defined using the Automated Anatomical Labeling (AAL) atlas (Tzourio-Mazoyer *et al.*, 2002), which has been used in other network-based studies in SVD (e.g., Lawrence *et al.*, 2014, 2018*b*). The AAL is a volumetric segmentation of 116 GM ROIs (58 per hemisphere) on the Colin brain in MNI space (Holmes *et al.*, 1998). Importantly, 26 of these regions were cerebellar regions, which were excluded from our analysis due to tractography being unreliable in these regions (i.e., due to complex geometry of the cerebellar decussation), leaving 90 nodes for our analysis.

The registration of the AAL atlas to each participant's DWI image was carried out using default parameters in ANTs (stnava.github.io/ANTs/). First, a linear affine transformation was used to register each participant's b0 image to their T1w image. Next, a symmetric diffeomorphic nonlinear transformation (Avants *et al.*, 2008) was used to register the T1w images to the Colin brain in MNI space. Finally, the linear and nonlinear

transformations were inverted, concatenated, then applied to the AAL image using nearest neighbour interpolation, bring the atlas image into each participant's DWI space. All registrations were visually inspected for errors.

Network edges were defined on the basis of connected node pairs. Two nodes, *i* and *j*, were connected by an edge, k_{ij}, if the endpoints of a tractography-reconstructed streamline lay between both regions. Edges were weighted, k_{ij}^{w}, by the length of the streamlines in mm, *l*, such that

$$k_{ij}^{w} = \frac{1}{2}\sum_{m=0}^{M} \quad \frac{1}{l}$$

where *M* is the set of streamlines connecting nodes *i* and *j*. Importantly, this formula scales k_{ij} to correct for the number of seeds per millimeter, as longer streamlines are seeded multiple times due to the tractography algorithm (Hagmann *et al.*, 2007; Lawrence *et al.*, 2014). Edges were then thresholded at $w_{ij} \geq 1$ to eliminate noise-related false-positives.

The result was a zero-diagonal symmetric connectivity matrix for each participant. The columns and rows of the matrix correspond to the 90 AAL ROIs, while each element of the matrix represents the corrected number of streamlines connecting each pair of ROIs. Graph theoretical quantities were then calculated.

4.2.4.2. Network measures

The density of a network is the ratio of observed edges to the total number of edges:

$$Density = \frac{2K}{N(N-1)}.$$

We also calculated measures of efficiency, which are based on the notion of shortest path lengths. The shortest path length is the path that minimises the nodes traversed to connect nodes *i* and *j*. The path length is thus a topological measure of distance between two nodes. These require a mapping of weight to distance, d_{ij}^{w}, which used the formula

$$d_{ij}^{w} = \frac{1}{w_{ij}},$$

such that higher connection weights correspond to shorter distances (Rubinov and Sporns, 2010).

Global efficiency is the average inverse shortest path length across the entire network, and reflects the overall ease of information transfer across the brain. Local efficiency, for each node, is the global efficiency, calculated using only first-degree neighbours of that node.

These are then averaged across all nodes to yield the average local efficiency, which is a measure of the average fault tolerance of a node in the brain.

Both global and local efficiency were calculated using edge weights. This is done by summing the distances associated with each edge along the shortest path length. The equation for weighted global efficiency is:

$$E^{w}_{global} = \frac{1}{n}\sum_{i \in N} \frac{\sum_{j \in N, j \neq i} \left(d^{w}_{ij}\right)^{-1}}{n-1}$$

The equation for weighted local efficiency in similar, but takes into account the weights of the connections between nodes *i* and *j*, w_{ij}, nodes *i* and *h*, w_{ih}, and the distance between nodes *j* and *h*, d^{w}_{ih}, which, in effect, quantifies the efficiency of the triangle that nodes *i*, *j*, and *h* form. This equation is:

$$E^{w}_{local} = \frac{1}{n}\sum_{i \in N} \frac{\sum_{j,h \in N, j \neq i} \left(w_{ij} w_{ih} \left[d^{w}_{jh}(N_i)\right]^{-1}\right)^{1/3}}{k_i(k_i - 1)}$$

4.2.5. Statistical analysis

Statistical analysis was carried out in R 3.4.3 (R Core Team, 2019), with supplemental functions from the psych (Revelle, 2018) and car (Fox and Weisberg, 2011) packages. Unless otherwise specified, all tests were two-tailed, statistical significance thresholded at $\alpha = 0.05$, and P values corrected for multiple comparisons using the Bonferroni-Holm method (Holm, 1979).

Descriptive statistics were used to summarise demographic and clinical information for all participants included in the study. Pearson product-moment correlation coefficients were calculated between all continuous variables.

4.2.5.1. Mediation analysis

First, we attempted to show that the relationship between SVD-related pathology and apathy was mediated by network measures. A mediation effect is when the effects of an independent variable, *X*, on a dependent variable, *Y*, is accounted for by a third, or mediating, variable, *M*. Classically, mediation models are framed using path analysis diagrams, with three paths of interest: *A*, the direct effect of *X* on *M*; *B*, the direct effect of the mediator on *Y*; and *C*, the direct effect of *X* on *Y*. The effects *A*, *B*, and *C* are tested using linear regressions.

The requirements for testing a mediation have been previously detailed, but are reproduced here. First, *X* must predict *Y*, which can be expressed as:

$$Y = \beta_{10} + \beta_{11}X + \epsilon_1, (1)$$

where β_{10} is the intercept, ϵ_1 is the error term, and β_{11} is the regression coefficient associated with *X*, which must be significant. Second, *X* must also predict *M*, such that:

$$M = \beta_{20} + \beta_{21}X + \epsilon_2, (2)$$

where β_{21} must also be significant. Third, and finally, *X* and *M* must be regressed on *Y*, such that:

$$Y = \beta_{30} + \beta_{31}X + \beta_{32}M + \epsilon_3, (3)$$

where β_{32} must be significant. For a true mediation effect, $\beta_{32} < \beta_{11}$. Since the difference between equations (1) and (3) is only the inclusion of *M*, the reduction in regression coefficients can only be explained by the mediating effect of *M*. A partial mediation effect is when β_{32} shrinks, but remains significant. A full mediation is when β_{32} shrinks and becomes non-significant.

Three mediation models were tested in the present study. The first and second models tested the mediating effect of global efficiency on the relationship between apathy and SVD markers (LI and WMH, respectively). The third model was a reverse mediation model, where WMH and LI mediated the relationship between global efficiency and apathy. A simple model for multiple mediators can be created by modifying equation 3, such that:

$$Y = \beta_{30} + \beta_{31}X + \beta_{32}M_1 + \beta_{33}M_2 + \epsilon_3, (4)$$

where M_1 and M_2 are the two mediators.

4.2.5.2. Linear regression analysis

To determine whether network integrity was related to apathy after controlling for other variables, we conducted a multiple linear regression analysis. In this model, apathy was the dependent variable, which was predicted by variables that were associated with it in our bivariate correlation analysis. Variables that remained predictors after this procedure were then carried forward as covariates for our whole-brain and regional network analyses.

4.2.5.3. Whole brain network analysis

In order to determine *how* white matter networks were disrupted in patients with apathy, a series of one-way analysis of covariance (ANCOVA) tests were used to compare the apathy only, depression only, comorbid, and control SVD groups (see section 2.2) on whole brain network measures of strength, density, global efficiency, and local efficiency (see section

2.4.2). Control variables were identified through our earlier multiple regression analysis (see section 2.5.2). Because of unbalanced group sizes, ANCOVAs were computed with type II sums of squares (Langsrud, 2003). After a significant result, between-group post hoc comparisons were conducted with the Tukey honest significant difference test.

4.2.5.4. Regional network analysis

Apathy may be characterised by a distinct structural subnetwork (i.e., a group of specific nodes and edges). In order to determine whether or not this was the case, we conducted a series of regional network analyses. In contrast to our whole-brain analysis, which investigated *how* network measures were disrupted, our regional analysis investigated *where* disruption had occurred, necessitating hypothesis testing at each edge within the connectivity matrices. Because edges are the component tested, inferences are fundamentally pairwise, as a single edge connects a pair of nodes.

Regional analyses were conducted using the Network Based Statistic (NBS) toolbox in MATLAB (Zalesky *et al.* (2010); nitrc.org/projects/nbs). The NBS implements statistical tests using the framework of the general linear model (Friston *et al.*, 1994), which has been previously detailed (Chapter 2).

The NBS starts by independently testing the hypothesis of interest at each edge with an appropriate statistical test. This endows each connection with a value of the test statistic quantifying the evidence in favour of the null hypothesis. Next, a test statistic threshold is chosen. Connections exceeding this threshold are then added to a set of supra-threshold connections. This set of connections represent the potential edges at which the null hypothesis can be rejected. Finally, topological clusters among these supra-threshold connections are identified. The basic unit of a cluster is a connected graph component (i.e., two nodes and their connecting edge). Connected graph components are a set of supra-threshold connections for which a path can be found between any two nodes.

Connected components are treated as evidence of a non-chance structure for which the null hypothesis can be rejected. In other words, a putative experimental effect is assumed to be represented by a component, rather than by a single connection or several connections that are spatially isolated from one another (Zalesky *et al.*, 2010). The experimental effect associated with this component can then be tested against the null hypothesis.

Hypothesis testing in the NBS is done by computing P values corrected for familywise error rates using permutation testing (Winkler *et al.*, 2014). The size of the largest connected component is recorded for each permutation, resulting in an empirical null

distribution for the largest component size. Component sizes can be identified in two ways: using the spatial extent of a component, which is simply the total number of significant connections it comprises, or the intensity of a component, which is the sum of all test statistic values across all connections of that component (Zalesky *et al.*, 2010). These are analogous to cluster area and mass in voxel-based statistical thresholding (Bullmore *et al.*, 1999). The resulting one-sided corrected P values are the proportion of permutations for which the largest component was of the same size or greater.

We conducted 3 regional analyses using the NBS. For the first analysis, we compared network matrices between the apathy group and the rest of the sample. Significant edges, in this context, reflect connections that differ between the apathy group and the rest of the sample. In other words, this analysis examined the unique network topology, or subnetwork, that characterised patients with apathy only.

Our second and third regional analysis leveraged our continuous scale data and large sample size by conducting multiple regression analyses in the whole sample using the full AES and CESD scales. For the second analysis, a general linear model was fitted at each edge with AES and CESD scores used as independent variables. Separate contrast vectors were specified to assess the significance of the apathy and depression regression coefficients, in both the positive and negative direction. The apathy contrast tested for a relationship between apathy and an edge while controlling for depression as a covariate and vice versa. Significant edges, in this context, reflect subnetworks that are associated with apathy after controlling for depression and vice versa. Our third analysis was similar to the second, but also included the other covariates identified in our earlier multiple regression analysis (see section 4.2.5.2).

Edges were deemed significant at $t \geq 3.1$, which corresponds to an approximate $P = 0.001$, and component sizes were determined from cluster extent, which is analogous to cluster size or area in voxel-based analyses (Bullmore *et al.*, 1999; Zalesky *et al.*, 2010). For each test, corrected P values were generated using 10000 permutation tests. As tests in the NBS are one-sided, significance levels were adjusted to $P < 0.025$ to test both tails of the distribution.

4.3. Results

Descriptive statistics for the 331 participants included in the study are presented in Table 1.

Table 1. Descriptive statistics for the study population.

Variable	RUN DMC
AES	27.3 (7.8)
CESD	10.3 (8.8)
MMSE	28.1 (2.2)
Age, years	68.9 (8.3)
Sex, female (%)	194 (58.6)
Education, years	11.2 (3.4)
WMH volume, mL	8.4 (12.2)
LI count	0.6 (1.5)
Antidepressant usage (%)	37 (11)

Note. Descriptive statistics are presented as means (standard deviation) unless otherwise noted. AES = Apathy Evaluation Scale – Clinician version; CESD = Center for Epidemiologic Studies Depression Scale; MMSE = Mini-Mental State Examination; WMH = white matter hyperintensities; LI = lacunar infarcts.

Interestingly, 11% of our sample was using antidepressants, indicating a prevalence of depression consistent with traditional samples. Importantly, this sample had a more moderate disease burden compared to other samples, with the average number of LI being < 1 and WMH burden of 8.4 mL.

Pearson product-moment correlations, with P values adjusted using Holm's method, are shown in Table 2. Due to the high magnitude of correlations between network measures (all r's > 0.85), only global efficiency was used in this analysis, in order to limit multiple comparisons.

Table 2. Pearson product-moment correlations between variables of interest.

	CESD	MMSE	Age	Education	WMH (mL)	LI count	Global efficiency
AES	0.50 (<0.001)	-0.42 (<0.001)	0.25 (<0.001)	-0.31 (<0.001)	0.23 (<0.001)	0.19 (0.006)	-0.30 (<0.001)
CESD		-0.17 (0.033)	0.07 (0.713)	-0.23 (0.001)	0.14 (0.114)	0.08 (0.713)	-0.10 (0.647)
MMSE			-0.34 (<0.001)	0.36 (<0.001)	-0.17 (0.027)	-0.10 (0.647)	0.30 (<0.001)
Age (years)				-0.10 (0.647)	0.40 (<0.001)	0.14 (0.150)	-0.58 (<0.001)
Education (years)					-0.07 (0.713)	-0.03 (0.713)	0.11 (0.426)
WMH						0.52 (<0.001)	-0.54 (<0.001)
LI count							-0.33 (<0.001)

As hypothesised, apathy was correlated with depression, cognition, and neurobiological measures such as SVD pathology and global network efficiency (Figure 1a). Network efficiency was also inversely correlated with SVD markers, implying that higher SVD burden led to lower network efficiency. Intriguingly, depression was not associated with either SVD pathology or network efficiency (Figure 1b). This suggests that depression, even at the univariate level, is distinct from apathy from a neurobiological standpoint, despite being highly correlated (at r = 0.50, so shared variance is 25%).

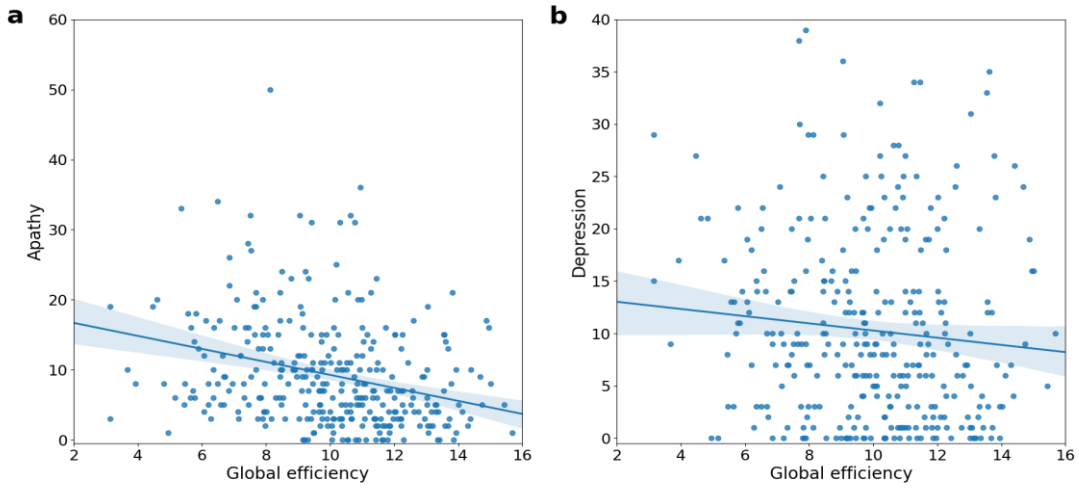

Figure 1. The relationships between apathy, depression, and global efficiency. **a,** Apathy is negatively associated with global efficiency. **b,** Depression is not associated with global efficiency.

The multiple regression analysis using all demographic and clinical variables correlated with apathy (Table 2) revealed that global efficiency remained a predictor of apathy ($\beta = -0.31$, $P = 0.028$), as did depression ($\beta = 0.16$, $P < 0.01$), cognition ($\beta = -0.259$, $P < 0.001$), and education ($\beta = -0.106$, $P = 0.024$). Age, WMH, and LI were no longer correlated (P's > 0.05), and were thus removed from the whole brain network analysis and regional network analysis.

4.3.1. Network measures mediate the relationship between apathy and SVD pathology

Results of the mediation analyses are shown in Figure 2. Path analysis models showed that the significant relationship between apathy and WMH volume ($\beta = 0.233$, $P < 0.001$), was fully mediated after controlling for global efficiency ($\beta' = 0.082$, $P = 0.205$) (Figure 2A). Similarly, LI number was related to apathy ($\beta = 0.176$, $P = 0.003$), but not after controlling for global efficiency ($\beta' = 0.077$, $P = 0.172$) (Figure 2B). In contrast, the relationship between global efficiency and apathy, ($\beta = -0.304$, $P < 0.001$), remained after controlling for both WMH volume and LI simultaneously ($\beta' = -0.244$, $P = 0.001$) (Figure 2C).

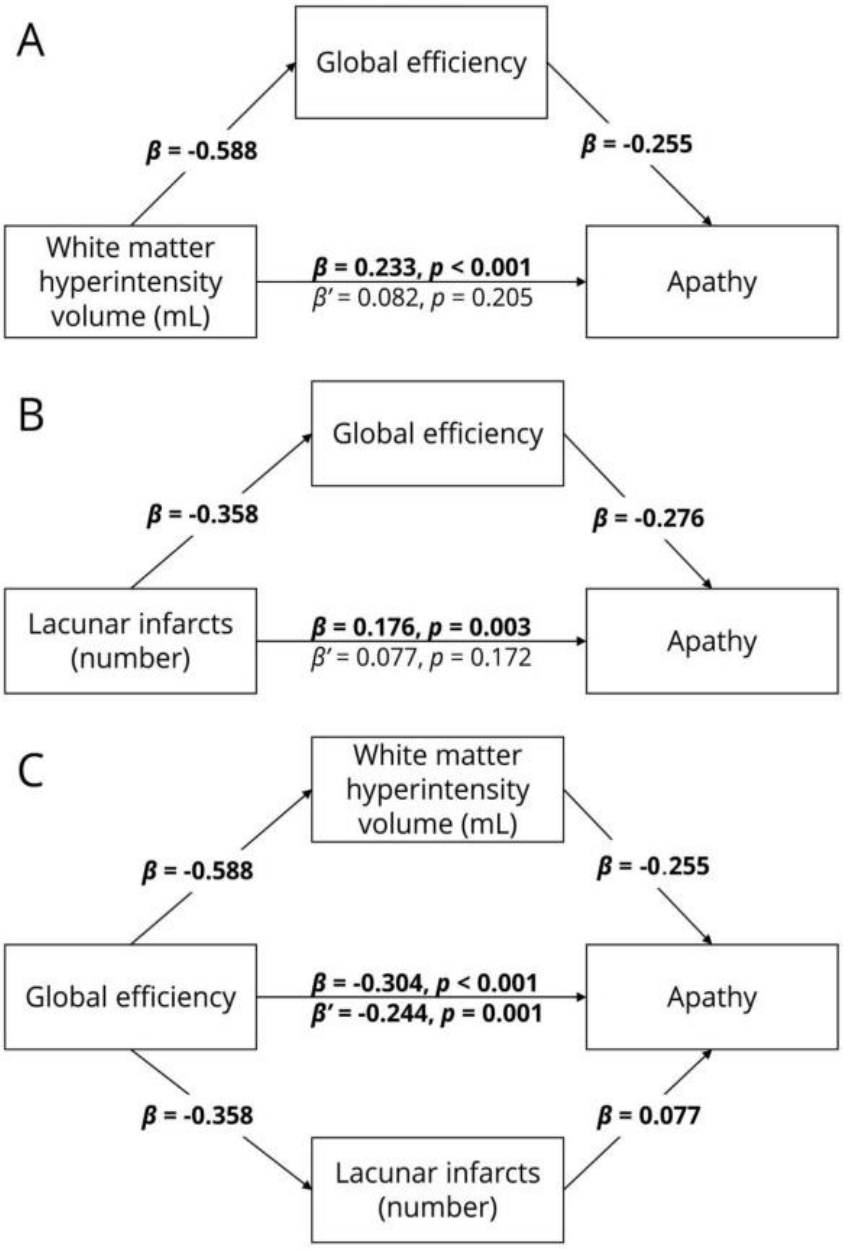

Figure 2. Results of the mediation analyses. (A) Mediating effect of global efficiency on the relationship on WMH volume and apathy. (B) Mediating effect of global efficiency on the relationship between LI number and apathy. (C) Mediating effect of WMH volume and LI number on the relationship between global efficiency and apathy. WMH = white matter hyperintensities, LI = lacunar infarcts. All numbers represent standardized beta coefficients. β = coefficient before mediation, β' = coefficient after mediation. Significant paths at $P < 0.01$ following Bonferroni-Holm adjustment are highlighted in bold.

4.3.2. Patients with apathy differ on measures of whole brain network integrity

Using established cut scores on the AES and CESD, participants were assigned to apathy (n = 26), depression (n = 48), comorbid apathy and depression (n = 32), and control SVD (n = 225) groups (Table 3). Between-group differences were found for antidepressant usage (χ^2 = 27.187, P < 0.001), but not sex (χ^2 = 4.123, P = 0.249). Antidepressant use differed between the depression and control groups (odds ratio (OR) = 0.238, P = 0.006) and comorbid and control groups (OR = 0.119, P < 0.001). The apathy group was older than both the depression and control groups (P's < 0.001). The apathy and comorbid groups had lower MMSE scores compared to the depression and control groups (P's < 0.01). The apathy and comorbid groups were less educated than the control group (P's < 0.05).

Table 3. Descriptive statistics for demographic and clinical variables of interest between groups.

Variable	Apathy group (n = 26)	Depression group (n = 48)	Comorbid group (n = 32)	Control SVD group (n = 225)	Test statistic	*P*
AES	39.5 (6.4)	27.6 (4.0)	41.2 (7.9)	23.8 (3.9)	F = 197.222	< 0.001
CESD	10.2 (4.3)	22.6 (5.2)	24.0 (6.0)	5.7 (4.5)	F = 262.968	< 0.001
MMSE	25.6 (3.8)	28.2 (1.5)	26.8 (2.7)	28.6 (1.6)	F = 23.130	< 0.001
Age, years	75.2 (7.6)	67.2 (8.6)	70.7 (7.9)	68.3 (8.1)	F = 6.933	< 0.001
Sex, female (%)	20 (77)	26 (54)	18 (56)	130 (58)	χ^2 = 4.123	0.249
Education, years	9.2 (3.3)	10.5 (3.2)	9.9 (3.3)	11.8 (3.4)	F = 7.586	< 0.001
WMH volume, mL	18.4 (21.1)	10.3 (13.4)	10.3 (15.5)	6.6 (9.1)	F = 8.791	< 0.001
LI count	1.3 (2.2)	0.8 (1.9)	0.7 (1.6)	0.5 (1.2)	F = 2.732	0.088
Antidepressant usage (%)	4 (15)	9 (19)	11 (32)	13 (6)	χ^2 = 27.187	< 0.001

Note. Descriptive statistics are presented as means (standard deviation) unless otherwise noted. AES = Apathy Evaluation Scale – Clinician version; CESD = Center for Epidemiologic Studies Depression Scale, MMSE = Mini-Mental State Examination, WMH = white matter hyperintensities, LI = lacunar infarcts.

ANCOVAs comparing whole-brain network measures revealed differences in density, global, and local efficiency whilst controlling for cognition and education (Table 4). Post-hoc tests revealed that the apathy group scored lower on all network measures compared to the control group, depression group, and comorbid group (Table 5). The depression, comorbid, and control groups did not differ on any network measure.

Table 4. One-way ANCOVAs comparing groups on whole-brain network measures.

Network parameter	Apathy group (n = 26)	Depression group (n = 48)	Comorbid group (n = 32)	Control SVD group (n = 225)	F	P
Density	0.10 (0.02)	0.11 (0.02)	0.11 (0.02)	0.12 (0.02)	4.788	0.003
Global efficiency	7.49 (2.15)	9.95 (2.72)	9.47 (2.73)	10.25 (2.37)	4.780	0.003
Local efficiency	6.51 (1.61)	7.80 (1.79)	7.46 (1.58)	7.93 (1.41)	3.120	0.026

Table 5. *P* values of pairwise *post hoc* comparisons on whole-brain network measures.

	Pairwise comparison					
Network measure	Apathy - depression	Apathy - comorbid	Apathy - control	Depression - comorbid	Depression - control	Comorbid - control
Density	**< 0.001**	**0.010**	**< 0.001**	0.840	0.976	0.530
Global efficiency	**< 0.001**	**0.013**	**< 0.001**	0.822	0.873	0.333
Local efficiency	**0.003**	0.079	**< 0.001**	0.757	0.950	0.356

Note. Significant results at $P < 0.05$ are highlighted in bold.

4.3.3. Apathy is associated with large-scale white matter network disruption

To investigate whether there were regional differences in white matter networks associated with apathy, we first performed an edgewise comparison between the apathy group and the rest of the sample. This revealed a single topological cluster, with edges connecting the bilateral supplementary motor area (SMA), t = 3.932, left SMA to left middle cingulate gyrus (MCG), t = 3.277, and left MCG to left anterior cingulate gyrus (ACG), t = 3.161 (Figure 3A).

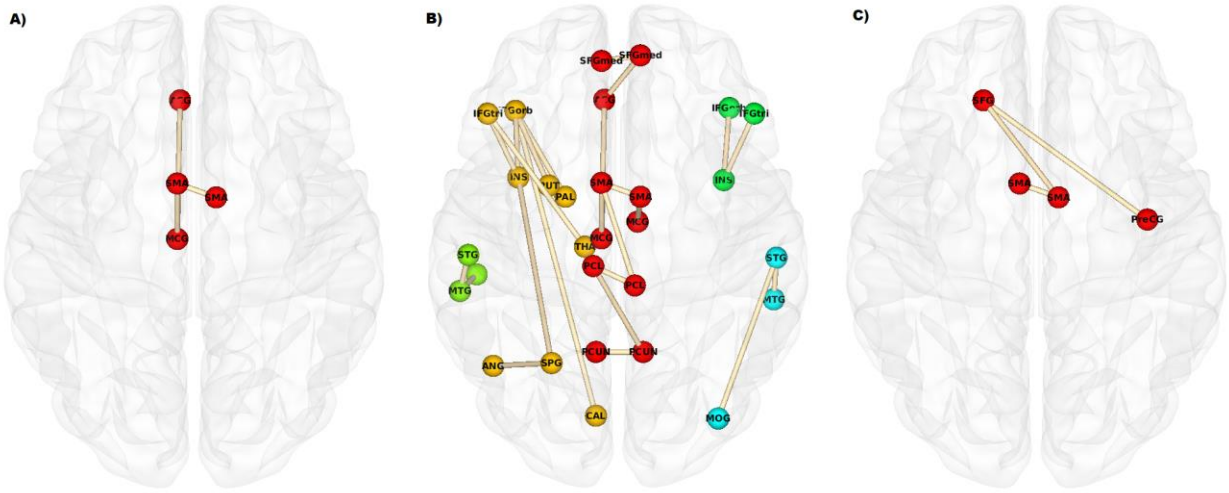

Figure 3. Topological clusters related to apathy. **A)** Cluster that differed between the apathy group and all other participants. **B)** Clusters associated with continuous apathy scores in all participants, whilst controlling for continuous depression scores. Nodes are coloured according to the unique clusters they form. See Table 6 for a full list of significant edges, grouped by topological cluster. **C)** Clusters associated with continuous apathy scores in all participants, while controlling for depression, cognition, and education. Networks were projected on the MNI152 standard space template, and visualized from the axial plane in neurological convention.

Following our comparison of the apathy only group to the rest of the sample, which yielded a significant result, we conducted an additional pairwise comparison between the apathy only and comorbid groups. This would allow us to determine whether the apathy only group had specific subnetworks that were impaired relative to the comorbid group. Both groups were compared using the same criteria as in the methods ($t > 3.1$, extent-based thresholding, 10000 permutations, $\alpha = 0.025$). No between-group regional differences were found.

We then examined edgewise correlations with continuous apathy scores while controlling for continuous depression scores, and vice-versa. Apathy was associated with five distinct topological clusters (Table 6 and Figure 3B). The first and largest cluster (red in Figure 3B) included the same structures and connections identified in the first regional analysis, as well as connections within the superior frontal and parietal lobes. The second cluster was a left-lateralized thalamo-cortico-striatal loop, which included the inferior frontal

gyrus pars orbitalis (IFGorb), insula, and putamen (gold in Figure 3B). The third cluster (yellow-green in Figure 3B) was located in the left temporal lobe. The fourth cluster included right insula and right inferior frontal gyrus (green in Figure 3B). The fifth cluster was a right-lateralised occipitotemporal circuit (cyan in Figure 3B). In contrast, the model examining depression while controlling for apathy yielded no edges.

The final analysis examined edgewise correlations with continuous apathy scores while controlling for depression, cognition, and education. This revealed a single cluster in the bilateral SMA, $t = 3.396$, right SMA and left SFG, $t = 3.135$, and left SFG to right precentral gyrus (PreCG), $t = 3.179$ (Figure 3C).

4.4. Discussion

Our study used graph theory to examine the relationship between white matter networks and apathy in patients with SVD. We found that network measures mediated the relationship between SVD markers and apathy, that patients with apathy, but not depression, had reduced whole brain measures of network density and efficiency, and that this disruption could be localised to specific structural subnetworks, which included parietal-premotor, frontostriatal, and occipitotemporal connections. Many of these connections became non-significant after controlling for general cognitive function, suggesting that apathy may share a common basis with cognitive dysfunction (Le Heron *et al.*, 2018*a*).

Using bivariate correlations, we replicated previous findings which show that WMH and LI are associated with apathy (Lavretsky *et al.*, 2008; Grool *et al.*, 2014). We were able to demonstrate that these relationships were fully mediated when controlling for whole brain measures of network efficiency. Conversely, WMH and LI only partially mediated the relationship between apathy and network measures, suggesting that WMH and LI lead to apathy through their effects on network disruption. This result suggests that the parenchymal changes associated radiological markers of SVD – which include demyelination, gliosis, and axonal loss (Gouw *et al.*, 2011) -– may lead to apathy through the disconnection of white matter networks. This contextualises previous research showing associations between apathy and radiological markers of SVD, providing a plausible underlying mechanism for the pathogenesis of apathy in this condition.

Our whole brain analysis revealed that patients with apathy had disrupted measures of network integrity when compared to all other SVD groups. In particular, whole brain networks of the apathy group had reduced network strength and density, and were less integrated on both a global and local scale. The strength and density of a network are simply

an approximation of the number of reconstructed streamlines present in the brain, and validate other work that has shown that apathy is associated with white matter microstructural damage. Global and local efficiency, on the other hand, express patterns of connectivity. A reduction in global efficiency reflects a loss of long-range connections that facilitate communication between segregated brain structures, while a reduction in local efficiency reflects a loss of short-range connections between neighbouring structures (Bullmore and Sporns, 2012). Measures of efficiency are closely related to, but are distinct from, measures of volume; axonal density within a white matter tract does not necessarily imply density between tracts. A concomitant decrease in measures of efficiency with measures of density suggests that apathy is a disconnection syndrome caused not only by a reduction in the number of streamlines, but also by a reduction in connectivity between tracts.

We also found that the depression group was not different with respect to the control group in terms of whole brain connectivity. This replicates the work of Hollocks *et al.* (2015), which was performed in a different cohort of patients with more severe SVD, characterised by symptomatic LI and confluent WMH. This does not imply that depression is not a symptom of SVD; indeed, depression was nearly twice as prevalent as apathy in our sample. It also does not imply that depression is not associated with any underlying neurobiological change. Our results suggest that the relationship between white matter microstructure and depressive symptomatology previously described in SVD (Brookes *et al.*, 2014) may be attributable to apathy, in part because measures used to assess depressive symptomatology in that study included apathy-related items (Hollocks *et al.*, 2015). However, this does not preclude depression from being associated with other measures of structural or functional integrity. For instance, previous literature has identified a robust relationship between unipolar depression and hippocampal volumes (Videbech and Ravnkilde, 2004), and studies show that depression is associated with the disruption of functional networks (Drysdale *et al.*, 2017). It is possible that depression is more strongly correlated with volumetric grey matter reduction or aberrant functional connectivity, rather than impaired white matter tract connectivity or structural network topology.

We also found that the comorbid apathy and depression group did not differ from the control SVD group. This was a surprising result, as one might expect the comorbid group to show similar, if not worse impairment, to the apathy group. Furthermore, the comorbid group had higher mean scores on the AES and CESD compared to the apathy and depression only groups. It is possible that this counterintuitive effect may be because the etiology of apathy differs between the apathy only and comorbid groups. For instance, apathy in our apathy only

group may have been the product of vascular pathology disrupting the structural networks underlying goal-directed behaviour. Apathy in our comorbid group, however, could be a product of depressive symptoms, which may not result in structural network change. Thus, despite a similar behavioural presentation, the neurobiological differences between these patients with apathy may reflect different etiologies, which may have important implications for differential diagnosis and treatment. That said, the regional between-group comparison between the apathy and comorbid group yielded no significant result, possibly due to the low sample sizes within each group. This result will need to be replicated in future studies, in order to ensure that our results did not stem from some spurious source such as sampling error. Until then, this result must be interpreted with caution.

We attempted to delineate distinct structural subnetworks associated with apathy by examining network matrices at the level of individual edges. Strikingly, significance was found in the bilateral SMA across all our analyses. First, we compared the apathy group to the rest of the sample, and found a single network consisting of the SMA and left ACG and MCG. After conducting our regression analysis, which controlled for depression, this cluster not only remained, but extended anteriorly to include the bilateral medial SFG, and posteriorly to include the bilateral paracentral lobule and bilateral precuneus. After conducting another regression while controlling for depression, cognition, and education, this cluster was reduced to a cluster spanning the bilateral SMA, left SFG, and right PreCG.

These results suggest a crucial role for the SMA in motivated behaviour. The parietal-premotor network we found in our regression analysis controlling for depression converges with the findings of Bonnelle *et al.* (2015), who investigated the functional correlates of apathy in healthy individuals. In their study, the authors found that individuals with higher levels of apathy had reduced functional activity in the SMA, ACG, and MCG as effort levels on a task increased. Furthermore, BOLD signal fluctuation in the SMA during effortful trials correlated with activity in ACG, MCG, primary motor cortex, and the superior parietal and frontal lobes, implying functional connectivity between these structures. This is supported by findings that apathy, but not depression, predicts the amplitude of SMA-localised resting-state fluctuations in patients with idiopathic Parkinson's disease (Skidmore *et al.*, 2013).

The premotor cluster we found was partially connected to a topological cluster that included superior and medial elements of the parietal lobes, including the somatosensory cortex. Importantly, these were not connected with any nodes in primary motor areas. These findings suggest that the parietal-premotor network, which has been hypothesised to underlie movement intention and awareness independently of motor execution (Desmurget and Sirigu,

2009), may play an important role in apathy. Human electrophysiological research has shown that neurons in medial premotor regions, particularly SMA, can accurately predict an impending decision to move up to hundreds of milliseconds before that decision reaches conscious awareness (Fried *et al.*, 2011). On the basis of these results, Fried *et al.* (2011) propose that volitional behaviour only occurs once neural activity in medial frontal regions reaches a certain threshold. It has been suggested that these regions transmit effort-related information directly to parietal regions, especially the somatosensory cortex (Zénon *et al.*, 2015). The findings presented in the current study suggest that the functional interactions between premotor and parietal regions are supported by a structural network consisting of white matter fibres. Pathology that damages these fibres, such as SVD, may result in the impaired activation or transmission of internally generated neural signals from premotor regions, which precede conscious decision-making (Fried *et al.*, 2011). This may cause a failure of neural ensembles to reach threshold, leading to a loss of volitional behaviour that manifests clinically as behavioural apathy.

We also identified clusters in both hemispheres that included the IFGorb, IFGtri, and INS. In the left hemisphere, this cluster also included the thalamus and parts of the basal ganglia, including the pallidum and putamen. Importantly, the putamen, as delineated by the AAL, includes portions of the nucleus accumbens (Tzourio-Mazoyer *et al.*, 2002). These structures, as well as their white matter connectivity, have been implicated in various processes that support effort-based decision-making, such as reward valuation and salience processing (Haber, 2016). Reward insensitivity has been suggested to be a factor underlying apathy in Parkinson's disease (Muhammed *et al.*, 2016), and it is possible that this generalises to SVD. If this is the case, then connections in the frontostriatal network we identified likely reflect denervation of dopaminergic projections connecting the ventral striatum to the frontal lobes. Dopamine enhances willingness to exert effort for rewards (Chong *et al.*, 2015), and indeed, apathy has been related to nucleus accumbens atrophy in Parkinson's disease patients (Carriere *et al.*, 2014). Our results suggest that apathy may, in part, be driven by disruption to the functional circuits underlying normal reward processing, leading to the inaccurate perception or valuation of stimuli which are important for approach-avoidance decision-making.

We also found bilateral topological clusters centred in the temporal lobes, with the left cluster extending to the occipital lobe. This likely reflects microstructural damage to the inferior fronto-occipital fasciculus, which has been shown in our TBSS analysis and in previous work of Hollocks et al. (2015). The functional significance of this finding is difficult

to interpret, in part because the anatomy and function of this tract remain poorly understood (Sarubbo *et al.*, 2013). However, the finding that these structures were associated with apathy in a different patient group, using different measures of apathy, makes them difficult to dismiss as false positives. Future studies are needed to investigate the relationship between the inferior fronto-occipital fasciculus and apathy.

Many of these subnetworks associated with apathy became non-significant after controlling for MMSE scores, supporting the notion that there is substantial overlap between the networks that underlie apathy and cognitive function. Unfortunately, due to the general nature of the MMSE, we could not explain specific associations between subnetworks, apathy symptoms, and cognitive domains such as executive function or processing speed. More specific analyses may be able to clarify network-specific disruption underlying cognitive symptoms, which may then lead to certain behavioural subtypes of apathy.

There were some limitations of our study. One was in our measurement of depression, which was assessed using a self-report scale rather than a structured clinical interview. Although the CESD has been shown to have good reliability and validity when compared to other scales in geriatric stroke patients (Shinar *et al.*, 1986; Agrell and Dehlin, 1989), psychometric research suggests that structured clinical interviews remain the "gold standard" for identifying depression (Stuart *et al.*, 2014), especially given an underreporting bias on some self-rated depression scales (Hunt *et al.*, 2003). Future work could more accurately diagnose patients into depressive subtypes, such as those outlined in DSM-5 (American Psychiatric Association, 2013), in order to examine if these results change. This was not feasible due to our large sample and extensive protocol, although future studies would be able to address this.

Another limitation is our method of reconstructing white matter pathways using tractography. Although the connections we identified correspond to real white matter pathways, diffusion tensor tractography has inherently limited accuracy in mapping structural connectomes, and complimentary histological and neurophysiological methods have been proposed to improve accuracy (Thomas *et al.*, 2014). In a similar vein, the AAL atlas, which we used for whole brain parcellation, is relatively coarse, with many nodes encompassing functionally heterogenous structures. Although other atlases with more fine-grained cortical parcellations exist (Glasser *et al.*, 2016), we were limited by the spatial resolution of our diffusion-weighted sequences (2.5 mm isotropic), which was partially chosen to improve the relatively low signal-to-noise ratio of images acquired at the 1.5 Tesla field strength of our MRI. This low field strength is another potential limitation on data quality, as higher field

strengths reduce uncertainty in the fitted values of the diffusion tensor (Polders *et al.*, 2011). Future studies that employ multimodal, high-resolution methods for fibre tracking may result in a more nuanced picture of the relationship between white matter topology and apathy.

A final limitation was the cross-sectional nature of our study. Due to changes in raters between the 2011 and 2015 visits, we were not able to analyse longitudinal AES scores. This means that conclusions about causality must be drawn with caution. To determine if damage to these networks leads to apathy, converging evidence from experimental neuroscience and longitudinal neuroimaging studies will be needed. Our current study was associational in nature, and as a result, we cannot firmly rule out alternative hypotheses, such as if apathy leads to changes in brain networks. Also, as we only examined apathy in the context of white matter connectivity, we can only draw conclusions about it in that regard. Further studies will be needed to examine other variables that may influence apathy, such as psychosocial factors (Marin, 1991).

In our study, we have shown that network disruption underlies the relationship between radiological markers of SVD and apathy. In addition, SVD patients with apathy have white matter networks that are sparser and less efficient when compared to other SVD patients. This includes SVD patients with depression, who were not impaired on whole brain measures of network integrity relative to control SVD patients with no apathy or depression. We also localise apathy to parietal-premotor, frontostriatal, and occipitotemporal networks. The anatomy of these networks is consistent with functional studies that show parietal-premotor regions to be associated with volitional behaviour, and frontostriatal regions to be associated with reward processing. Future studies could investigate the topology of these specific networks *a priori*, leading to focused experiments with greater statistical power. The connectivity of these white matter networks also offers a potential biomarker for detecting motivational deficits in neurological disorders.

Chapter 5: Depressive symptoms are associated with distinct patterns of cortical atrophy

5.1. Introduction

Having investigated the neurobiological basis of apathy in SVD in previous chapters (Chapters 2 - 4), we now turn our attention to depression. Depression is the leading cause of disability worldwide (World Health Organization, 2017) and a major determinant of quality of life in SVD (Hollocks *et al.*, 2015). We have shown that apathy, but not depression, appears to be more closely related white matter network changes in SVD (Chapter 3), supporting the notion that apathy, in cerebrovascular disease, is a syndrome of network disconnection. This, however, leaves a lingering question: what is the underlying neurobiology of depression?

One reproducible finding on the neurobiology of early-onset major depression is an association with focal hippocampal atrophy (Videbech and Ravnkilde, 2004). If depression is not associated with white matter network damage, then perhaps it is instead associated with focal patterns of grey matter atrophy, which also occurs as the result of SVD pathology (Lambert *et al.*, 2016). Furthermore, specific symptoms of depression, such as low mood, anhedonia, or somatic symptoms (American Psychiatric Association, 2013) may have different neural correlates, and pooling them together may attenuate results.

In the present study, we aim to investigate whether specific symptoms of depression are associated with longitudinal volumetric grey matter atrophy in SVD. First, we attempt to determine whether specific symptoms of depression are longitudinally dissociable in SVD. Next, we chart the trajectory of these symptoms in tandem with atrophy in specific grey matter regions.

5.2. Methods

5.2.1. Study population and measures

The sample investigated participants with neuroimaging data from the Radboud University Nijmegen Diffusion tensor and Magnetic resonance imaging Cohort (RUN DMC) study described previously (Chapter 2). The depression measure used was the Center for Epidemiologic Studies Depression Scale (CESD) whilst cognition assessed using the Mini Mental State Examination (MMSE) (Section 2.2.2).

Two hundred and seventy-six participants underwent MRI at all three timepoints (2006, 2011, and 2015), while 93 had MRI at two timepoints only (i.e., 2006 and either 2011 or 2015). This left a total of 369 participants with MRI assessments at more than one timepoint, with a total of 1014 MRI assessments overall. These 369 participants constituted the sample for the current analysis.

5.2.2. MRI acquisition protocol

MR images were acquired on a 1.5 Tesla MRI scanner (2006: Siemens, Magnetom Sonata; 2011 and 2015: Siemens, Magnetom Avanto). The protocol included a T1-weighted (T1w) three-dimensional magnetization prepared rapid gradient echo (MPRAGE) sequence (voxel size = 1.0 mm x 1.0 mm x 1.0 mm).

5.2.3. Freesurfer analysis

Freesurfer was used to longitudinally process T1w images. The cross-sectional steps of this pipeline have been described previously (Chapter 2). After processing all T1w images for each participant at all time points, the longitudinal stream in Freesurfer was used to obtain reliable volume and thickness estimates. This involved the creation of an unbiased participant-specific template image using a robust, inverse consistent registration of cross-sectional T1w images (Reuter *et al.*, 2010). Several steps in Freesurfer are then re-initialized using common information from the participant-specific template, thereby leveraging longitudinal information to improve the accuracy and reliability of cortical thickness estimates, resulting in increasing statistical power (Reuter *et al.*, 2012).

Freesurfer is a widely-used software suite that has been extensively validated in comparisons against manual measurements (Kuperberg *et al.*, 2003; Salat *et al.*, 2004) and histological analysis (Rosas *et al.*, 2002). Furthermore, Freesurfer shows good test-retest reliability across scanner manufacturers and field strengths (Han *et al.*, 2006; Reuter *et al.*, 2012), making it a good choice for the analysis of longitudinal T1w images in RUN DMC, due to the scanner upgrade between 2006 and 2011.

5.2.4. Correction for scanner changes

Despite using the same acquisition and processing pipeline for all T1w images, differences may still exist due to the scanner upgrade between 2006 and 2011. We therefore attempted to quantify and correct the degree of change between these timepoints, as failing to do so may lead to an over- or underestimation of volumes in 2006. For instance, underestimating

volume in 2006 may make the change from 2011 to 2015 appear steeper than it is, leading one to incorrectly conclude a non-linear (e.g., quadratic) change over time when only a linear one exists.

To do so, we compared cross-sectional estimates of total intracranial volume (TIV) derived from FreeSurfer. TIV generally increases linearly from birth until approximately the second decade of life, after which it remains fairly constant (Davis and Wright, 1977). Since an inclusion criterion in the RUN DMC study was an age of at least 50 years, TIV should remain fixed in this population throughout the duration of the study. Differences in TIV between time points should therefore only be attributable to measurement error, such as in the MRI scan or in the pipeline.

In a subset of 276 participants with MRI scanning at all 3 timepoints, we compared ratios of TIV estimates by dividing the 2006 scan by the 2011 scan, and the 2015 scan by the 2011 scan. This yielded a percentage difference for the 2006 and 2015 scans, with reference to the 2011 scan. These were then averaged across participants to estimate the total magnitude of change. We found that the difference between the 2006 and 2011 scans was +3%, while the difference between the 2011 and 2015 scans was -0.3%.

As the absolute value of these changes differed by an order of magnitude, we attempted to correct this by multiplying all estimates of volume in 2006 by 1.03, thereby proportionally increasing regional volumes. Multiplying all 2006 volumes by a constant factor, rather than a participant-specific value, allowed us to compensate for the systematic bias created by the scanner upgrade while preserving inter-participant and inter-regional variability.

5.2.5. Statistical analysis

Statistical analyses were conducted in R 3.6.1 (R Core Team, 2019). Confirmatory factor analyses utilized the lavaan 0.6-4 (Rosseel, 2012) and semTools 0.5-1 (Jorgensen *et al.*, 2018) packages, while linear mixed-effect modeling utilized the lme4 1.1-21 (Bates *et al.*, 2015) and lmerTest 3.1-0 (Kuznetsova *et al.*, 2017) packages. All tests were two-tailed, with $\alpha = 0.05$.

5.2.5.1. Confirmatory factor analysis

First, we sought to confirm the multifactorial structure of the CESD in RUN DMC. This was done using confirmatory factor analysis (CFA) in lavaan. CFA is an application of structural equation modeling (SEM). SEM is a theory-driven statistical technique that allows a

researcher to specify regression- and correlation-based relationships between observed and latent (unobserved) variables. Hence, a researcher can *a priori* specify a causal structure describing inter-variable relationships. This yields an *implied* covariance matrix, which can be compared to the real, *observed* covariance matrix, in order to provide a measure of model fit. It is important to note that causal relationships in SEM merely represent a hypothesized relationship which, if significant, can only be evidence of causality if supported by the experimental design.

CFA is a special case of SEM, whereby one or more latent factors are driving responses on a scale. The items that correspond to each factor must be specified by the user, and thus, are usually used to confirm theoretical structures.

In the present study, we attempt to confirm a recently-proposed factor structure of the CESD, as well as establish its longitudinal invariance, if any. This new factor structure is derived from the original, which proposed that the CESD loaded onto four factors: depressed affect, absence of positive affect or anhedonia, somatic activity or inactivity, and interpersonal difficulties (Radloff, 1991). This new solution drops the interpersonal factor, as only two items loaded on it, thus restricting its reliability, and eliminated a sex-related question from the depressed affect scale (17. "I had crying spells"), to avoid over-inflating estimates of depression in women (Carleton *et al.*, 2013). The remaining factors are easily interpretable, as they converge with DSM-5 criteria for major depressive disorder (American Psychiatric Association, 2013). The items on this scale can be seen in Table 1.

Table 1. Subscales on the CESD.

Item	Subscale
1. I was bothered by things that usually don't bother me.	Somatic
2. I did not feel like eating; my appetite was poor.	Somatic
3. I felt that I could not shake off the blues.	Mood
4. I felt I was just as good as other people.	Anhedonia
5. I had trouble keeping my mind on what I was doing.	Somatic
6. I felt depressed.	Mood
7. I felt that everything I did was an effort.	Somatic
8. I felt hopeful about the future.	Anhedonia
9. I thought my life had been a failure.	-
10. I felt fearful.	-
11. My sleep was restless.	Somatic
12. I was happy.	Anhedonia
13. I talked less than usual.	-
14. I felt lonely.	Mood
15. People were unfriendly.	-
16. I enjoyed life.	Anhedonia
17. I had crying spells.	-
18. I felt sad.	Mood
19. I felt that people dislike me.	-
20. I could not get "going".	Somatic

First, we attempted to establish whether or not this 3-factor model of the CESD was superior to the originally proposed 4-factor model. We did this by fitting both models longitudinally, and compared their fit indices. For the purposes of model selection, we compared the Akaike Information Criterion (AIC) and Bayesian Information Criterion (BIC), which are relative fit indices. Both the AIC and BIC estimate the amount of information explained by the model while penalizing model complexity, and for both, lower values indicate a better fitting model (Burnham and Anderson, 2004). A difference of 15 is sufficient to claim that one model outperforms another (Burnham and Anderson, 2004).

We then assessed the reliability of the 3-factor model using ω (Bollen, 1980), an estimate of internal factor consistency that relaxes assumptions about uncorrelated errors, normality, and unidimensionality, which are necessary in the more restrictive Cronbach's α (Viladrich *et al.*, 2017). ω was calculated for each subscale at each timepoint.

Next, we sought to answer whether the 3-factor solution of the CESD was longitudinally invariant. Factorial invariance has four distinct levels (Widaman and Reise, 1997):

1. Configural invariance (invariant factor structure);
2. Weak factorial invariance (invariant factor structure and loadings);
3. Strong factorial invariance (invariant factor structure, loadings, and intercepts) and;
4. Strict factorial invariance (invariant factor structure, loadings, intercepts, means, and unique factor invariances).

Configural and weak invariance are insufficient to reliably identify the same construct longitudinally, and either strong or strict invariance must hold across all times of measurement (Widaman *et al.*, 2010).

Factorial invariance was tested by fitting a series of increasingly restricted models. For the configural model, all parameters are estimated freely. For the weak factorial invariance model, item loadings are fixed, followed by intercepts for the strong factorial model.

Factorial invariance was established by comparing the fit indices of these nested models. For this comparison, we examined the confirmatory fit index (CFI) and root mean square error of the approximation (RMSEA), measures of the overall goodness- and badness-of-fit, respectively. Due to these models being increasingly restrictive, it is common for the fit of these indices to progressively worsen, as data is rarely drawn from an ideal sample. Here, it is important to examine the change in fit indices. A lack of invariance was defined as a decrease of CFI ≥ 0.010 or an increase in RMSEA ≥ 0.015 (Moreira *et al.*, 2018).

For all models, parameters were estimated using maximum likelihood estimation with robust standard errors calculated using the Huber-White method (Freedman, 2006). Test statistics were scaled to adjust for non-normal distributions using Yuan-Bentler's F-statistic (Bentler and Yuan, 1999). Missing values were incorporated into the analysis model using full information maximum likelihood, which is appropriate for longitudinal missing data (Wothke, 2000).

5.2.5.2. Missing data analysis

Some data was missing on the depression subscales, as well as for antidepressant usage, which were key variables for linear mixed-effect modeling (section 2.6.2). In order to avoid losing power, missing data was imputed using the mice package version 3.6.0 in R (van

Buuren and Groothuis-Oudshoorn, 2010). mice generates multiple imputations using the method of chained equations (van Buuren *et al.*, 2006), which is described in more detail in Chapter 2, section 2.2.1.

Imputed values were generated using predictive mean matching, which draws imputed values from the observed values (Rubin, 1986; Little, 1988*b*). As a general rule of thumb, the number of imputations generated should be proportional to the amount of missing data, so 20 imputations should be generated for 10% to 30% missing data (Graham *et al.*, 2007). Missing data points comprised 0.37% of all the data used in the present study, so 10 imputations were generated with a maximum of 10 iterations.

Linear mixed-effect models, which are subsequently described, were fit using all imputed datasets. Parameter estimates were then averaged across all models, and the total variance over repeated analyses pooled using Rubin's rules (Rubin, 1987), with degrees of freedom calculated using the Barnard-Rubin adjustment for sample size (Barnard and Rubin, 1999). Henceforth, all reported linear mixed-effect estimates refer to the estimates which were pooled across all imputed datasets.

5.2.5.3. Linear mixed-effect modeling

We used a series of linear mixed-effect models to assess longitudinal relationships between regional grey matter atrophy and depressive symptoms. A key characteristic of mixed-effect models are the ability to model both fixed (population-level) and random (participant-level) effects (Laird and Ware, 1982). The general form of a linear mixed-effect model is

$$y = X\beta + Zu + \epsilon,$$

where y, the dependent variable, is an $N \times 1$ column vector, X is an $N \times p$ matrix of p predictor variables, β is a $p \times 1$ vector of fixed effect regression coefficients, Z is the $N \times q$ matrix for the q random effects, u is a $q \times 1$ vector of random effects, and ϵ is a vector of residuals not explained by $X\beta + Zu$.

Random effects can be used to model hierarchical structures in the data, including situations where observations are not independent. In our case, observations were not independent, and hence were grouped hierarchically by participant across time. This flexible approach to modeling allows for imbalanced group sizes and missing data.

In effect, a linear mixed-effect model can estimate the longitudinal relationship between y and p, while accounting for inter-individual variability in y.

Our analysis attempted to examine how change in the grey matter volume of a region covaried with changes in specific depressive symptoms whilst controlling for age, sex, and

antidepressant use. Brain regions of interest were defined using the Desikan-Killiany parcellation of the FreeSurfer-processed T1w images (Desikan *et al.*, 2006). This took the form of linear mixed-effects models with the general formula:

$$Y_{ij}^{k} = Depression_{ij}^{l} + Antidepressant_{ij} + Age_{ij} + Sex_{i} + Zu + \epsilon,$$

where the response *Y* at area *k* for individual *i* at time *j* is estimated by the time-varying depressive symptom *l*, with *l* being either the longitudinal somatic, mood, or anhedonia subscale score. Covariates of no interest included antidepressant usage, age, sex, and with a random effect, *Zu*, of intercept-by-participant. Importantly, the scaling of volumes by timepoint and TIV simplifies this model considerably, as these terms do not need to be added as covariates for the analysis. Unfortunately, the addition of a random slope-by-time could not be added, as preliminary analyses revealed that the addition of this term led to models failing to converge or singular fit. Both of these issues are symptomatic a random-effects structure that is too complicated to estimate, and as a result, this term was not included in any model.

All linear mixed-effect estimates were chosen to minimize the restricted maximum likelihood criterion, and parameters were optimized using the Nelder-Mead simplex method (Nelder and Mead, 1965). The false discovery rate across brain regions was corrected per depressive symptom using the Benjamini-Hochberg procedure (Benjamini and Hochberg, 1995).

5.3. Results

5.3.1. Mood, anhedonia, and somatic symptoms of depression are longitudinally dissociable and reliable

Comparison of AIC and BIC values for the 3- and 4-factor models of the CESD are shown in Table 2. The 3-factor model had both a lower AIC (28058 vs. 31879) and BIC (28065 vs. 32935). The difference in AIC and BIC was > 15 (3821 and 4870, respectively), which strongly suggests that the 3-factor model should be preferred.

Table 1. Fit indices for 3- and 4-factor models of the CESD.

	3-factor model	4-factor model	Δ
df	741	1107	366
AIC	28058	31879	3821
BIC	28065	32935	4870

Note. Smaller AIC and BIC values indicate better fit.

Estimates of ω for the somatic, mood, and anhedonia subscales can be seen in Table 3. All subscales showed acceptable fit, $\omega > 75$, with stable reliability over time, with the absolute difference of ω between two adjacent timepoints < 0.07.

Table 2. ω for CESD subscales.

	Somatic	Mood	Anhedonia
2006	0.76	0.85	0.84
2011	0.81	0.81	0.79
2015	0.78	0.80	0.86

Finally, factorial invariance testing revealed that the 3-factor model met conditions for strict factorial invariance. Not only were changes within acceptable limits, all $\Delta CFI < 0.10$ and all $\Delta RMSEA < 0.015$, but the strict factorial invariance model with unique factor variance showed acceptable fit indices overall, CFI = 0.928, RMSEA = 0.036. These can be seen in Table 4. This factorial invariance testing, together with the stable values of ω, imply that the CESD subscales genuinely measure the same constructs across all timepoints within this population.

Table 3. Longitudinal factorial invariance models.

	df	Δdf	CFI	ΔCFI	RMSEA	ΔRMSEA
Configural	741	0	0.937	0.000	0.036	0.000
Loadings	763	22	0.936	-0.001	0.035	-0.001
Intercepts	785	22	0.934	-0.002	0.035	0.000
Means	791	6	0.932	-0.002	0.036	0.001
Residuals	819	28	0.928	-0.004	0.036	0.000

Note. CFI = confirmatory fit index; RMSEA = root mean square error of the approximation.

5.3.2. Depressive symptoms are modestly correlated with apathy

In a subset of 334 participants at 2011, we found that apathy was correlated with anhedonic (r = .42), mood (r = 0.38), and somatic (r = 0.46) symptoms of depression (P's < 0.001) (Figure 1).

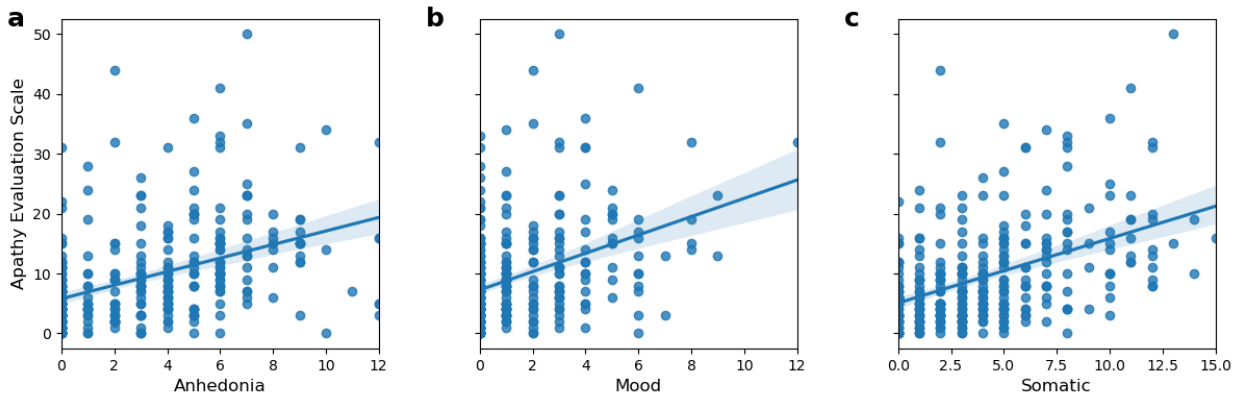

Figure 1. Association between apathy and depressive symptoms. Apathy is associated with all depressive factors, including **a,** anhedonia, **b,** mood, and **c,** somatic factors.

5.3.3. Depressive symptoms are associated with distinct patterns of brain atrophy

Linear mixed effect models revealed that, after controlling for age, sex, and antidepressant usage, each specific symptom of depression was associated with longitudinal atrophy in distinct areas. These are shown in Tables 4-6.

Table 4. Areas associated with anhedonic depressive symptoms.

Area	β (s.e.)	$P_{uncorrected}$
L ENT	-3.06e-06 (1.42e-06)	0.031
L lOFG	-7.19e-06 (2.26e-06)	0.002
L PHG	-1.98e-06 (8.92e-07)	0.027
L rACG	-2.71e-06 (9.38e-07)	0.004
L rMFG	-1.17e-05 (5.59e-06)	0.037
L SMAR	-8.61e-06 (3.76e-06)	0.022
R IPL	-1.13e-05 (4.55e-06)	0.013
R ITG	-7.88e-06 (3.33e-06)	0.018
R mOFG	-4.31e-06 (1.83e-06)	0.019
R MTG	-8.97e-06 (3.91e-06)	0.022
R pORB	-3.78e-06 (1.2e-06)	0.002
R rMFG	-1.22e-05 (6.19e-06)	0.050
R STG	-8.38e-06 (3.66e-06)	0.023
R FP	-1.74e-06 (7.86e-07)	0.027
R PUT	-6.47e-06 (2.16e-06)	0.003
R PALL	-2.45e-06 (8.74e-07)	0.005

Table 5. Areas associated with mood depressive symptoms.

Area	β (s.e.)	$P_{uncorrected}$
L ENT	-4.47e-06 (2.04e-06)	0.029
L ITG	-1.12e-05 (5.2e-06)	0.031
L lOFG	-7.44e-06 (3.31e-06)	0.025
L PHG	-3.45e-06 (1.25e-06)	0.006
L TP	-4.48e-06 (2.17e-06)	0.039
R ENT	-4.42e-06 (2.01e-06)	0.028
R ITG	-1.27e-05 (4.8e-06)	0.008
R lOFG	-6.46e-06 (3.28e-06)	0.050
R PHG	-3.12e-06 (1.05e-06)	0.003
R TP	-5.18e-06 (2.3e-06)	0.025
R HIPP	-4.63e-06 (2.21e-06)	0.036

Table 6. Areas associated with somatic depressive symptoms.

Area	β (s.e.)	$P_{uncorrected}$
L TP	-2.95e-06 (1.41e-06)	0.037
R IPL	-8.72e-06 (4.28e-06)	0.042
R ITG	-6.66e-06 (3.13e-06)	0.034
R pCC	-2.68e-06 (1.16e-06)	0.020
R preCG	-1.25e-05 (5.35e-06)	0.019
R TP	-3.84e-06 (1.51e-06)	0.011
R THAL	-5.82e-06 (2.6e-06)	0.025
R ACCU	-7.52e-07 (3.12e-07)	0.016

The somatic factor was primarily right-lateralised, and included atrophy in inferior parietal lobule (IPL), inferior temporal gyrus (ITG), posterior cingulate cortex (pCC), precentral gyrus (preCG), temporal pole (TP), thalamus (THAL), and accumbens area (ACCU). Atrophy of the left TP was also found.

The mood factor was associated with bilateral atrophy in temporal areas, including bilateral entorhinal cortex (ENT), bilateral ITG, bilateral parahippocampal gyrus (PHG), bilateral TP, and right hippocampus (HIPP). Additionally, bilateral atrophy in the lateral orbitofrontal gyrus (lOFG) was also found.

Finally, anhedonia was associated with bilateral effects across the cortex and basal ganglia. Affected regions included left ENT, left lOFG, left PHG, left rostral anterior cingulate gyrus (rACG), left rostral middle frontal gyrus (rMFG) left supermarginal gyrus (SMAR) right IPL, right ITG, right medial orbitofrontal gyrus (mOFG), right MTG, right inferior frontal gyrus pars orbitalis (pORB), right superior temporal gyrus (STG), right FP, right putamen (PUT), and right pallidum (PALL).

The full list of uncorrected associations with depressive symptoms and atrophy can be seen in Table 4. Multiple comparisons were adjusted for the false discovery rate on a per-contrast basis across all models using the Benjamini-Hochberg procedure (Benjamini and Hochberg, 1995; Abdi and Williams, 2010). Following this correction, no significant areas were found, indicating that the strength of the overall signal was weak.

5.4. Discussion

We have shown that the somatic, mood, and anhedonic symptoms of depression can be dissociated and are longitudinally reliable in patients with SVD. Furthermore, each of these symptoms are associated with overlapping and distinct patterns of grey matter atrophy over the course of 9 years.

CFA analyses suggest that the somatic, mood, and anhedonic symptoms of depression can be derived from the CESD in patients with SVD (Carleton *et al.*, 2013). Furthermore, longitudinal CFA results showed that these constructs were stable and internally consistent over nearly a decade, suggesting that the assessment of these depressive symptoms using the CESD is reliable in this population.

Analysis of longitudinal relationships between these symptoms and grey matter volumes derived from a robust longitudinal participant-specific template (Reuter *et al.*, 2012) showed that each symptom was associated with distinct patterns of atrophy. Intriguingly, all symptoms were associated with atrophy in the temporal lobes, a finding that converges with a recent report showing that temporal lobe atrophy and WMH predicted incidence of major depression over 10 years in individuals over 70 (Gudmundsson *et al.*, 2015).

Notably, this finding differs from studies on the neuroanatomical correlates of depression in adolescence and early adulthood, which generally find an association with hippocampal atrophy (Videbech and Ravnkilde, 2004). We did find an association with mood symptoms and atrophy of the right hippocampus, supporting this general finding, but we also found all symptoms to be associated with distributed atrophy across the medial temporal and lateral temporal lobes. This included the entorhinal cortex, as well as the superior, middle,

and inferior temporal gyri. This suggests that the grey matter basis of so-called "vascular depression" is a distinct entity from depression observed in early adulthood. This suggests a possible association between depressive symptoms and dementia, particularly Alzheimer's dementia, which is characterised by progressive medial temporal lobe atrophy (Pettigrew *et al.*, 2017). Supporting this is the finding that WMH and temporal lobe atrophy predicted the incidence of both depression and dementia (Pettigrew *et al.*, 2017), suggesting a common neuroanatomical basis for both syndromes. The associations between depressive symptoms and dementia in SVD are explored later (Chapter 6).

Before discussing the distinct associations found with specific depressive symptoms, it is important to think about the content validity of the items of the CESD that contributed to each. The mood subscale is readily interpretable as many items have face validity, such as the items that ask about sadness and loneliness.

The anhedonia subscale, however, was defined as a lack of positive emotion (Carleton *et al.*, 2013), in which participants did not endorse the positive items of the CESD (e.g., "I felt happy"). This item may not reflect anhedonia *per se*, which is generally defined as a loss of pleasure (American Psychiatric Association, 2013). Anhedonia is generally defined as consummatory or anticipatory, reflecting a loss of pleasure while experiencing something versus a failure to experience excitement or anticipation for future events. Some of the items on the subscale, such as those about enjoying life and feeling hopeful about the future, can be interpreted as reflecting anhedonia. The other items, however, such as feeling happy or feeling as good as other people, could be debated as reflecting mood (i.e., not endorsing these positive items could be interpreted as feeling unhappy or having feelings of worthlessness, which may reflect mood more than anhedonia). Thus, the interpretation of the anhedonia construct in this study should strictly be in terms of a lack of positive emotion, rather than a loss of consummatory or anticipatory pleasure, which is a more standard definition of anhedonia in the literature.

Finally, the somatic subscale reflects many different factors. It includes restless sleep, poor appetite, and difficulties concentrating, which are clearly defined as possible symptoms of major depression (American Psychiatric Association, 2013). Other items, however, are more difficult to classify, such as the item about being bothered about things, which may reflect irritability. Furthermore, the items about everything being an effort and being unable to get going could be thought to reflect anergia, fatigue, or even apathy. The relatively non-specific wording of these questions make it difficult to discern what construct these are truly assessing.

Despite these caveats about the definitions of each CESD subscale, however, it should be noted that our CFA revealed adequate support for these constructs, indicating that the items are genuinely grouping together empirically. This is supported by our finding that the factor structure of the CESD is stable longitudinally, with invariant loadings, intercepts, means, and residuals. If these items genuinely assessed different latent constructs, one could expect more variability within factors across time, causing a greater reduction in fit, particularly with regards to factor loadings. This did not occur, however, and so we can conclude that this 3-factor structure of the CESD has some degree of empirical validity.

A key finding was that somatic symptoms were associated with atrophy in primarily right-lateralised structures. The issue of laterality related to somatic symptoms has rarely been explored. One early report, which looked at somatic symptoms across depressive disorders, anxiety disorders, and somatization disorders found that somatic symptoms, such as pain, were primarily found in the left half of the body, implying right hemisphere lateralisation (Min and Lee, 1997). In accordance with this, we found somatic symptoms to be associated with right-lateralised atrophy in sensorimotor areas, such as IPL, pCC, preCG, and the thalamus.

Why somatic symptoms should be associated with lateralised patterns of atrophy, in contrast to the mood and anhedonic symptoms, which showed bilateral effects, is not clear. Research on lateralisation in depression suggests that hyperactivity in the right hemisphere leads to increased processing of negative emotions and pessimistic thoughts, which lead to stress and pain associated with the illness (Hecht, 2010). Pain sensitivity and negative affect may have a mutual basis in the right hemisphere (Pauli *et al.*, 1999), and if this applies to somatic symptoms in general, may explain why depression can be accompanied by aberrant sleep and appetite. Our findings give insight into the grey matter regions that may mediate these somatic symptoms, although future research will need to clarify whether these effects are domain-specific (i.e., one area to one symptom) or if atrophy in all of them is the general factor underlying all somatic symptoms.

Our findings regarding the mood factor clearly point towards an association between the temporal lobes and negative affect. Much of the work on this topic focuses on the role of the hippocampus in the pathophysiology of depression, with theoretical work suggesting many possible mechanistic links. One classic explanation that links depressive symptoms and the hippocampus is dysregulation of the hypothalamic-pituitary-adrenal axis, which leads to an elevation of cortisol levels (Byers and Yaffe, 2011). Chronically high levels of cortisol have neurotoxic effects on the hippocampus, leading to atrophy (Byers and Yaffe, 2011).

The neurotoxic effects of cortisol may explain hippocampal atrophy in depression, but less attention has been focused on general temporal lobe atrophy related to depression. Preliminary evidence using positron emission tomography (PET) to image tau *in vivo* has found modest associations between depressive symptoms and tau deposition in the inferior temporal lobes and entorhinal cortex (Gatchel *et al.*, 2017). This suggests a neurodegenerative mechanism underlying depression-related atrophy in the lateral and medial temporal lobes, which may be distinct, or have mutual influences with, depression-related hippocampal atrophy.

Related to these findings is that major depression is the most common psychiatric comorbidity with temporal lobe epilepsy (Edeh and Toone, 1987). The relationships between temporal lobe epilepsy and major depression appear to be bidirectional, and both are risk factors for one another (Forsgren and Nyström, 1990; Hesdorffer *et al.*, 2000), suggesting a shared etiology (Kessler and Price, 1993). Recent research on the shared mechanisms underlying temporal lobe atrophy and depression generally find common deficits in monoaminergic neurotransmission, particularly with ascending serotonergic and noradrenergic systems that terminate in the prefrontal cortex (Kumar *et al.*, 2016). If this is the case, then it is unsurprising that we have found bilateral patterns of atrophy in lOFG to be associated with mood symptoms *in conjunction with* temporal atrophy. That said, there are only modest associations between temporal lobe epilepsy and hippocampal atrophy (Caciagli *et al.*, 2017), and as far as we are aware, no investigations into general temporal lobe atrophy. Thus, our results support the notion of hippocampal and prefrontal atrophy being associated with negative affect.

Finally, our results with anhedonia suggested widespread atrophy throughout the cerebral cortex. This included many of the temporal areas previously mentioned, but also the left rACG, bilateral rMFG, left lOFG, right mOFG, and right pORB. These regions cover large parts of the prefrontal cortex, which in context with the atrophy found in right putamen and pallidum, suggests that mutual atrophy of basal ganglia-prefrontal regions underlies anhedonia. The neuroanatomical regions associated with anhedonia are remarkably similar to the white matter network regions associated with apathy (Chapter 3), possibly due to their high correlation. If atrophy in these basal ganglia and prefrontal structures are correlated, it might suggest the disruption of mutually trophic influences (Seeley *et al.*, 2009), which may be mediated by white matter network connectivity. If this is the case, it would be evidence to support the hypothesis of a shared neurobiology between apathy and anhedonia (Husain and

Roiser, 2018). Our work is primarily exploratory but this avenue may be explored in the future through the analysis of anatomical covariance networks (Evans, 2013).

At any rate, these findings support the notion that the emotional subtype of apathy and anhedonia share common neuroanatomical substrates, which is unsurprising given the partial overlap due to the common definitions of the two constructs (Chapter 1). Both may be the product of disrupted effort-based decision-making for rewarding outcomes (Husain and Roiser, 2018).

It is important to note that, after correcting multiple comparisons for the false discovery rate, no depressive symptom was associated with atrophy in any area. This implies an overall weak effect, which, although generally consistent with the literature on depression and atrophy (Schmaal *et al.*, 2016), implies some limitations with the cohort in question. A notable issue was the relatively small number of longitudinal observations, with about 25% of the initial cohort dropping out after baseline. This led to too few observations to adequately estimate a complex random effects structure, such as one that includes a random effect for slope-by-time. Furthermore, it may have reduced our power to detect significant associations between longitudinal atrophy and change in depressive symptoms. For these reasons, our results will need to be replicated with a larger sample, as this would not only increase power to detect true positives but also allow for the modeling of more complex random effects structures.

These weak effects may also be affected by scanner changes from 2006 to 2011. Although we attempted to compensate for this, the validity of our method has yet to be externally verified.

Another limitation, as previously alluded to, was the overall validity of the items used to assess the somatic, mood, and anhedonic symptoms of depression. Although our CFA yielded adequate support for these constructs, it should be noted that specific scales to assess these symptoms have been developed, which may yield more criterion validity than the CESD subscales we use here.

Finally, we were not able to assess change in apathy, given that our measure of apathy (Section 2.2.2) was not administered at baseline, and was administered by different raters in 2011 and 2015. As a consequence of this, we were not able to assess depression-related covariance alongside apathy, which may have substantiated our discussion about atrophy associated with somatic and anhedonic symptoms. That said, given the overlap between the content of these subscales of the CESD and apathy, our results might be viewed as a

preliminary look into what grey matter atrophy associated with apathy in SVD might look like.

We have shown that somatic, mood, and anhedonic symptoms of depression as measured by the CESD are reliable and longitudinally stable in SVD. Further, we show that these symptom dimensions are associated with atrophy in overlapping and distinct areas of the cerebral cortex. This suggests the importance of distinguishing these symptoms when examining a construct such as "depression", as neurobiological associations may be driven by specific symptom clusters.

Chapter 6: Apathy, but not depression, predicts all-cause dementia in cerebral small vessel disease

6.1. Introduction

Having investigated the neurobiology of apathy (Chapters 2 - 4) and depression (Chapter 5), we now turn our attention to their relationships with dementia. SVD is the leading vascular cause of dementia, accounting for 32% of the relationship between age and dementia risk (Power *et al.*, 2018) while playing a major role in exacerbating cognitive decline in Alzheimer's disease (Pantoni, 2010; Wardlaw *et al.*, 2013).

The most common pattern of pathology in vascular dementia is subcortical vascular encephalopathy, which is a severe form of SVD characterised by confluent WMH (Jellinger and Attems, 2010). This may lead to dementia through a disconnection syndrome, whereby WMH lead to the progressive damage of cortical and subcortical white matter tracts (Lawrence *et al.*, 2013). Additionally, single strategic lacunar infarcts may also lead to dementia when the focally damaged territory, or cortical regions connected to the infarct via white matter tracts (Duering *et al.*, 2015), play a role in cognitive function (Benjamin *et al.*, 2014). The cognitive domains affected by SVD-related pathology are primarily processing speed and executive function, with relatively preserved long-term memory (Prins *et al.*, 2005; Lawrence *et al.*, 2013). It should be noted, however, that pure vascular dementia is rare, with many post-mortem cases showing evidence of mixed pathologies in 90% to 95% of all cases (Jellinger and Attems, 2010; Thal *et al.*, 2012).

This pattern of SVD-related parenchymal damage may also underlie apathy (Chapter 5). If this is the case, then apathy may be symptomatic of a prodromal form of dementia in SVD patients. Many of the white matter network connections related to apathy in SVD overlap with those related to cognitive function (Chapter 3; (Lawrence *et al.*, 2014). In accordance with this, apathy has been found to be associated with deficits in processing speed and executive function in SVD patients (Lohner *et al.*, 2017). In contrast, depression, after controlling for apathy, has not been found to be related to cognitive deficits (Lohner *et al.*, 2017). This may be due to depressive symptoms in SVD being related to grey matter atrophy over time (Chapter 6), as opposed to focal grey matter or white matter damage.

We test the hypothesis that apathy, but not depression, predicts all-cause dementia using two independent cohorts of SVD patients: the St. George's Cognition and Neuroimaging Study (SCANS) and Radboud University Nijmegen Diffusion tensor and

Magnetic resonance Cohort (RUN DMC). We had two primary predictions: that baseline apathy, but not depression, would predict dementia after controlling for SVD-related cognitive impairment; and that longitudinal changes in apathy, but not depression, would also predict dementia.

6.2. Methods

6.2.1. Participants

6.2.1.1. SCANS

Details of the full sample have been published elsewhere (Lawrence *et al.*, 2013, 2018*b*), but are reproduced in full here for clarity. Participants were recruited between 2007 to 2010 from stroke services at 3 UK hospitals (St. George's, King's College, and St. Thomas') covering a geographically contiguous region of South London. Participants included had to have symptomatic SVD, defined as a clinical lacunar stroke syndrome (Bamford *et al.*, 1991) with magnetic resonance imaging (MRI) evidence of an anatomically appropriate lacunar infarct, which was either a high-signal lesion on diffusion-weighted imaging or a cavitated lacune on T1-weighted imaging of maximum diameter ≤ 1.5 cm. In order to recruit a cohort with moderate to severe SVD, participants also had to have confluent white matter hyperintensities (WMH) of modified Fazekas grade ≥ 2, corresponding to early confluence (Fazekas *et al.*, 1987).

Exclusion criteria included the following: any stroke mechanism other than SVD, including cortical infarcts, cardioembolic sources (Adams Jr *et al.*, 1993), intracranial or extracranial arterial vessel stenosis > 50%, or subcortical infarct diameter > 1.5 cm, as these striatocapsular-type infarcts are often embolic in nature; other major central nervous system disorders; major psychiatric diseases excepting depression; any cause for WMH other than SVD, such as multiple sclerosis; not fluent in English; MRI contraindications including claustrophobia; or unable to give written informed consent.

SCANS received ethical approval from the London–Wandsworth regional ethics committee, and the study is registered with the UK Clinical Research Network (ukctg.nihr.ac.uk; study ID: 4577). All participants provided written informed consent. All assessments were conducted a minimum of 3 months post-stroke in order to minimise the acute effects of stroke on outcomes.

One hundred and eighty patients were screened for eligibility, of whom 137 volunteered to participate. One hundred and twenty-one of the 137 patients completed the baseline assessment. Of the 16 individuals who could not complete the assessment, 6 withdrew due to the length of the neuropsychological examination, 2 were unable to complete the MRI scan, 6 became unwell between consent and the baseline visit, and 2 were found to meet exclusion criteria after being consented, 1 due to narcolepsy and 1 due to schizophrenia.

Following the baseline assessment, participants were approached for follow-up assessments annually for up to five years. Participants who subsequently experienced a new clinical stroke were allowed to remain in the study, provided the new stroke was lacunar. Of the 121 participants recruited at baseline, 18 completed only one assessment because of death (n = 7), study withdrawal (n = 6), relocation (n = 1), lost to follow-up (n = 2), or withdrawal from full neuropsychological testing (n = 2). This left 103 participants with more than one assessment for the longitudinal analysis.

6.2.1.2. RUN DMC

Details on the inclusion and exclusion criteria for RUN DMC have been documented previously (Chapter 2).

Five hundred and three participants were recruited to the baseline assessment in 2006. Of the 503 recruited, 398 were able to attend follow-up in 2011. As our apathy measure was not administered at baseline, we analyze only the 2011 data. Reasons for missing the assessment included death (n = 49), illness (n = 19), relocation (n = 5), lack of time (n = 30), or lost to follow-up (n = 2). An additional 45 were excluded due to reaching an endpoint before the 2011 assessment (n = 15), or missing data (n = 30), leaving 353 participants with complete data for the analysis.

6.2.2. Clinical assessment

6.2.2.1. SCANS

Demographic variables such as age, sex, and education were recorded. Hypertension was defined as either systolic blood pressure (BP) > 140 mmHg, diastolic BP > 90 mmHg, or use of antihypertensive medication. Hypercholesterolaemia was defined as either a random total cholesterol of > 5.2 mmol/L or use of statin medications. Smoking was defined as an ordinal variable with three categories: never smoked, former smoker, and current smoker. Diabetes mellitus was diagnosed as being on oral antidiabetic drugs or insulin treatment.

Anthropomorphic measurements were taken after the removal of shoes and bulky items of clothing, and body mass index (BMI) was defined as weight (in kg) divided by height (in m^2).

6.2.2.2. RUN DMC

Demographic variables such as age, sex, and education were recorded. Hypertension was defined as either systolic blood pressure > 140 mmHg, diastolic BP > 90 mmHg, or use of antihypertensive medication. Hypercholesterolaemia was defined as the use of lipid-lowering drugs. Smoking was defined as an ordinal variable with three categories: never smoked, former smoker, and current smoker. Diabetes mellitus was diagnosed as being on oral antidiabetic drugs or insulin treatment. Anthropomorphic measurements were taken after the removal of shoes and bulky items of clothing, and BMI was defined as weight (in kg) divided by height (in m^2).

6.2.3. Apathy and depression

6.2.3.1. SCANS

Apathy and depression were assessed using the Geriatic Depression Scale (GDS) (Yesavage *et al.*, 1982). The GDS is a 30-item self-report scale of depressive symptoms. However, recent research suggests that the GDS reflects more than just a single factor, and includes 6 items that assess apathy, rather than depression. These apathy and depression subscales of the GDS can be dissociated in SVD (Hollocks *et al.*, 2015), and reflect genuine differences in neurobiology and quality of life.

One question assessing memory (14. Do you feel you have more problems with memory than most?) was excluded in the calculation of the depression scores, as previous work has shown that this item is biased in assessments of dementia (van Dalen *et al.*, 2018*b*), leaving 23 depression-related items. The items used to make each scale are listed in Table 1.

Table 1. Apathy and depression items on the Geriatric Depression Scale.

Apathy (Cronbach α = 0.62)
2. Have you dropped many of your activities and interests?
12. Do you prefer to stay at home, rather than going out and doing new things?
19. Do you find life very exciting?
20. Is it hard for you to get started on new projects?
21. Do you feel full of energy?
28. Do you prefer to avoid social gatherings?
Depression (Cronbach α = 0.90)
1. Are you basically satisfied with your life?
3. Do you feel that your life is empty?
4. Do you often get bored?
5. Are you hopeful about the future?
6. Are you bothered by thoughts you can't get out of your head?
7. Are you in good spirits most of the time?
8. Are you afraid that something bad is going to happen to you?
9. Do you feel happy most of the time?
10. Do you often feel helpless?
11. Do you often get restless and fidgety?
13. Do you frequently worry about the future?
15. Do you think it is wonderful to be alive now?
16. Do you often feel downhearted and blue?
17. Do you feel pretty worthless the way you are now?
18. Do you worry a lot about the past?
22. Do you feel that your situation is hopeless?
23. Do you think that most people are better off than you are?
24. Do you frequently get upset over little things?
25. Do you frequently feel like crying?

In order to analyze how change in apathy and depression may relate to dementia risk, intercept and slope terms for both variables were derived from individuals who attended more than one assessment (Section 2.2.1). This was done using linear mixed-effect models, which were implemented using the lme4 package version 1.1-21 in R (Bates *et al.*, 2015). A more detailed discussion of the implementation and interpretation of linear mixed-effect models can be found in Section 5.2.5.3.

Separate linear mixed-effect models were used to predict apathy and depression, with a fixed effect of time and a random uncorrelated intercept and slope of time-by-participant being used to predict longitudinal apathy and depression scores. All estimates were chosen to optimise the restricted maximum likelihood criterion. The estimated model coefficients were used to predict participant-specific intercepts and slopes for apathy and depression, corresponding to the initial measurement and the linear change of the measurement over time, respectively.

6.2.3.2. RUN DMC

Apathy was assessed using the 18-item clinician-rated Apathy Evaluation Scale (AES) (Marin *et al.*, 1991). The AES was only administered at 2011 and 2015, precluding an analysis of baseline AES scores. However, data on progression to dementia is not available past 2015, preventing a meaningful analysis of apathy change past 2011. Additionally, AES raters changed between 2011 and 2015, further restricting an analysis of longitudinal change in apathy scores (see Chapter 2). Hence, our analysis of RUN DMC is restricted to a cross-sectional analysis of the 2011 apathy scores only.

Depression was assessed using the Centre for Epidemiological Studies Depression Scale (CESD), a 20-item self-report measure of depression (Radloff, 1977). Two items related to motivation were removed (7. I felt that everything I did was an effort; 20. I could not get "going"), leaving 18 depression-related items for the analysis.

6.2.4. Cognitive assessment

Both studies administered neuropsychological tasks sensitive to processing speed (PS). Deficits in PS are an early and prominent manifestation of vascular cognitive impairment, and are robustly associated with pathological white matter changes in SVD (Duering *et al.*, 2014). Raw scores on individual tasks were converted into age-, sex-, and education-adjusted z-scores, then averaged to produce a composite measure of PS. The administration of these tasks has been described for both for SCANS (Lawrence *et al.*, 2013) and RUN DMC (van Norden *et al.*, 2011), but the tasks and scoring used for the PS index are listed in Table 2.

Table 2. Neuropsychological tests used for processing speed index.

Neuropsychological task	Task scoring	Dataset
BMIPB Speed of Information Processing	Total correct, adjusted for motor score	SCANS
Digit Symbol Substitution	Total correct	SCANS
Grooved Pegboard Task	Time to complete (best hand)	SCANS
Paper-Pencil Memory Scanning Task	Time to complete 1-character subtask	RUN DMC
Letter Digit Substitution Test	Total correct	RUN DMC

Note. BMIPB = Brain Injury and Rehabilitation Trust Memory and Information Processing Battery.

6.2.4.1. SCANS

PS tasks included the Brain Injury and Rehabilitation Trust (BIRT) Memory and Information Processing Battery (BMIPB) (Coughlan *et al.*, 2007), the Digit Symbol Substitution Test (DSST) (Wechsler, 1997), and the Grooved Pegboard Test (Dawson *et al.*, 2010). The BMIPB is a collection of seven psychological tests that assess various aspects of cognitive function (Coughlan *et al.*, 2007), although for the purposes of assessing processing speed, only the Speed of Information Processing subtask was used. In this task, participants are presented with several rows of numbers, and are asked to cross out the second highest number in each row. After 4 minutes, the total number of correctly completed rows is used as a participant's total score. Next, participants are tested on their motor speed. They are given a page of figures, and are asked to cross out as many as possible within 25 seconds. A composite score is then created by adjusting the raw total for the motor score, thus assessing processing speed while controlling for differences in motor function.

In the DSST, participants are given two sheets: one is a test sheet with numbers and empty boxes below the numbers, while the other is a key sheet with numbers and corresponding symbols (Wechsler, 1997). The participant is then asked to fill out as many empty boxes on the test sheet with symbols that match the corresponding number from the key sheet. After 2 minutes, the total number of boxes filled out correctly is used as the participant's total score.

In the Grooved Pegboard Task, participants are given a board with pegs and grooves, and are asked to put pegs into all the grooves using a single hand (Dawson *et al.*, 2010). The grooves are randomly rotated across the board, requiring participants to rotate the pegs in their hand in order to properly fit them into the grooves. The task is first done with the

dominant hand, then again with the non-dominant hand, with the time taken to complete the task recorded for each individual hand. Although the task is typically scored by averaging the time taken to complete the task for both hands, we instead used the best score regardless of hand. This was done in order to eliminate potentially confounding unilateral motor deficits, which may be caused by strategic lacunar infarction (Steinke and Ley, 2002).

6.2.4.2. RUN DMC

PS tasks included the Paper and Pencil Memory Scanning Test (PPMST) (Brand and Jolles, 1987) and Letter Digit Substitution Test (LDST). In the PPMST, participants are given a paper showing one to four random digits (Brand and Jolles, 1987). After a 5 second delay, they are shown a matrix of 120 numbers, and are asked to cross out digits that were part of the original set. In the first round of the trial, participants are only asked to cross out a single digit. As such, the total time taken in seconds on the first round of the test is a measure of processing speed, as demands on memory are minimal.

The LDST is a modified version of the DSST (Wechsler, 1997), where symbols on the key sheet are replaced with 'over-learned' signs (Jolles *et al.*, 1995). This means that participants only need to learn the letter-digit association, rather than learning the association between a digit and an abstract symbol, which relies more heavily on working memory and complex visual perception. Similarly to the DSST, participants are scored based on the total number of boxes correctly filled.

It is important to note that several neuropsychological tests are developed and normed in a population of native English speakers, while participants in RUN DMC were primarily native Dutch speakers. In order to avoid possible language-based confounds, the PPMST and LDST were scored using norms derived from a large Dutch-speaking population (Van der Elst *et al.*, 2006; Van Der Elst *et al.*, 2007).

6.2.5. All-cause dementia diagnosis

6.2.5.1. SCANS

Dementia was defined using the DSM-5 definition of major neurocognitive disorder (American Psychiatric Association, 2013). Participants were diagnosed with dementia if they met one of the following criteria:

1. dementia was diagnosed in a memory clinic or equivalent clinical service;

2. upon blind review of all available medical records and cognitive assessments, consensus between a neurologist and clinical neuropsychologist that the clinical picture met DSM-5 criteria for major neurocognitive disorder;
3. an MMSE score < 24, which is indicative of major cognitive impairment (Tombaugh and McIntyre, 1992), as well as an Instrumental Activities of Daily Living (IADL) scale (Lawton and Brody, 1969) score ≤ 7, indicating a significant reduction in capabilities of daily living (Barberger-Gateau *et al.*, 1992).

The date of dementia was defined as the date of the diagnosis. If the exact date was not known, and the diagnosis was based on review of medical records or cognitive performance, the midpoint date between the visit at which the diagnosis was established and the previous visit was used as the date of dementia.

6.2.5.2. RUN DMC

Dementia was defined using DSM-IV-TR criteria (American Psychiatric Association, 2000), which is broadly synonymous with the DSM-5 definition of major neurocognitive disorder (Sachdev *et al.*, 2014), and was considered present if:

1. dementia was diagnosed in a memory clinic or equivalent clinical service;
2. upon blind review of all available medical records and cognitive assessments, panel consensus between a neurologist, clinical neuropsychologist, and geriatrician that the clinical picture met DSM-5 criteria for major neurocognitive disorder;
3. an MMSE score < 24 with concurrent IADL score ≤ 7.

The date of dementia was defined as the date the clinical symptoms became compatible with the diagnosis. If the exact date was unknown, such as in the case of review of medical records or cognitive assessments, the midpoint between the baseline date and the date of the diagnosis was used, or failing this, the date the patient was admitted to a nursing home because of dementia.

6.2.6. Statistical analysis

All statistical analyses were conducted using functions in R 3.6.1 (R Core Team, 2019) and the 'survival' package 2.44-1.1 (Therneau and Grambsch, 2000; Therneau, 2015). All tests were two-tailed with $\alpha = 0.05$. Analyses were conducted identically for SCANS and RUN DMC unless otherwise specified.

Relevant baseline demographic and clinical data were compared in three contexts:

1. between SCANS and RUN DMC, to assess differences between datasets;
2. between individuals who developed dementia or not *within* both datasets; and
3. between individuals who attended more than one assessment or not in SCANS, to see if any variables biased longitudinal assessments.

Continuous variables were compared using Welch's t-tests if normally distributed and Mann-Whitney U tests if not. Categorical or binary variables were compared using Pearson's χ^2 with Yates' correction for continuity.

For the multivariate dementia analyses, we had two primary questions:

1. would apathy and depression, at baseline, predict dementia?; and
2. would longitudinal change in apathy and depression be associated with dementia?

We used Cox proportional hazards regression models to answer both questions. The exponentiated regression coefficients for each covariate in a Cox model are hazard ratios (HRs), which represent the change in the dementia hazard function per unit change in the covariate following adjustment for other variables in the model (Singer and Willett, 2003). HRs <1 are protective factors, while HRs > 1 are risk factors.

To answer the first question, baseline apathy and depression scores were used to predict dementia while controlling for age, education, and PS. Event times, in years, were calculated from the first visit that apathy was assessed (SCANS: baseline; RUN DMC: 2011) until the onset of dementia, death, or the date of the most recent assessment. Individuals who did not develop dementia were right-censored.

To better visualize the role of apathy and depression in this model, covariate-adjusted Kaplan-Meier product-limit survival curves were produced after stratifying Model 1 survival estimates based on median apathy and depression scores (Therneau *et al.*, 2015).

To answer the second question, SCANS was restructured into a person-period dataset, with each case corresponding to a (start, stop] interval of time between assessments (Singer and Willett, 2003). Apathy and depression scores, as well as if the participant had developed dementia at that point, were allowed to vary between intervals. To adjust for non-independent observations, a participant-specific cluster variance was added as a term in the model.

C-statistics were used to assess the goodness-of-fit or classification accuracy of each model, and range from 0.5 (chance classification) to 1.0 (perfect classification) (Harrell *et al.*, 1996). In all models, Efron's method was used to approximate partial likelihoods for tied cases, variance inflation factors for covariates < 10, indicating minimal multicollinearity (Yoo *et al.*, 2014), and proportionality of hazards verified by non-significant variable- and

model-level scaled Schoenfeld residual tests (Therneau and Grambsch, 2000). Due to skewed distributions, depression scores were transformed using the natural logarithm in both datasets, as were apathy scores in RUN DMC. Cases with partially missing data in SCANS were excluded on a list-wise basis (Model 1: n = 3; Model 2: n = 2).

6.3. Results

Demographic characteristics of SCANS and RUN DMC are summarized and compared in Table 3. Participants in SCANS had a higher burden of vascular disease compared to those in RUN DMC, evidenced by a greater proportion of hypertension and hyperlipidemia. Consistent with this, participants in SCANS showed lower IADL scores, indicating more impairment in activities of daily living.

Table 3. Characteristics of participants included in SCANS and RUN DMC.

	SCANS (n = 121)	RUN DMC (n = 352)	P
Age	70.0 (9.7)	69.1 (8.2)	0.123
Sex, Female (%)	43 (35.5)	142 (40.3)	0.41
Education, Low/Medium/High	56 (46.7)/43 (35.8)/21 (17.5)	34 (9.7)/198 (56.2)/120 (34.1)	<0.001
Hypertension (%)	112 (92.6)	283 (80.4)	0.003
Diabetes (%)	22 (18.2)	52 (14.8)	0.575
Hypercholesterolemia (%)	104 (86.0)	175 (49.7)	<0.001
Smoking, Never/Ex/Current	48 (39.7)/49 (40.5)/24 (19.8)	103 (29.3)/205 (58.2)/44 (12.5)	0.003
BMI	27.0 (4.9)	27.8 (4.5)	0.023
MMSE	27.5 (2.7)	28.0 (2.2)	0.099
IADL	7.4 (1.2)	7.7 (1.0)	<0.001

6.3.1. Baseline characteristics of participants who developed dementia

Follow-up data on progression to dementia was available for all participants. In SCANS, 24 of 121 participants (19.8%) developed dementia, while in RUN DMC, 38 of 352 participants (10.8%) developed dementia. Comparisons between individuals who developed dementia and those dementia-free, at baseline, are shown in Table 4. In both datasets, participants with

dementia were characterized by higher apathy scale scores, but did not differ in depression scores.

Table 4. Baseline characteristics of participants who developed all-cause dementia.

	SCANS			RUN DMC		
	Dementia (n = 24)	No dementia (n = 97)	P	Dementia (n = 38)	No dementia (n = 314)	P
Age	72.1 (10.5)	69.5 (9.5)	0.189	78.5 (4.5)	68.0 (7.8)	<0.001
Sex, Female (%)	5 (20.8)	38 (39.2)	0.149	26 (68.4)	130 (41.4)	0.322
Education, Low/Medium/High	12 (52.2)/11 (47.8)/0 (0.0)	44 (45.4)/32 (33.0)/21 (21.6)	0.043	9 (23.7)/23 (60.5)/6 (15.8)	25 (8.0)/175 (55.7)/114 (36.3)	0.002
Hypertension (%)	23 (95.8)	89 (91.8)	0.804	30 (78.9)	253 (80.6)	0.982
Diabetes (%)	7 (29.2)	15 (15.5)	0.207	8 (22.2)	44 (14.6)	0.342
Hypercholesterolemia (%)	23 (95.8)	81 (83.5)	0.219	27 (75.0)	148 (49.2)	0.006
Smoking, Never/Ex/Current	9 (37.5)/9 (37.5)/6 (25.0)	39 (40.2)/40 (41.2)/18 (18.6)	0.777	8 (21.1)/23 (60.5)/7 (18.4)	95 (30.3)/182 (58.0)/37 (11.8)	0.331
BMI	25.6 (5.7)	27.3 (4.6)	0.032	26.6 (5.9)	28.0 (4.3)	0.218
Apathy	3.6 (1.7)	2.8 (1.7)	0.046	35.6 (11.6)	26.6 (7.0)	<0.001
Depression	6.4 (6.0)	5.5 (5.1)	0.527	10.3 (7.4)	8.6 (7.6)	0.142
MMSE	24.9 (3.8)	28.2 (1.8)	<0.001	24.3 (3.5)	28.5 (1.4)	<0.001
PS index	-2.0 (0.4)	-0.8 (0.8)	<0.001	-1.9 (0.5)	-1.2 (0.7)	<0.001
IADL	6.4 (2.0)	7.7 (0.7)	<0.001	6.2 (2.1)	7.9 (0.5)	<0.001

6.3.2. Longitudinal cohort characteristics

In SCANS, 104 participants attended at least one follow-up assessment over the 5-year course of the study. Comparisons of baseline characteristics between the 104 individuals and the 17 individuals who only attended one assessment are shown in Table 5. 20 of the individuals in the longitudinal cohort developed dementia (19.2%). Individuals who only attended the baseline assessment were older and more cognitively impaired, but did not differ with regards to apathy and depression scores or dementia prevalence.

Table 5. Characteristics of participants with longitudinal data in SCANS.

	Only attended baseline (n = 17)	Longitudinal cohort (n = 104)	P
Age	74.9 (8.0)	69.2 (9.8)	0.015
Sex, Female (%)	7 (41.2)	36 (34.6)	0.802
Education, Low/Medium/High	12 (70.6)/4 (23.5)/1 (5.9)	44 (42.7)/39 (37.9)/20 (19.4)	0.091
Hypertension (%)	16 (94.1)	96 (92.3)	1.000
Diabetes (%)	5 (29.4)	17 (16.3)	0.339
Hypercholesterolemia (%)	15 (88.2)	89 (85.6)	1.000
Smoking, Never/Ex/Current	9 (52.9)/6 (35.3)/2 (11.8)	39 (37.5)/43 (41.3)/22 (21.2)	0.436
BMI	27.7 (3.3)	26.9 (5.1)	0.327
Dementia	4 (23.5)	20 (19.2)	0.933
Apathy	3.0 (1.6)	2.9 (1.8)	0.982
Depression	4.9 (5.0)	5.8 (5.4)	0.500
MMSE	25.6 (3.1)	27.8 (2.5)	<0.001
PS index	-1.3 (1.0)	-0.9 (0.9)	0.074
IADL	6.9 (1.7)	7.5 (1.1)	0.075

6.3.3. Multivariate Cox regression analyses

The results of all multivariate Cox regressions are shown in Table 6. Model 1, which evaluated baseline apathy and depression scores in predicting dementia in both datasets, showed that higher apathy scores were associated with an increased dementia risk in SCANS, as were log-transformed apathy scores in RUN DMC, even after controlling for age, education, and PS. In contrast, log-transformed depression scores in both datasets were not associated with dementia.

Table 6. Multivariate Cox regression models predicting all-cause dementia.

	SCANS			RUN DMC		
	HR	95% CI	P	HR	95% CI	P
Model 1	C = 0.904 (0.022)			C = 0.914 (0.019)		
Apathy	1.49	1.05-2.11	0.024	5.64	1.38-23.03	0.016
Depression	1.18	0.59-2.37	0.638	0.92	0.65-1.32	0.664
Age	1.07	1.00-1.14	0.047	1.17	1.11-1.23	<0.001
Education	0.92	0.42-2.03	0.844	0.68	0.39-1.18	0.166
PS	0.03	0.01-0.12	<0.001	0.27	0.13-0.54	<0.001
Model 2	C = 0.937 (0.027)					
Apathy	1.53	1.08-2.17	0.017			
Depression	0.65	0.10-4.38	0.654			
Age	1.21	1.02-1.45	0.033			
Education	4.00	1.50-10.70	0.006			
PS	0.00	0.00-0.03	<0.001			

Note. Model 1 tests apathy and depression at baseline, whilst Model 2 tests longitudinal change in apathy and depression scores.

To evaluate whether the addition of apathy increased the utility of these models for predicting dementia, apathy was removed from the model, which was then re-run using only depression, age, education, and PS as covariates. Since this alternative model was nested within Model 1, both models could be compared using likelihood ratio tests. These revealed that the inclusion of apathy led to improved model fit in both SCANS (χ^2=5.30, P=0.021) and RUN DMC (χ^2=5.67, P=0.017).

Results in Model 1 were consistent for Model 2, which analyzed longitudinal apathy and depression in SCANS. Increasing apathy over time was associated with a greater dementia risk, but not depression. C-statistics for all tested models were excellent ($C \geq 0.90$).

In order to better illustrate the impact of apathy and depression on dementia risk, Model 1 was re-run using median apathy and depression scores. Covariate-adjusted Kaplan-

Meier survival curves visually demonstrated that higher apathy scores were consistently associated with a greater dementia risk over time in both SCANS and RUN DMC (Figure 1A), while depression scales showed more mixed results (Figure 1B).

6.4. Discussion

In two independent cohorts of SVD patients, we showed that higher baseline apathy scores, as well as increasing apathy over time, were associated with an increased dementia risk. In contrast, baseline depression scores, as well as change in depression, did not predict dementia, highlighting the importance of distinguishing between these symptoms. The relationship between apathy and dementia remained even after controlling for age, education, and cognition, which are well-established risk factors for dementia (Barnes *et al.*, 2009). Furthermore, the addition of apathy to a model with terms for age, education, and cognition led to a better model fit. This suggests that apathy may have some utility in building predictive models for dementia, and can still be useful clinically even after a detailed cognitive assessment. These results support the hypothesis that apathy, but not depression, may be a prodromal symptom of dementia in patients with SVD.

A major strength of the study was that our findings were replicated in two independent cohorts, which were recruited at different centers, had differing levels of SVD pathology, and were assessed using different measures of apathy and depression. SCANS, by virtue of its inclusion criteria, had a higher burden of SVD pathology when compared to RUN DMC. This was reflected in a higher proportion of vascular risk factors such as hypertension and hyperlipidemia, as well as more severe impairment in activities of daily living. This may explain why the prevalence of dementia was nearly double in SCANS compared to RUN DMC (19.8% vs 10.8%) despite similar dementia criteria and follow-up durations. The fact that our findings converged in these two different populations, with RUN DMC representing a more general population with mild SVD and SCANS representing symptomatic patients with more advanced SVD, suggests that these results may be generalizable to individuals with a broad range of pathology.

Our results, at first glance, appear to diverge with recent findings from the Prevention of Dementia by Intensive Vascular Care (PreDIVA) trial, which showed that apathy and depression, assessed by an abbreviated form of the GDS, predicted incident dementia in a large sample of community-dwelling individuals (van Dalen *et al.*, 2018*b*). The investigators, however, found that the associations between depression and dementia were largely driven by the GDS item that assessed memory complaints. After removal of that item from the

calculation of depression scores, which we have done *a priori*, this association was no longer significant. Furthermore, the authors also found that an interaction between apathy and a history of stroke predicted incident dementia. This interaction may partially have been driven by SVD patients with lacunar stroke, which was explored in our study. Our results therefore converge with those in the PreDIVA trial, and may also partially contextualize their findings regarding individuals with cerebrovascular disease.

These findings may also clarify why there are inconsistent reports of associations between late-life depression or depressive symptoms and dementia risk (Byers and Yaffe, 2011). Clinical scales that assess depressive symptoms may also assess apathy, as evidenced by motivation-related questions on the GDS and CESD, the depression scales used in our study. These apathy items may be a factor underlying the relationship between depressive symptoms and dementia in the elderly. This is an important consideration for future studies that utilize clinical scales for measuring depression. We found that the removal of apathy-related items from longer depression scales ($\geq$ 20 items) is unlikely to have a serious effect on internal consistency (Hollocks *et al.*, 2015), suggesting that removing these items is a valid approach for assessing a more 'pure' depression construct. It is important to note that this only applies to depressive *symptoms*, rather than depressive *syndromes*, which may include apathy items by definition (American Psychiatric Association, 2013).

The number of people living with dementia worldwide has been projected to triple by 2050 (Prince *et al.*, 2013), making the issue of early diagnosis and intervention increasingly important. Recent evidence suggests that late-life cognitive functioning can be maintained or improved by targeting modifiable factors such as cardiovascular risk, physical activity, and diet (Ngandu *et al.*, 2015). Our results support the notion that measuring apathy may be clinically useful as a non-invasive, inexpensive, and easily implementable method for identifying patients at-risk for developing dementia (van Dalen *et al.*, 2018*b*). Additionally, our longitudinal findings suggest that continued monitoring of apathy may be a way to assess changes in dementia risk. Individuals identified as having high apathy, or increasing apathy over time, could be sent for a more detailed neurocognitive or neuropathological examination, or be selected for behavioral or pharmacological interventions.

Our work also suggests that another area for future research lies in identifying the mechanisms linking apathy to dementia onset. Recent neuroimaging work in sporadic and genetic SVD suggests that similar white matter networks underlie motivation and normal cognitive function (Le Heron *et al.*, 2018*b*; Tay *et al.*, 2019). It is possible that cerebrovascular pathology that damages these networks leads to a prodromal form of

dementia which presents with apathy and cognitive deficits. Over time, SVD-related pathology increases (van Leijsen *et al.*, 2019), which is paralleled by increasing cognitive and motivational impairment (Brodaty *et al.*, 2013), eventually becoming severe enough to meet criteria for a dementia state. This implies that apathy is not a risk factor for dementia *per se*, but rather, an early symptom of white matter network damage.

Treating apathy is an important issue in itself, as apathy is detrimental to quality of life (Hollocks *et al.*, 2015). Preliminary evidence suggests that post-stroke patients treated with escitalopram, a selective serotonin reuptake inhibitor, were three times less likely to develop apathy a year after the stroke when compared to those on placebo (Mikami *et al.*, 2013*a*), although longer follow-up with a larger sample is necessary. Treating apathy in individuals who have already developed it is another major concern, with recent pharmacological and behavioral interventions showing mixed or negative results (Skidmore *et al.*, 2015; Starkstein *et al.*, 2016). There is an urgent need for high-quality randomized controlled trials to address this.

It is possible that dropout rates in SCANS may have affected longitudinal estimates of apathy. By definition, apathy is a reduction in motivation, and highly apathetic individuals may have been more likely to not attend sessions after the initial baseline visit. As a consequence of this, the 103 individuals included in the longitudinal analysis may have been a self-selecting population of individuals with lower apathy scores overall. This may have led to HRs that were systematic underestimates of the true association between apathy and dementia risk.

Finally, it should be noted that all dementia cases were defined on the basis of clinical results, rather than on the basis of any neuropathological examination. This is a limitation in the sense that we cannot claim to have found an association between apathy and pathologically confirmed dementia. We have, however, found an association between apathy and a *clinical presentation consistent with dementia*. This suggests that our results may be clinically applicable, and as stated before, that apathy may be used as a rapid screening tool to select individuals who will later undergo a more detailed examination for a pathologically confirmed diagnosis of dementia. This can then be combined with an accurate diagnosis of dementia subtype (e.g., pure vascular dementia, Alzheimer's dementia, etc.) to gauge the true association between apathy and dementia.

Our work has shown that apathy, but not depression, predicted all-cause dementia in SVD, supporting the hypothesis that apathy is a prodromal symptom of dementia. This shows that distinguishing between these symptoms has important implications for clinical practice

and research. It also suggests that apathy may be useful in predictive models of dementia, and that the assessment of apathy over time may be informative for dementia diagnosis. Finally, it paves the way for future studies attempting to understand the mechanisms underlying apathy, vascular cognitive impairment, and dementia.

Chapter 7: General conclusion

7.1. Main findings

This thesis has attempted to explore the underlying neurobiology of apathy and depression in patients with cerebral small vessel disease (SVD). First, we reviewed the constructs of apathy and depression, highlighting their similarities and differences, as well as the impact of apathy on functional outcomes (Chapter 1). We also present a network neuroscience framework for investigating apathy in cerebrovascular disease (Chapter 1). The primary cohort used in the thesis, the Radboud University Nijmegen Diffusion tensor and Magnetic resonance Cohort (RUN DMC), was then briefly introduced (Chapter 2). We then explored the structural basis of potential network changes by examining grey and white matter correlates of apathy and depression (Chapter 3). We found that apathy was associated with focal grey matter damage and distributed white matter damage, whilst depression was associated with focal grey matter change in the basal ganglia and not associated with white matter change. We then showed that apathy, but not depression, was associated with large-scale white matter network damage, and that SVD pathology led to apathy through network damage (Chapter 4). Following our finding that depression was associated with grey matter changes, we then explored longitudinal correlations between regional grey matter volumes and the anhedonic, somatic, and mood symptoms of depression (Chapter 5). We found that these symptoms of depression had partially overlapping but distinct correlates, possibly explaining the differential expression of these symptoms. was associated with increased dementia risk in SVD patients, possibly owing to these different neurobiological etiologies (Chapter 6).

One consistent finding throughout this work was the contrast between focal grey matter changes and distributed white matter changes. Apathy and depression may be associated with the former, but apathy alone appears to be associated with the latter. This is likely a reflection of the pathological processes underlying SVD, which can result in both focal infarcts or diffuse white matter changes (Wardlaw *et al.*, 2019). With regards to focal grey matter damage, apathy appeared to be associated with primarily subcortical and prefrontal changes (Chapter 3), consistent with known lacunar infarct distributions and associated cortical thinning (Wardlaw *et al.*, 2013; Duering *et al.*, 2015). In contrast, depression was associated with atrophy in temporal structures (Chapter 5), which are generally spared from the effects of SVD (Lambert *et al.*, 2016). This may well suggest a different etiology for depression in SVD that can be partially attributable to other pathologies

such as Alzheimer's disease, which is known to be co-morbid with cerebrovascular pathology (Power *et al.*, 2018).

In contrast to this, apathy alone was found to be associated with widespread white matter damage, suggesting that goal-directed behaviour is supported by large-scale integrated networks (Chapters 3 and 4). It is therefore unlikely that any one area underlies motivation, although some structures may serve as important hubs for communication (Chapter 3). This shares a common basis with executive deficits often seen in severe SVD (Lawrence *et al.*, 2014), and accordingly, we found that apathy was associated with an increased dementia risk (Chapter 6).

7.2. Neurocognitive mechanisms underlying apathy

One consistent finding across studies was a relationship between apathy and cognitive function. Voxel-based grey matter and white matter changes depended in part on general cognitive function (Chapter 3), as did white matter subnetworks (Chapter 4). Accordingly, apathy was associated with conversion to dementia (Chapter 6).

If damage to distinct networks leads to the behavioral symptoms of apathy, then they may do so through defined neurocognitive mechanisms. For the purposes of this review, we will consider apathy to be a deficit in the cognitive processes underlying effort-based decision making due to the conceptual simplicity and operationalisability of this approach (Le Heron *et al.*, 2018*a*, 2019). This view suggests that behavior can be thought of in three distinct phases:

1. Deciding whether to pursue a behavior;
2. Performing and persisting with the behavior; and
3. Evaluating and learning the costs and benefits of a behavior.

7.2.1. Reward-based decision-making

Prior to any behavior occurring, an individual must decide whether or not that behavior is worth engaging in. This engages networks that underlie cost-benefit valuation, as rewards and effort costs must be appraised. Apathy may therefore be the result of reductions in reward sensitivity, which is typically operationalized as an tendency to respond in proportion to the value of a rewarding stimulus during a behavioral task.

Recent evidence suggests that reduced incentivization to rewards may underlie apathy in cerebrovascular disease. Decreased reward-related task speeding is associated with apathy

in chronic stroke patients (Rochat *et al.*, 2013). Similarly, CADASIL patients with apathy rejected more opportunities to exert effort during a task, and were slower in making effort-related decisions, when compared to patients without apathy (Le Heron *et al.*, 2018*b*). This was paralleled by reduced FA in the anterior cingulum, white matter of the OFC, and the anterior internal capsule. Rejection of opportunities to exert effort suggests that apathy in these patients reflects a devaluation of rewards, while the increased decision-making time and concurrent white matter damage may reflect disrupted network efficiency. This is directly supported by a study of white matter subnetworks in sporadic SVD patients, which showed that the global efficiency of a reward-related subnetwork was more correlated with apathy than motor or visual subnetworks (Lisiecka-Ford *et al.*, 2018). The reward-related subnetwork included nodes such as ACC, OFC, and putamen (including ventral striatum), among others (Lisiecka-Ford *et al.*, 2018). Changes in the connectivity between these frontostriatal structures was also associated with apathy in our study, which used an independent cohort of sporadic SVD patients (Chapter 3).

This collective evidence suggests a direct pathway between cerebrovascular pathology, network change, cognitive deficits, and apathy. First, neuropathological changes lead to frontostriatal network damage, either through cortical or subcortical infarcts that lead to secondary neurodegenerative cascades down white matter tracts (Duering *et al.*, 2015; Schaapsmeerders *et al.*, 2016), or through frontal WMH, which represent areas of ischemic demyelination and axonal loss (Gouw *et al.*, 2011). Both infarcts and WMH may also lead to incident cortical atrophy in connected regions (Duering *et al.*, 2015; Lambert *et al.*, 2016). The progressive destruction or disruption of these frontal white matter tracts may lead to a decrease in the efficiency of information transfer along these tracts, making the integration of reward-related signals between structures such as ACC, ventral striatum, and PFC (Haber and Knutson, 2010) more difficult. In turn, these can lead to a decrease in the perceived rewarding value of a stimulus, manifesting as a reduction in GDB and apathy.

These changes may be modulated by dopaminergic neurons, which originate in the ventral tegmental area and substantia nigra and project to the ventral striatum, ACC, ventromedial PFC, and OFC (Chong and Husain, 2016). Dopamine may promote approach behaviors by attributing incentive salience to rewarding stimuli (Chong and Husain, 2016). Accordingly, case studies show that the administration of dopamine agonists alleviates apathy in stroke patients. These include bromocriptine (Catsman-Berrevoets and Harskamp, 1988; Barrett, 1991; Parks *et al.*, 1992; Marin *et al.*, 1995; Powell *et al.*, 1996), and ropinirole (Kohno *et al.*, 2010; Adam *et al.*, 2013).

Changes in dopaminergic neurotransmission may explain associations between apathy and inflammation (Eurelings *et al.*, 2015; Chen *et al.*, 2018). Systemic inflammation can be estimated by circulating plasma C-reactive protein (CRP) levels, which are elevated following an inflammatory response (Pepys and Baltz, 1983). Elevated acute phase CRP levels are associated with increasing post-stroke apathy over six months (Chen *et al.*, 2018). Similarly, apathy was correlated with higher CRP levels over several years in community-dwelling individuals (Eurelings *et al.*, 2015). This relationship may be driven by inflammation-associated decreases in dopamine synthesis and availability, reducing neural responses toward rewarding stimuli (Felger and Treadway, 2017). It should be noted, however, that inflammation itself is related to incident vascular disease (Gounis *et al.*, 2015), meaning that the relationship between inflammatory markers and apathy may additionally be mediated by other factors such as WMH (Yao *et al.*, 2019). Clearly dissociating the direct and indirect effects of inflammation on apathy is an important topic for future research.

7.2.2. Attentional control during behavior

After a behavior is initiated, it must be sustained until completion to achieve the desired outcome. This involves not only monitoring current outcomes of a task, but also comparing the potential value of completing the current task to others which are potentially more rewarding. If this is the case, then it is possible that patients with apathy may also show deficits in cognitive flexibility.

There is some indirect evidence to support this hypothesis. Apathy is associated with worse performance on composite cognitive indices that include the Trail Making Test Part B (TMT-B) (Reitan, 1958) in stroke and SVD (Lohner *et al.*, 2017; Douven *et al.*, 2018*a*). TMT-B performance requires individuals to draw a line between alternating numbers and letters in consecutive order, and completion requires the maintenance of a long sequence of behaviors as well as the ability to switch between two contexts (numbers and letters) (Kortte *et al.*, 2002). The reduction in TMT-B performance may reflect patient difficulties in completing a long sequence of behaviors and in switching between contexts, leading to difficulties in sustaining motivation through a task and switching to other, more rewarding tasks. These associations, however, are indirect, as TMT-B performance in both studies was included in a larger composite index that included other measures of executive functioning (Lohner *et al.*, 2017; Douven *et al.*, 2018*a*). Although these composite cognitive indices are robust and easy to interpret, variance in the measures used to construct them may obfuscate true associations. For instance, another study that measured executive function using the

TMT-B found no correlation between executive function and apathy scores (Brodaty *et al.*, 2005). This may be due to that executive function index including a color-form sorting task, which may assess different cognitive abilities than TMT-B (Tamkin and Kunce, 1982). The inclusion of both, therefore, may have dampened associations with apathy. More direct testing of these constructs, as well as careful consideration towards tests used to create composite cognitive indices, is required before any definitive conclusions can be drawn.

The deficits discussed above may be due to impairment of the fronto-parietal and cingulo-opercular networks, two intrinsic connectivity networks derived from resting-state functional MRI data (Seeley *et al.*, 2007). The fronto-parietal network includes the dorsolateral PFC, inferior parietal lobule, intraparietal sulcus, precuneus, and middle cingulate, while the cingulo-opercular network includes anterior PFC, anterior insula, dorsal ACC, and thalamus (Seeley *et al.*, 2007). Both networks have been implicated in attentional control processes, with fronto-parietal network initiating and adjusting behavior on a task-to-task basis, while the cingulo-opercular network provides stable maintenance of task goals over the entire behavioral period (Dosenbach *et al.*, 2008).

In Chapter 4, we showed that apathy in SVD patients was associated with altered connectivity in white matter networks that have a similar topological organization to these intrinsic connectivity networks. Furthermore, after controlling for general cognitive functioning, which included measures of attention, we found that apathy was no longer associated with these particular white matter networks. Although no direct analysis of resting-state functional connectivity was conducted, structural connectivity has been shown to constrain functional connectivity in the human brain (Honey *et al.*, 2009). Therefore, structural damage to the nodes or edges supporting the fronto-parietal and cingulo-opercular networks may result in attentional deficits. These make the maintenance of task-related GDB more difficult, manifesting as apathy. It should be noted that all current evidence that supports this notion is indirect, highlighting the need for more focused, theory-driven network analyses of apathy.

7.2.3. Learning and remembering rewarding behaviors

After a behavior has been completed, outcomes reveal whether the behavior was a success or failure. The magnitude of the success or failure, in relation to the effort exerted to complete the task, informs individuals of how worthwhile the task was. Deficits in learning this action-outcome contingency may impair individuals from learning rewarding behaviors, which may manifest as apathy (Husain and Roiser, 2018).

Evidence, in general, supports an association between apathy and impaired measures of verbal recall and recognition in stroke and SVD (Brodaty *et al.*, 2005; Lohner *et al.*, 2017; Fishman *et al.*, 2018*b*), although some studies do not find this association (Douven *et al.*, 2018*a*). In accordance with this, apathy has been found to be associated with reduced FA in the fornix, the major output tract of the hippocampus, in sporadic SVD (Hollocks *et al.*, 2015), as well as with reduced nodal degree in left hippocampus in ischemic stroke patients (Yang *et al.*, 2015*a*). These reductions in white matter connectivity may be related to grey matter changes in the hippocampus, which were associated with apathy in our research (Chapter 3).

Apathy has also been documented as a comorbidity with amnesia following thalamic stroke (Guberman and Stuss, 1983; Catsman-Berrevoets and Harskamp, 1988; Carrera and Bogousslavsky, 2006). This may be due to the reciprocal connections between the thalamus and the hippocampus via the mammillo-thalamic tract, which includes the fornix (Carlesimo *et al.*, 2011). Interpreting this is not straightforward, however, as disrupted white matter connectivity between the thalamus and PFC may also underlie apathy (Chapter 4). Future research could clarify whether thalamic-hippocampal connectivity plays a role in learning and memory deficits associated with apathy by examining tract-specific white matter microstructure in patients with vascular thalamic amnesia and apathy.

The evidence to support a link between cerebrovascular disease, network damage, learning and memory deficits, and apathy therefore remains inconclusive. These associations may be further complicated by depression and Alzheimer's disease pathology in elderly patients, both of which are associated with medial temporal lobe changes that may interact with cerebrovascular pathology to produce age-related changes in learning and memory (Geerlings *et al.*, 2008; van Leijsen *et al.*, 2019). More focused behavioral experiments, together with more rigorous sample population phenotyping, may be able to better clarify these relationships.

Links between these components of GDB, underlying cognitive functions, and potential subnetworks that may support these are shown in Figure 1. It is important to note that the way we have presented these is, overall, a simplified view of how neurobiological networks might be related to apathetic behaviors. It is unlikely that one single subnetwork or connection underlies a specific behavior or cognition, as this is quite contrary to the notion of networks in general. For instance, attention must be sustained throughout all phases of behavior, as a lack of attention may impair decision-making and learning. Instead, we have highlighted specific cognitive functions that may be particularly important to a certain phase

of behavior, and have related that to properties of established functional networks that may be disrupted in cerebrovascular disease. Interactions between these networks, which could be mediated by GDB-related hub nodes, may well play a role in determining multiple components of behavior.

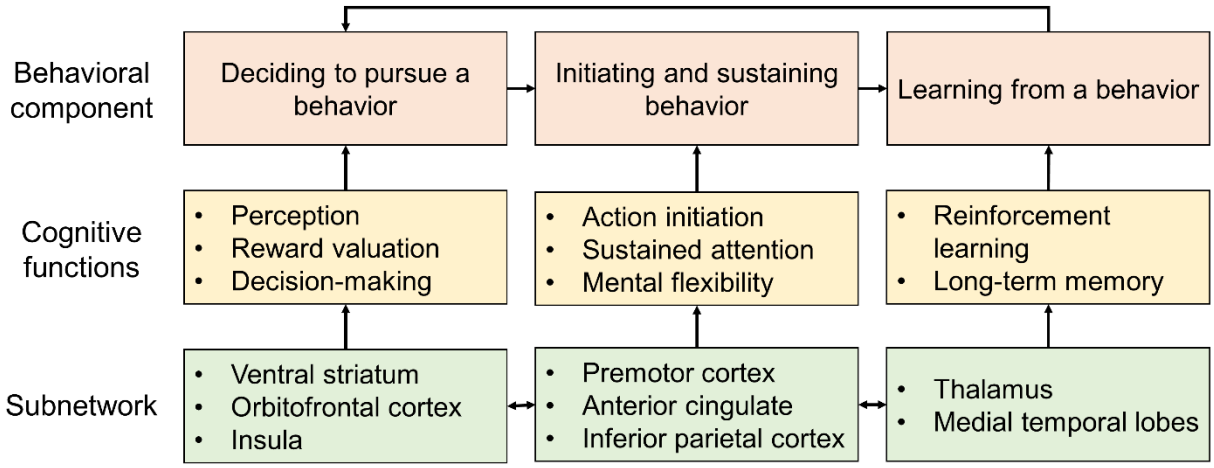

Figure 1. Potential relationships between subnetworks, cognition, and components of goal-directed behavior. Behavior may be thought of in three temporal phases: before, during, and after. Prior to behavior occurring, individuals must evaluate whether a behavior is worth engaging in. After a decision has been made, the behavior must be initiated and sustained. Once the behavior has been completed, the outcome of the behavior influences future decision-making. These may be supported by specific subnetworks implicated in incentive salience, executive control, and learning and memory. Some nodes may be part of multiple subnetworks, such as the anterior cingulate cortex (ACC) and ventral striatum (VS), as these may be hub nodes for goal-directed behavior. For simplicity, only one subnetwork has been listed per phase of behavior, though it should be noted that multiple subnetworks with more nodes than the ones listed may be involved.

7.3. Overlap between apathy and depression

Another consistent finding throughout the work was the high correlation between apathy and depression (Chapter 2). Despite these high correlations, both were not synonymous, and showed diverging correlations with other clinical variables (Chapter 2), neurobiology (Chapter 3 and 4), and all-cause dementia (Chapter 6). This supports the notion that the two may appear behaviourally similar, and can present co-morbidly, but are different entities with distinct neurobiological underpinnings (Chapter 1).

From the results presented in this thesis, apathy appears to be more strongly related to white matter microstructure and network function in SVD (Chapters 3 and 4). Although both are associated with grey matter change, particularly in the striatum, apathy appears to be associated with more distributed grey matter changes across the cortex (Chapter 3). Results from Chapter 5 suggest that depression may be associated with weak effects across the cortex that disappear after applying a correction for multiple comparisons.

What symptoms underlie the relationship between apathy and depression? Although anhedonia may appear the most similar to apathy from a theoretical standpoint (Chapter 1), this only received partial empirical support, as apathy was also moderately correlated with somatic and mood symptoms in 2011 (Chapter 5). This suggests that apathy, as measured using the AES, may actually be correlated with a more diverse range of depressive symptomatology than initially thought. It may be possible that this is partly driven by similar patterns of grey matter change (Chapters 3 and 5), or by further behavioural similarities, such as somatic symptoms possibly appearing similarly to apathy. Further investigation of these constructs, especially those that use different scales to measure apathy and depressive symptoms, is warranted.

7.4. Limitations

One important limitation in our data was our lack of reliable longitudinal apathy measurements in the RUN DMC study. As previously mentioned, the clinician-rated Apathy Evaluation Scale (AES), the measure of apathy in that population, was not administered at baseline, and was administered by a different rater between two follow-ups (2011 and 2015). This precluded a longitudinal analysis of change in RUN DMC, which limited our ability to assess whether apathy was associated with progressive neurobiological change, such as transneuronal degeneration or cortical atrophy. It is therefore left to future studies to establish

longitudinal network changes associated with apathy in SVD and cerebrovascular disease more generally.

Another limitation was that we could not directly test functional network change associated with apathy or depression. Although functional networks assessed using techniques such as perfusion MRI or functional MRI are important for understanding cognitive function (Seeley *et al.*, 2007), these measures are inherently confounded in patients with cerebrovascular disease. For instance, changes to perfusion in certain areas could reflect cerebrovascular reactivity in addition to changes in neural activity (Lythgoe *et al.*, 1999). This may have consequences for the reproducibility of functional networks, which has been shown in SVD (Lawrence *et al.*, 2018*a*). Therefore, conclusions about functional changes associated with apathy and depression must be made cautiously until the effects of cerebrovascular pathology on measures of brain function are better understood.

7.5. Future directions

The network-based view of apathy that we have proposed, along with the potential cognitive mechanisms that may link network damage to apathy, provide a fruitful basis for future hypotheses. Validation of the specific hub nodes and subnetworks underlying apathy in stroke and SVD (Yang *et al.*, 2015*a*; Tay *et al.*, 2019) may lead to a better understanding of the structural and functional connections and subnetworks that are impaired in individuals with specific cerebrovascular pathologies. These pathologies may include the under-explored areas of post-stroke neuroinflammation or the ischemic penumbra, which may play roles in exacerbating or alleviating apathy. Moreover, a clearer understanding of specific subnetwork connectivity related to GDB could lead to *a priori* investigations using networks of interest (e.g., Lisiecka-Ford et al., 2018). These subnetworks could also be examined in the context of other comorbidities, such as depression and fatigue (Douven *et al.*, 2017*b*), in order to identify common underlying mechanisms.

Studies on the trajectories of post-stroke apathy could investigate whether functional diaschisis underlies apathy in the acute phase. Longitudinal research could examine whether patients who recovery from apathy show corresponding improvements in intrahemispheric connectivity or vicariation, and if individuals who develop apathy show transneuronal degeneration in connected cortical regions. These network pathologies should help explain why apathy develops after lesions in certain areas.

Further inquiry into the validity of the presented neurocognitive framework for apathy is needed, as well as the subnetworks that support these cognitive functions. This could

involve behavioral paradigms or cognitive tests that assess specific constructs that may be related to apathy, with additional consideration to any comorbidities that a patient might show. Doing so may identify which components of GDB are disrupted in patients with cerebrovascular disease. Additionally, work on how some cognitive mechanisms may be related to multiple phases of GDB is needed, as this evidence is largely absent.

All of these lines of research could lead to targeted interventions for treating apathy. For instance, an apathetic patient with damage in a defined apathy-related subnetwork might be treated with rTMS, which requires *a priori* knowledge of which nodes may be disrupted. Such rTMS approaches have some preliminary support (Mitaki *et al.*, 2016; Sasaki *et al.*, 2017). Alternatively, subnetwork-specific neurotransmitter deficits could be addressed with pharmacological agents, such as dopamine agonists, which lead to a reinstatement of the related component of GDB (Adam *et al.*, 2013). Treating apathy may not only lead to improvements in patient functional outcomes, but also lower the risk of future vascular disease.

This network-based hypothesis of apathy may also be applied to other conditions. For instance, different neurodegenerative diseases target distinct large-scale networks (Seeley *et al.*, 2009), making it reasonable to assume that disease-specific patterns of network damage could lead to different symptoms of apathy. This could lead to a better understanding of the nature of motivational impairments in specific diseases, which could assist in clinical phenotyping. Findings could then be integrated across diseases to identify core networks underlying goal-directed behavior.

Other areas of progress that may be made in the understanding of apathy in cerebrovascular disease include more focused testing of specific cognitive and behavioral deficits seen. This can take the form of quantitative behavioral tasks that assess reinforcement-related speeding or effort-based decision making (Rochat *et al.*, 2013; Le Heron *et al.*, 2018*b*), which may then be assessed in the context of structural network changes. This may lead to a better understanding of the cognitive deficits that specifically underlie apathy given a certain pathology, such as white matter hyperintensities (WMH) or focal infarction in a certain network.

Understanding the neurobiology of depression could be greatly improved by adopting a dimensional approach and examining specific symptoms (Cuthbert and Insel, 2013). This approach, as we have shown, reveals similar and distinct neuroanatomical correlates (Chapter 5). This methodological approach could help clarify what types of neurobiological changes are characteristic of depression *in general*, as well as changes that may underlie some

symptoms, but not others. Specific attention to anhedonia in particular may also prove useful in understanding apathy. As others have suggested, similar behavioural presentations may reflect a common underlying neurobiology (Husain and Roiser, 2018).

This could then pave the way for targeted treatment approaches. For example, these approaches could include repetitive transcranial magnetic stimulation (rTMS), a non-invasive therapy that involves magnetic stimulation over specific sites. rTMS applied over medial prefrontal cortex has already shown some efficacy in improving symptoms of apathy in stroke patients (Mitaki *et al.*, 2016; Sasaki *et al.*, 2017). These could be applied to other sites depending on symptomatic presentations, leading to patient-centric care. A similar principle could be applied to the use of pharmacological agents that target specific neurotransmitter systems.

Apathy in itself may be a useful prognostic marker for individuals with vascular cognitive impairment. Given that the inclusion of apathy leads to a quantitative improvement in predictive models of dementia over and above the effects of age, cognition, and education (Chapter 6), we can surmise that it may be a useful marker to identify individuals at-risk for developing more severe cognitive deficits. This may then be used to select patients for more detailed neuropathological testing, or be used to identify candidates for clinical trials.

Finally, understanding the neurobiological basis of apathy could lead to insights into the nature of goal-directed behaviour. This has important societal implications, as motivation influences important facets of life such as job-seeking and life satisfaction (Vansteenkiste *et al.*, 2005). On a deeper level, goal-directed behaviour is a reflection on volitional behavior, which contrasts with autonomic or reflexive behaviors (Passingham *et al.*, 2010). Understanding the neural basis of volitional behavior could well have important implications for decision-making, free will, and consciousness, which are key elements of the human experience.

Abbreviations

AAL = Automated Anatomical Labeling

ACC = anterior cingulate cortex

ACG = anterior cingulate gyrus

ADL = activities of daily living

AES = Apathy Evaluation Scale

AIC = Akaike Information Criterion

ANCOVA = analysis of covariance

ANTs = Advanced Normalization Tools

BET = Brain Extraction Toolkit

BIC = Bayesian Information Criterion

BMI = body mass index

BMIPB = Brain Injury and Rehabilitation Trust Memory and Information

BOLD = blood oxygen level dependent

BP = blood pressure

BV = brain volume

CADASIL = Cerebral Autosomal Dominant Arteriopathy with Subcortical Infarcts and Leukoencephalopathy

CESD = Center for Epidemiologic Studies Depression Scale

CFA = confirmatory factor analysis

CRP = C-reactive protein

CSF = cerebrospinal fluid

DSM = Diagnostic and Statistical Manual of Mental Disorders

DSM-IV-TR = Diagnostic and Statistical Manual of Mental Disorders, Fourth Edition, Text Revision

DSM-5 = Diagnostic and Statistical Manual of Mental Disorders, Fifth Edition

DSST = Digit Symbol Substitution Task

DTI = diffusion tensor imaging

DWI = diffusion-weighted imaging

EPI = echo planar imaging

FA = fractional anisotropy

FLAIR = fluid-attenuated inversion recovery

FLIRT = FMRIB's Linear Image Registration Tool

GABA = gamma aminobutyric acid

GDB = goal-directed behaviour

GDS = Geriatric Depression Scale

GM = grey matter

HR = hazard ratio

IADL = instrumental activities of daily living

ICD-10-CM = International Classification of Diseases, Tenth Revision, Clinical Modification

IFG = inferior frontal gyrus

LDST = Letter Digit Symbol Task

LI = lacunar infarct

MCAR = missing completely at random

MCG = middle cingulate gyrus

MD = mean diffusivity

MMSE = Mini-Mental State Examination

MNI = Montreal Neurological Institute

MPRAGE = magnetization-prepared rapid gradient echo

MRI = magnetic resonance imaging

NAA = N-acetylaspartate

NBS = network-based statistic

OFC = orbitofrontal cortex

OR = odds ratio

PCA = principal component analysis

PFC = prefrontal cortex

PreCG = precentral gyrus

PreDIVA = Prevention of Dementia by Intensive Vascular Care

PPMST = Paper and Pencil Memory Scanning Task

PS = processing speed

rCBF = regional cerebral blood flow

RMSEA = root mean square error of approximation

ROI = region of interest

rTMS = repetitive transcranial magnetic stimulation

RUN DMC = Radboud University Nijmegen Diffusion tensor and Magnetic resonance Cohort

SAS = Starkstein Apathy Scale

SCANS = St. George's Cognition And Neuroimaging in Stroke

SD = standard deviation

SEM = structural equation modeling

SFG = superior frontal gyrus

SMA = supplementary motor area

SPM = Statistical Parametric Mapping

SVD = small vessel disease

T1w = T1-weighted

TBSS = tract-based spatial statistics

TE = echo time

TI = inversion time

TIV = total intracranial volume

TMT-B = Trail Making Test, Part B

TR = repetition time

TPM = tissue probability map

VBM = voxel-based morphometry

WM = white matter

WMH = white matter hyperintensities

References

Abdi H, Williams L. Contrast analysis. In: Salkind N, editor(s). Encyclopedia of research design. Thousand Oaks, CA: SAGE Publishing; 2010. pp. 243–251.

Adam R, Leff A, Sinha N, Turner C, Bays P, Draganski B, et al. Dopamine reverses reward insensitivity in apathy following globus pallidus lesions. Cortex 2013; 49: 1292–1303.

Adams Jr HP, Bendixen BH, Kappelle LJ, Biller J, Love BB, Gordon DL, et al. Classification of subtype of acute ischemic stroke. Definitions for use in a multicenter clinical trial. TOAST. Trial of Org 10172 in Acute Stroke Treatment. Stroke 1993; 24: 35–41.

Agrell B, Dehlin O. Comparison of six depression rating scales in geriatric stroke patients. Stroke 1989; 20: 1190–1194.

American Psychiatric Association. Diagnostic and statistical manual of mental disorders: DSM-IV-TR. 4th ed., Text Revision. Washington, DC: American Psychiatric Association; 2000

American Psychiatric Association. Diagnostic and statistical manual of mental disorders: DSM-5. 5th ed. Washington, DC: American Psychiatric Association; 2013.

Andersson JL, Hutton C, Ashburner J, Turner R, Friston K. Modeling geometric deformations in EPI time series. Neuroimage 2001; 13: 903–919.

Andersson S, Krogstad J, Finset A. Apathy and depressed mood in acquired brain damage: Relationship to lesion localization and psychophysiological reactivity. Psychol Med 1999; 29: 447–456.

Ang Y-S, Lockwood P, Apps MA, Muhammed K, Husain M. Distinct subtypes of apathy revealed by the apathy motivation index. PLoS One 2017; 12: e0169938.

Ashburner J, Friston KJ. Unified segmentation. Neuroimage 2005; 26: 839–851.

Ashtari M, Greenwald B, Kramer-Ginsberg E, Hu J, Wu H, Patel M, et al. Hippocampal/amygdala volumes in geriatric depression. Psychol Med 1999; 29: 629–638.

Assaf Y, Pasternak O. Diffusion tensor imaging (DTI)-based white matter mapping in brain research: A review. J Mol Neurosci 2008; 34: 51–61.

Autret K, Arnould A, Mathieu S, Azouvi P. Transient improvement of poststroke apathy with zolpidem: A single-case, placebo-controlled double-blind study. BMJ Case Rep 2013; 2013: bcr2012007816.

Avants BB, Epstein CL, Grossman M, Gee JC. Symmetric diffeomorphic image registration with cross-correlation: Evaluating automated labeling of elderly and neurodegenerative brain. Med Image Anal 2008; 12: 26–41.

Azur MJ, Stuart EA, Frangakis C, Leaf PJ. Multiple imputation by chained equations: What is it and how does it work? Int J Methods Psychiat Res 2011; 20: 40–49.
Bamford J, Sandercock P, Dennis M, Burn J, Warlow C. Classification and natural history of clinically identifiable subtypes of cerebral infarction. Lancet 1991; 337: 1521–1526.
Barberger-Gateau P, Commenges D, Gagnon M, Letenneur L, Sauvel C, Dartigues J-F. Instrumental activities of daily living as a screening tool for cognitive impairment and dementia in elderly community dwellers. J Am Geriatr Soc 1992; 40: 1129–1134.
Barnard J, Rubin DB. Small-sample degrees of freedom with multiple imputation. Biometrika 1999; 86: 948–955.
Barnes D, Covinsky K, Whitmer R, Kuller L, Lopez O, Yaffe K. Predicting risk of dementia in older adults: The late-life dementia risk index. Neurology 2009; 73: 173–179.
Baron J, Rougemont D, Soussaline F, Bustany P, Crouzel C, Bousser M, et al. Local interrelationships of cerebral oxygen consumption and glucose utilization in normal subjects and in ischemic stroke patients: A positron tomography study. J Cereb Blood Flow Metab 1984; 4: 140–149.
Barrett K. Treating organic abulia with bromocriptine and lisuride: Four case studies. J Neurol Neurosur Psychiatry 1991; 54: 718–721.
Basser PJ, Mattiello J, LeBihan D. Estimation of the effective self-diffusion tensor from the NMR spin echo. J Magn Reson B 1994a; 103: 247–254.
Basser PJ, Mattiello J, LeBihan D. MR diffusion tensor spectroscopy and imaging. Biophys J 1994b; 66: 259–267.
Basser PJ, Pajevic S, Pierpaoli C, Duda J, Aldroubi A. In vivo fiber tractography using DT-MRI data. Magn Reson Med 2000; 44: 625–632.
Basser PJ, Pierpaoli C. Microstructural and physiological features of tissues elucidated by quantitative-diffusion-tensor MRI. J Magn Reson B 1996; 111: 209–219.
Bassett DS, Bullmore ET, Meyer-Lindenberg A, Apud JA, Weinberger DR, Coppola R. Cognitive fitness of cost-efficient brain functional networks. Proc Natl Acad Sci 2009; 106: 11747–11752.
Bates D, Mächler M, Bolker B, Walker S. Fitting linear mixed-effects models using lme4. J Stat Softw 2015; 67: 1–48.
Benjamin P, Lawrence AJ, Lambert C, Patel B, Chung AW, MacKinnon AD, et al. Strategic lacunes and their relationship to cognitive impairment in cerebral small vessel disease. Neuroimage Clin 2014; 4: 828–837.

Benjamini Y, Hochberg Y. Controlling the false discovery rate: A practical and powerful approach to multiple testing. J R Stat Soc B 1995; 57: 289–300.
Bentler PM, Yuan K-H. Structural equation modeling with small samples: Test statistics. Multivariate Behav Res 1999; 34: 181–197.
Bhatia KP, Marsden CD. The behavioural and motor consequences of focal lesions of the basal ganglia in man. Brain 1994; 117: 859–876.
Bollen KA. Issues in the comparative measurement of political democracy. Am Sociol Rev 1980: 370–390.
Bonnelle V, Manohar S, Behrens T, Husain M. Individual differences in premotor brain systems underlie behavioral apathy. Cereb Cortex 2015; 26: 807–819.
Brand N, Jolles J. Information processing in depression and anxiety. Psychol Med 1987; 17: 145–153.
Brodaty H, Liu Z, Withall A, Sachdev PS. The longitudinal course of post-stroke apathy over five years. J Neuropsychiatry Clin Neurosci 2013; 25: 283–291.
Brodaty H, Sachdev PS, Withall A, Altendorf A, Valenzuela MJ, Lorentz L. Frequency and clinical, neuropsychological and neuroimaging correlates of apathy following stroke–the Sydney Stroke Study. Psychol Med 2005; 35: 1707–1716.
Brookes RL, Herbert V, Lawrence AJ, Morris RG, Markus HS. Depression in small-vessel disease relates to white matter ultrastructural damage, not disability. Neurology 2014; 83: 1417–1423.
Buckner RL, Head D, Parker J, Fotenos AF, Marcus D, Morris JC, et al. A unified approach for morphometric and functional data analysis in young, old, and demented adults using automated atlas-based head size normalization: Reliability and validation against manual measurement of total intracranial volume. Neuroimage 2004; 23: 724–738.
Bullmore E, Sporns O. Complex brain networks: Graph theoretical analysis of structural and functional systems. Nat Rev Neurosci 2009; 10: 186–198.
Bullmore E, Sporns O. The economy of brain network organization. Nat Rev Neurosci 2012; 13: 336.
Bullmore ET, Suckling J, Overmeyer S, Rabe-Hesketh S, Taylor E, Brammer MJ. Global, voxel, and cluster tests, by theory and permutation, for a difference between two groups of structural MR images of the brain. IEEE Trans Med Imaging 1999; 18: 32–42.
Burnham KP, Anderson DR. Multimodel inference: Understanding AIC and BIC in model selection. Sociol Methods Res 2004; 33: 261–304.

Byers AL, Yaffe K. Depression and risk of developing dementia. Nat Rev Neurol 2011; 7: 323–331.
Caciagli L, Bernasconi A, Wiebe S, Koepp MJ, Bernasconi N, Bernhardt BC. A meta-analysis on progressive atrophy in intractable temporal lobe epilepsy: Time is brain? Neurology 2017; 89: 506–516.
Caeiro L, Ferro JM, Pinho e Melo T, Canhão P, Figueira ML. Post-stroke apathy: An exploratory longitudinal study. Cerebrovasc Dis 2013; 35: 507–513.
Caeiro L, Ferro JM, Santos CO, Figueira ML. Depression in acute stroke. J Psychiatry Neurosci 2006; 31: 377.
Calamante F, Tournier J-D, Jackson GD, Connelly A. Track-density imaging (TDI): Super-resolution white matter imaging using whole-brain track-density mapping. Neuroimage 2010; 53: 1233–1243.
Carlesimo GA, Lombardi MG, Caltagirone C. Vascular thalamic amnesia: A reappraisal. Neuropsychologia 2011; 49: 777–789.
Carleton RN, Thibodeau MA, Teale MJ, Welch PG, Abrams MP, Robinson T, et al. The center for epidemiologic studies depression scale: A review with a theoretical and empirical examination of item content and factor structure. PLoS One 2013; 8: e58067.
Carrera E, Bogousslavsky J. The thalamus and behavior: Effects of anatomically distinct strokes. Neurology 2006; 66: 1817–1823.
Carrera E, Tononi G. Diaschisis: Past, present, future. Brain 2014; 137: 2408–2422.
Carriere N, Besson P, Dujardin K, Duhamel A, Defebvre L, Delmaire C, et al. Apathy in Parkinson's disease is associated with nucleus accumbens atrophy: A magnetic resonance imaging shape analysis. Mov Disord 2014; 29: 897–903.
Castellanos-Pinedo F, Hernández-Pérez JM, Zurdo M, Rodríguez-Fúnez B, Hernández-Bayo JM, García-Fernández C, et al. Influence of premorbid psychopathology and lesion location on affective and behavioral disorders after ischemic stroke. J Neuropsychiatry Clin Neurosci 2011; 23: 340–347.
Catsman-Berrevoets CE, Harskamp F. Compulsive pre-sleep behavior and apathy due to bilateral thalamic stroke: Response to bromocriptine. Neurology 1988; 38: 647–649.
Chabriat H, Joutel A, Dichgans M, Tournier-Lasserve E, Bousser M-G. CADASIL. Lancet Neurol 2009; 8: 643–653.
Chase TN. Apathy in neuropsychiatric disease: Diagnosis, pathophysiology, and treatment. Neurotox Res 2011; 19: 266–278.

Chen L, Xiong S, Liu Y, Lin M, Wang J, Zhong R, et al. C-reactive protein can be an early predictor of poststroke apathy in acute ischemic stroke patients. J Stroke Cerebrovasc Dis 2018; 27: 1861–1869.
Chiu PH, Deldin PJ. Neural evidence for enhanced error detection in major depressive disorder. Am J Psychiatry 2007; 164: 608–616.
Chong T-J, Husain M. The role of dopamine in the pathophysiology and treatment of apathy. In: Progress in brain research. Elsevier; 2016. pp. 389–426
Chong TT-J, Bonnelle V, Manohar S, Veromann K-R, Muhammed K, Tofaris GK, et al. Dopamine enhances willingness to exert effort for reward in Parkinson's disease. Cortex 2015; 69: 40–46.
Clark CA, Barrick TR, Murphy MM, Bell BA. White matter fiber tracking in patients with space-occupying lesions of the brain: A new technique for neurosurgical planning? Neuroimage 2003; 20: 1601–1608.
Cohen J. A coefficient of agreement for nominal scales. Educ Psychol Meas 1960; 20: 37–46.
Coleman M. Axon degeneration mechanisms: Commonality amid diversity. Nat Rev Neurosci 2005; 6: 889–898.
Collin G, Sporns O, Mandl RC, van den Heuvel MP. Structural and functional aspects relating to cost and benefit of rich club organization in the human cerebral cortex. Cereb Cortex 2013; 24: 2258–2267.
Coughlan AK, Oddy M, Crawford JR. The BIRT Memory and Information Processing Battery (B-MIPB). 3rd ed. Wakefield, UK: The Brain Injury; Rehabilitation Trust (BIRT); 2007.
Craufurd D, Thompson JC, Snowden JS. Behavioral changes in Huntington disease. Cogn Behav Neurol 2001; 14: 219–226.
Cumming TB, Packer M, Kramer SF, English C. The prevalence of fatigue after stroke: A systematic review and meta-analysis. Int J Stroke 2016; 11: 968–977.
Cummings J, Friedman JH, Garibaldi G, Jones M, Macfadden W, Marsh L, et al. Apathy in neurodegenerative diseases: Recommendations on the design of clinical trials. J Geriatr Psychiatry Neurol 2015; 28: 159–173.
Cuthbert BN, Insel TR. Toward the future of psychiatric diagnosis: The seven pillars of RDoC. BMC Med 2013; 11: 126.
Dale AM, Fischl B, Sereno MI. Cortical surface-based analysis: I. Segmentation and surface reconstruction. Neuroimage 1999; 9: 179–194.

Dale AM, Sereno MI. Improved localizadon of cortical activity by combining EEG and MEG with MRI cortical surface reconstruction: A linear approach. J Cogn Neurosci 1993; 5: 162–176.
Dancause N. Vicarious function of remote cortex following stroke: Recent evidence from human and animal studies. Neuroscientist 2006; 12: 489–499.
Davis P, Wright E. A new method for measuring cranial cavity volume and its application to the assessment of cerebral atrophy at autopsy. Neuropathol Appl Neurobiol 1977; 3: 341–358.
Dawson JD, Uc EY, Anderson SW, Johnson AM, Rizzo M. Neuropsychological predictors of driving errors in older adults. J Am Geriatr Soc 2010; 58: 1090–1096.
Demirtas-Tatlidede A, Bahar SZ, Gurvit H. Akinetic mutism without a structural prefrontal lesion. Cogn Behav Neurol 2013; 26: 59–62.
den Brok MG, van Dalen JW, van Gool WA, Moll van Charante EP, de Bie RM, Richard E. Apathy in Parkinson's disease: A systematic review and meta-analysis. Mov Disord 2015; 30: 759–769.
de Oliveira Lanna ME, Alves CEO, Sudo FK, Alves G, Valente L, Moreira DM, et al. Cognitive disconnective syndrome by single strategic strokes in vascular dementia. J Neurol Sci 2012; 322: 176–183.
Der-Avakian A, Markou A. The neurobiology of anhedonia and other reward-related deficits. Trends Neurosci 2012; 35: 68–77.
Desikan RS, Ségonne F, Fischl B, Quinn BT, Dickerson BC, Blacker D, et al. An automated labeling system for subdividing the human cerebral cortex on MRI scans into gyral based regions of interest. Neuroimage 2006; 31: 968–980.
Desmurget M, Sirigu A. A parietal-premotor network for movement intention and motor awareness. Trends Cogn Sci 2009; 13: 411–419.
Dosenbach NU, Fair DA, Cohen AL, Schlaggar BL, Petersen SE. A dual-networks architecture of top-down control. Trends Cogn Sci 2008; 12: 99–105.
Douven E, Köhler S, Rodriguez MM, Staals J, Verhey FR, Aalten P. Imaging markers of post-stroke depression and apathy: A systematic review and meta-analysis. Neuropsychol Rev 2017a; 27: 202–219.
Douven E, Köhler S, Schievink SH, van Oostenbrugge RJ, Staals J, Verhey FR, et al. Temporal associations between fatigue, depression, and apathy after stroke: Results of the cognition and affect after stroke, a prospective evaluation of risks study. Cerebrovasc Dis 2017b; 44: 330–337.

Douven E, Köhler S, Schievink SH, van Oostenbrugge RJ, Staals J, Verhey FR, et al. Baseline vascular cognitive impairment predicts the course of apathetic symptoms after stroke: The CASPER study. Am J Geriatr Psychiatry 2018a; 26: 291–300.
Douven E, Staals J, Schievink SH, van Oostenbrugge RJ, Verhey FR, Wetzels-Meertens S, et al. Personality traits and course of symptoms of depression and apathy after stroke: Results of the CASPER study. J Psychosomatic Res 2018b; 111: 69–75.
Drysdale AT, Grosenick L, Downar J, Dunlop K, Mansouri F, Meng Y, et al. Resting-state connectivity biomarkers define neurophysiological subtypes of depression. Nat Med 2017; 23: 28.
Duering M, Gesierich B, Seiler S, Pirpamer L, Gonik M, Hofer E, et al. Strategic white matter tracts for processing speed deficits in age-related small vessel disease. Neurology 2014; 82: 1946–1950.
Duering M, Righart R, Wollenweber FA, Zietemann V, Gesierich B, Dichgans M. Acute infarcts cause focal thinning in remote cortex via degeneration of connecting fiber tracts. Neurology 2015; 84: 1685–1692.
Edeh J, Toone B. Relationship between interictal psychopathology and the type of epilepsy: Results of a survey in general practice. Br J Psychiatry 1987; 151: 95–101.
Eickhoff SB, Stephan KE, Mohlberg H, Grefkes C, Fink GR, Amunts K, et al. A new SPM toolbox for combining probabilistic cytoarchitectonic maps and functional imaging data. Neuroimage 2005; 25: 1325–1335.
Eurelings LS, Richard E, Eikelenboom P, van Gool WA, Moll van Charante EP. Low-grade inflammation differentiates between symptoms of apathy and depression in community-dwelling older individuals. Int Psychogeriatr 2015; 27: 639–647.
Eurelings LS, van Dalen JW, ter Riet G, Moll van Charante EP, Richard E, van Gool WA, et al. Apathy and depressive symptoms in older people and incident myocardial infarction, stroke, and mortality: A systematic review and meta-analysis of individual participant data. Clin Epidemiol 2018; 10: 363–379.
Evans AC. Networks of anatomical covariance. Neuroimage 2013; 80: 489–504.
Evans AC, Collins DL, Mills S, Brown E, Kelly R, Peters TM. 3D statistical neuroanatomical models from 305 MRI volumes. In: 1993 IEEE Conference Record Nuclear Science Symposium and Medical Imaging Conference. San Francisco, CA: IEEE; 1993. pp. 1813–1817.
Evans AC, Kamber M, Collins D, MacDonald D. An MRI-based probabilistic atlas of neuroanatomy. In: Magnetic resonance scanning and epilepsy. Springer; 1994. pp. 263–274.

Fazekas F, Chawluk JB, Alavi A, Hurtig HI, Zimmerman RA. MR signal abnormalities at 1.5 T in Alzheimer's dementia and normal aging. Am J Roentgenol 1987; 149: 351–356.
Fazekas F, Kleinert R, Offenbacher H, Schmidt R, Kleinert G, Payer F, et al. Pathologic correlates of incidental MRI white matter signal hyperintensities. Neurology 1993; 43: 1683–1689.
Felger JC, Treadway MT. Inflammation effects on motivation and motor activity: Role of dopamine. Neuropsychopharmacology 2017; 42: 216–241.
Fernando MS, Simpson JE, Matthews F, Brayne C, Lewis CE, Barber R, et al. White matter lesions in an unselected cohort of the elderly: Molecular pathology suggests origin from chronic hypoperfusion injury. Stroke 2006; 37: 1391–1398.
Fervaha G, Foussias G, Agid O, Remington G. Motivational deficits in early schizophrenia: Prevalent, persistent, and key determinants of functional outcome. Schizophr Res 2015; 166: 9–16.
Figved N, Klevan G, Myhr K, Glad S, Nyland H, Larsen J, et al. Neuropsychiatric symptoms in patients with multiple sclerosis. Acta Psychiatrica Scand 2005; 112: 463–468.
Firbank M, Minett T, O'Brien J. Changes in DWI and MRS associated with white matter hyperintensities in elderly subjects. Neurology 2003; 61: 950–954.
Fischl B, Dale AM. Measuring the thickness of the human cerebral cortex from magnetic resonance images. Proc Natl Acad Sci 2000; 97: 11050–11055.
Fischl B, Liu A, Dale AM. Automated manifold surgery: Constructing geometrically accurate and topologically correct models of the human cerebral cortex. IEEE Trans Med Imaging 2001; 20: 70–80.
Fischl B, Salat DH, Busa E, Albert M, Dieterich M, Haselgrove C, et al. Whole brain segmentation: Automated labeling of neuroanatomical structures in the human brain. Neuron 2002; 33: 341–355.
Fischl B, Salat DH, Van Der Kouwe AJ, Makris N, Ségonne F, Quinn BT, et al. Sequence-independent segmentation of magnetic resonance images. Neuroimage 2004a; 23: S69–S84.
Fischl B, Sereno MI, Tootell RB, Dale AM. High-resolution intersubject averaging and a coordinate system for the cortical surface. Hum Brain Mapp 1999; 8: 272–284.
Fischl B, Van Der Kouwe A, Destrieux C, Halgren E, Ségonne F, Salat DH, et al. Automatically parcellating the human cerebral cortex. Cereb Cortex 2004b; 14: 11–22.
Fishman KN, Ashbaugh AR, Lanctôt KL, Cayley ML, Herrmann N, Murray BJ, et al. Apathy, not depressive symptoms, as a predictor of semantic and phonemic fluency task

performance in stroke and transient ischemic attack. J Clin Exp Neuropsychol 2018a; 40: 449–461.
Fishman KN, Ashbaugh AR, Lanctôt KL, Cayley ML, Herrmann N, Murray BJ, et al. The role of apathy and depression on verbal learning and memory performance after stroke. Arch Clin Neuropsychol 2018b; 34: 327–336.
Folstein MF, Folstein SE, McHugh PR. 'Mini-mental state': A practical method for grading the cognitive state of patients for the clinician. J Psychiat Res 1975; 12: 189–198.
Fornito A, Zalesky A, Breakspear M. The connectomics of brain disorders. Nat Rev Neurosci 2015; 16: 159–172.
Forsgren L, Nyström L. An incident case-referent study of epileptic seizures in adults. Epilepsy Res 1990; 6: 66–81.
Fox J, Weisberg S. An R companion to applied regression. Second. Thousand Oaks CA: Sage; 2011.
Freedman DA. On the so-called 'Huber sandwich estimator' and 'robust standard errors'. Am Stat 2006; 60: 299–302.
Fried I, Mukamel R, Kreiman G. Internally generated preactivation of single neurons in human medial frontal cortex predicts volition. Neuron 2011; 69: 548–562.
Friedman D, Cycowicz YM, Gaeta H. The novelty P3: An event-related brain potential (ERP) sign of the brain's evaluation of novelty. Neurosci Biobehav Rev 2001; 25: 355–373.
Friston KJ, Holmes AP, Worsley KJ, Poline J-P, Frith CD, Frackowiak RS. Statistical parametric maps in functional imaging: A general linear approach. Hum Brain Mapp 1994; 2: 189–210.
Gatchel JR, Donovan NJ, Locascio JJ, Schultz AP, Becker JA, Chhatwal J, et al. Depressive symptoms and tau accumulation in the inferior temporal lobe and entorhinal cortex in cognitively normal older adults: A pilot study. J Alzheimers Dis 2017; 59: 975–985.
Geerlings M, den Heijer T, Koudstaal PJ, Hofman A, Breteler M. History of depression, depressive symptoms, and medial temporal lobe atrophy and the risk of Alzheimer disease. Neurology 2008; 70: 1258–1264.
Ghafoorian M, Karssemeijer N, van Uden IW, de Leeuw F-E, Heskes T, Marchiori E, et al. Automated detection of white matter hyperintensities of all sizes in cerebral small vessel disease. Med Phys 2016; 43: 6246–6258.
Ghika-Schmid F, Bogousslavsky J. The acute behavioral syndrome of anterior thalamic infarction: A prospective study of 12 cases. Ann Neurol 2000; 48: 220–227.

Ginsberg MD, Castella Y, Dietrich WD, Watson BD, Busto R. Acute thrombotic infarction suppresses metabolic activation of ipsilateral somatosensory cortex: Evidence for functional diaschisis. J Cereb Blood Flow Metab 1989; 9: 329–341.
Glasser MF, Coalson TS, Robinson EC, Hacker CD, Harwell J, Yacoub E, et al. A multi-modal parcellation of human cerebral cortex. Nature 2016; 536: 171.
Glimcher PW. Understanding dopamine and reinforcement learning: The dopamine reward prediction error hypothesis. Proc Natl Acad Sci 2011; 108: 15647–15654.
Glodzik-Sobanska L, Slowik A, Kieltyka A, Kozub J, Sobiecka B, Urbanik A, et al. Reduced prefrontal N-acetylaspartate in stroke patients with apathy. J Neurol Sci 2005; 238: 19–24.
Gounis MJ, Marel K van der, Marosfoi M, Mazzanti ML, Clarençon F, Chueh J-Y, et al. Imaging inflammation in cerebrovascular disease. Stroke 2015; 46: 2991–2997.
Gouw AA, Seewann A, Van Der Flier WM, Barkhof F, Rozemuller AM, Scheltens P, et al. Heterogeneity of small vessel disease: A systematic review of MRI and histopathology correlations. J Neurol Neurosur Psychiatry 2011; 82: 126–135.
Graham JW, Olchowski AE, Gilreath TD. How many imputations are really needed? Some practical clarifications of multiple imputation theory. Prev Sci 2007; 8: 206–213.
Grefkes C, Fink GR. Connectivity-based approaches in stroke and recovery of function. Lancet Neurol 2014; 13: 206–216.
Grool AM, Geerlings MI, Sigurdsson S, Eiriksdottir G, Jonsson PV, Garcia ME, et al. Structural MRI correlates of apathy symptoms in older persons without dementia: AGES-Reykjavik Study. Neurology 2014; 82: 1628–1635.
Guberman A, Stuss D. The syndrome of bilateral paramedian thalamic infarction. Neurology 1983; 33: 540–546.
Gudmundsson P, Olesen P, Simoni M, Pantoni L, Östling S, Kern S, et al. White matter lesions and temporal lobe atrophy related to incidence of both dementia and major depression in 70-year-olds followed over 10 years. Eur J Neurol 2015; 22: 781–e50.
Haber SN. Corticostriatal circuitry. Neurosci 21st Century 2016: 1–21.
Haber SN, Calzavara R. The cortico-basal ganglia integrative network: The role of the thalamus. Brain Res Bulletin 2009; 78: 69–74.
Haber SN, Knutson B. The reward circuit: Linking primate anatomy and human imaging. Neuropsychopharmacology 2010; 35: 4–26.
Hagmann P, Cammoun L, Gigandet X, Meuli R, Honey CJ, Wedeen VJ, et al. Mapping the structural core of human cerebral cortex. PLoS Biol 2008; 6: e159.

Hagmann P, Kurant M, Gigandet X, Thiran P, Wedeen VJ, Meuli R, et al. Mapping human whole-brain structural networks with diffusion MRI. PLoS One 2007; 2: e597.
Hahn C, Lim H-K, Won WY, Ahn KJ, Jung W-S, Lee CU. Apathy and white matter integrity in Alzheimer's disease: A whole brain analysis with tract-based spatial statistics. PLoS One 2013; 8: e53493.
Hama S, Yamashita H, Shigenobu M, Watanabe A, Hiramoto K, Kurisu K, et al. Depression or apathy and functional recovery after stroke. Int J Geriatr Psychiatry 2007a; 22: 1046–1051.
Hama S, Yamashita H, Shigenobu M, Watanabe A, Hiramoto K, Takimoto Y, et al. Sitting balance as an early predictor of functional improvement in association with depressive symptoms in stroke patients. Psychiatry Clin Neurosci 2007b; 61: 543–551.
Han X, Jovicich J, Salat D, van der Kouwe A, Quinn B, Czanner S, et al. Reliability of MRI-derived measurements of human cerebral cortical thickness: The effects of field strength, scanner upgrade and manufacturer. Neuroimage 2006; 32: 180–194.
Harrell FE, Lee KL, Mark DB. Multivariable prognostic models: Issues in developing models, evaluating assumptions and adequacy, and measuring and reducing errors. Stat Med 1996; 15: 361–387.
Harris AL, Elder J, Schiff ND, Victor JD, Goldfine AM. Post-stroke apathy and hypersomnia lead to worse outcomes from acute rehabilitation. Transl Stroke Res 2014; 5: 292–300.
Hecht D. Depression and the hyperactive right-hemisphere. Neurosci Res 2010; 68: 77–87.
Hervé D, Mangin J-F, Molko N, Bousser M-G, Chabriat H. Shape and volume of lacunar infarcts: A 3D MRI study in cerebral autosomal dominant arteriopathy with subcortical infarcts and leukoencephalopathy. Stroke 2005; 36: 2384–2388.
Hesdorffer DC, Hauser WA, Annegers JF, Cascino G. Major depression is a risk factor for seizures in older adults. Ann Neurol 2000; 47: 246–249.
Hollocks MJ, Lawrence AJ, Brookes RL, Barrick TR, Morris RG, Husain M, et al. Differential relationships between apathy and depression with white matter microstructural changes and functional outcomes. Brain 2015; 138: 3803–3815.
Holm S. A simple sequentially rejective multiple test procedure. Scand J Stat 1979: 65–70.
Holmes CJ, Hoge R, Collins L, Woods R, Toga AW, Evans AC. Enhancement of MR images using registration for signal averaging. J Comput Assist Tomogr 1998; 22: 324–333.
Honey C, Sporns O, Cammoun L, Gigandet X, Thiran J-P, Meuli R, et al. Predicting human resting-state functional connectivity from structural connectivity. Proc Natl Acad Sci 2009; 106: 2035–2040.

Hunt M, Auriemma J, Cashaw AC. Self-report bias and underreporting of depression on the BDI-II. J Pers Assess 2003; 80: 26–30.
Husain M, Roiser JP. Neuroscience of apathy and anhedonia: A transdiagnostic approach. Nat Rev Neurosci 2018; 19: 470–484.
Jang SH, Kim SH, Kwon HG. Injury of the prefronto-caudate tract in a patient with apathy following intracerebral hemorrhage in the caudate nucleus. Acta Neurol Belg 2019; 119: 143–145.
Jang SH, Kwon YH. Abulia due to injury of the prefrontocaudate tract in a stroke patient. Am J Phys Med Rehabil 2018; 97: e76–e77.
Jellinger KA, Attems J. Is there pure vascular dementia in old age? J Neurol Sci 2010; 299: 150–154.
Jenkinson M, Bannister P, Brady M, Smith S. Improved optimization for the robust and accurate linear registration and motion correction of brain images. Neuroimage 2002; 17: 825–841.
Jenkinson M, Smith S. A global optimisation method for robust affine registration of brain images. Med Image Anal 2001; 5: 143–156.
Jolles J, Houx P, Van Boxtel M, Ponds R. The Maastricht Aging Study: Determinants of cognitive aging. Maastricht, The Netherlands: Neuropsych Publishers; 1995.
Jorgensen, D. T, Pornprasertmanit, S., Schoemann, M. A, et al. semTools: Useful tools for structural equation modeling. 2018.
Juntu J, Sijbers J, Van Dyck D, Gielen J. Bias field correction for MRI images. In: Computer recognition systems. Springer; 2005. pp. 543–551
Keedwell PA, Andrew C, Williams SC, Brammer MJ, Phillips ML. The neural correlates of anhedonia in major depressive disorder. Biological Psychiatry 2005; 58: 843–853.
Kessler RC, Price RH. Primary prevention of secondary disorders: A proposal and agenda. Am J Community Psychol 1993; 21: 607–633.
Kim JW, Lee DY, Choo IH, Seo EH, Kim SG, Park SY, et al. Microstructural alteration of the anterior cingulum is associated with apathy in Alzheimer disease. Am J Geriatr Psychiatry 2011; 19: 644–653.
Kohno N, Abe S, Toyoda G, Oguro H, Bokura H, Yamaguchi S. Successful treatment of post-stroke apathy by the dopamine receptor agonist ropinirole. J Clin Neurosci 2010; 17: 804–806.
Kortte KB, Horner MD, Windham WK. The trail making test, part B: Cognitive flexibility or ability to maintain set? Appl Neuropsychol 2002; 9: 106–109.

Kos C, van Tol M-J, Marsman J-BC, Knegtering H, Aleman A. Neural correlates of apathy in patients with neurodegenerative disorders, acquired brain injury, and psychiatric disorders. Neurosci Biobehav Rev 2016; 69: 381–401.
Kringelbach ML. The human orbitofrontal cortex: Linking reward to hedonic experience. Nat Rev Neurosci 2005; 6: 691.
Kumar U, Medel-Matus J-S, Redwine HM, Shin D, Hensler JG, Sankar R, et al. Effects of selective serotonin and norepinephrine reuptake inhibitors on depressive-and impulsive-like behaviors and on monoamine transmission in experimental temporal lobe epilepsy. Epilepsia 2016; 57: 506–515.
Kumral E, Erdoğan CE, Bayam FE, Arslan H. Cingulate infarction: A neuropsychological and neuroimaging study. J Neurol Sci 2019; 402: 1–6.
Kuperberg GR, Broome MR, McGuire PK, David AS, Eddy M, Ozawa F, et al. Regionally localized thinning of the cerebral cortex in schizophrenia. Arch Gen Psychiatry 2003; 60: 878–888.
Kuznetsova A, Brockhoff PB, Christensen RHB. lmerTest package: Tests in linear mixed effects models. J Stat Softw 2017; 82: 1–26.
Kybic J, Thévenaz P, Nirkko A, Unser M. Unwarping of unidirectionally distorted EPI images. IEEE Trans Med Imaging 2000; 19: 80–93.
Laird NM, Ware JH. Random-effects models for longitudinal data. Biometrics 1982; 38: 963–974.
Lambert C, Benjamin P, Zeestraten E, Lawrence AJ, Barrick TR, Markus HS. Longitudinal patterns of leukoaraiosis and brain atrophy in symptomatic small vessel disease. Brain 2016; 139: 1136–1151.
Langsrud Ø. ANOVA for unbalanced data: Use Type II instead of Type III sums of squares. Stat Comput 2003; 13: 163–167.
Latora V, Marchiori M. Efficient behavior of small-world networks. Phys Rev Lett 2001; 87: 198701.
Lavretsky H, Zheng L, Weiner MW, Mungas D, Reed B, Kramer JH, et al. The MRI brain correlates of depressed mood, anhedonia, apathy, and anergia in older adults with and without cognitive impairment or dementia. Int J Geriatr Psychiatry 2008; 23: 1040–1050.
Lawrence AJ, Chung AW, Morris RG, Markus HS, Barrick TR. Structural network efficiency is associated with cognitive impairment in small-vessel disease. Neurology 2014: 10–1212.

Lawrence AJ, Patel B, Morris RG, MacKinnon AD, Rich PM, Barrick TR, et al. Mechanisms of cognitive impairment in cerebral small vessel disease: Multimodal MRI results from the St George's cognition and neuroimaging in stroke (SCANS) study. PLoS One 2013; 8: e61014.
Lawrence AJ, Tozer DJ, Stamatakis EA, Markus HS. A comparison of functional and tractography based networks in cerebral small vessel disease. Neuroimage Clin 2018a; 18: 425–432.
Lawrence AJ, Zeestraten EA, Benjamin P, Lambert CP, Morris RG, Barrick TR, et al. Longitudinal decline in structural networks predicts dementia in cerebral small vessel disease. Neurology 2018b; 90: e1898–e1910.
Lawton MP, Brody EM. Assessment of older people: Self-maintaining and instrumental activities of daily living. Gerontologist 1969; 9: 179–186.
Lefaucheur J-P, André-Obadia N, Antal A, Ayache SS, Baeken C, Benninger DH, et al. Evidence-based guidelines on the therapeutic use of repetitive transcranial magnetic stimulation (rTMS). Clin Neurophysiol 2014; 125: 2150–2206.
Le Heron C, Apps M, Husain M. The anatomy of apathy: A neurocognitive framework for amotivated behaviour. Neuropsychologia 2018a; 118: 54–67.
Le Heron C, Holroyd CB, Salamone J, Husain M. Brain mechanisms underlying apathy. J Neurol Neurosur Psychiatry 2019; 90: 302–312.
Le Heron C, Manohar S, Plant O, Muhammed K, Griffanti L, Nemeth A, et al. Dysfunctional effort-based decision-making underlies apathy in genetic cerebral small vessel disease. Brain 2018b; 141: 3193–3210.
Levy R, Dubois B. Apathy and the functional anatomy of the prefrontal cortex–basal ganglia circuits. Cereb Cortex 2006; 16: 916–928.
Lépine J-P, Briley M. The increasing burden of depression. Neuropsychiatric Dis Treatment 2011; 7: 3.
Li X, Ma C, Sun X, Zhang J, Chen Y, Chen K, et al. Disrupted white matter structure underlies cognitive deficit in hypertensive patients. Eur Radiol 2016; 26: 2899–2907.
Lisiecka-Ford DM, Tozer DJ, Morris RG, Lawrence AJ, Barrick TR, Markus HS. Involvement of the reward network is associated with apathy in cerebral small vessel disease. J Affect Disord 2018; 232: 116–121.
Little RJ. A test of missing completely at random for multivariate data with missing values. J Am Stat Assoc 1988a; 83: 1198–1202.
Little RJ. Missing-data adjustments in large surveys. J Bus Econ Stat 1988b; 6: 287–296.

Lohner V, Brookes RL, Hollocks MJ, Morris RG, Markus HS. Apathy, but not depression, is associated with executive dysfunction in cerebral small vessel disease. PLoS One 2017; 12: e0176943.
Lythgoe DJ, Williams SC, Cullinane M, Markus HS. Mapping of cerebrovascular reactivity using bold magnetic resonance imaging. Magn Reson Imaging 1999; 17: 495–502.
MacDonald AW, Cohen JD, Stenger VA, Carter CS. Dissociating the role of the dorsolateral prefrontal and anterior cingulate cortex in cognitive control. Science 2000; 288: 1835–1838.
Manjón JV, Coupé P, Concha L, Buades A, Collins DL, Robles M. Diffusion weighted image denoising using overcomplete local PCA. PLoS One 2013; 8: e73021.
Manohar SG, Chong TT-J, Apps MA, Batla A, Stamelou M, Jarman PR, et al. Reward pays the cost of noise reduction in motor and cognitive control. Curr Biol 2015; 25: 1707–1716.
Marin RS. Apathy: A neuropsychiatric syndrome. J Neuropsychiatry Clin Neurosci 1991; 3: 243–254.
Marin RS, Biedrzycki RC, Firinciogullari S. Reliability and validity of the Apathy Evaluation Scale. Psychiatry Res 1991; 38: 143–162.
Marin RS, Fogel BS, Hawkins J, Duffy J, Krupp B. Apathy: A treatable syndrome. J Neuropsychiatry Clin Neurosci 1995; 7: 23–30.
Mathieu S, Autret K, Arnould A, Travers C, Charveriat S, Vandenhelsken C, et al. Treatment of apathy with Zolpidem (Stilnox): Two double-blind, placebo-controlled single case studies. Ann Phys Rehabil Med 2011; 54: e214.
Matsuoka K, Yasuno F, Taguchi A, Yamamoto A, Kajimoto K, Kazui H, et al. Delayed atrophy in posterior cingulate cortex and apathy after stroke. Int J Geriatr Psychiatry 2015; 30: 566–572.
Matsuzaki S, Hashimoto M, Yuki S, Koyama A, Hirata Y, Ikeda M. The relationship between post-stroke depression and physical recovery. J Affect Disord 2015; 176: 56–60.
Mayo NE, Anderson S, Barclay R, Cameron JI, Desrosiers J, Eng JJ, et al. Getting on with the rest of your life following stroke: A randomized trial of a complex intervention aimed at enhancing life participation post stroke. Clin Rehabil 2015; 29: 1198–1211.
Mayo NE, Fellows LK, Scott SC, Cameron J, Wood-Dauphinee S. A longitudinal view of apathy and its impact after stroke. Stroke 2009; 40: 3299–3307.
Mihalov J, Mikula P, Budiš J, Valkovič P. Frontal cortical atrophy as a predictor of poststroke apathy. J Geriatr Psychiatry Neurol 2016; 29: 171–176.

Mikami K, Jorge RE, Moser DJ, Arndt S, Jang M, Solodkin A, et al. Prevention of poststroke apathy using escitalopram or problem-solving therapy. Am J Geriatr Psychiatry 2013a; 21: 855–862.
Mikami K, Jorge RE, Moser DJ, Jang M, Robinson RG. Incident apathy during the first year after stroke and its effect on physical and cognitive recovery. Am J Geriatr Psychiatry 2013b; 21: 848–854.
Miller EK. The prefontral cortex and cognitive control. Nat Rev Neurosci 2000; 1: 59.
Miller EK, Cohen JD. An integrative theory of prefrontal cortex function. Annu Rev Neurosci 2001; 24: 167–202.
Min SK, Lee BO. Laterality in somatization. Psychosomatic Med 1997; 59: 236–240.
Mitaki S, Onoda K, Abe S, Oguro H, Yamaguchi S. The effectiveness of repetitive transcranial magnetic stimulation for poststroke apathy is associated with improved interhemispheric functional connectivity. J Stroke Cerebrovasc Dis 2016; 25: e219–e221.
Moffett JR, Ross B, Arun P, Madhavarao CN, Namboodiri AM. N-acetylaspartate in the CNS: From neurodiagnostics to neurobiology. Prog Neurobiol 2007; 81: 89–131.
Moreira PS, Santos N, Castanho T, Amorim L, Portugal-Nunes C, Sousa N, et al. Longitudinal measurement invariance of memory performance and executive functioning in healthy aging. PLoS One 2018; 13: e0204012.
Moretti R, Cavressi M, Tomietto P. Gait and apathy as relevant symptoms of subcortical vascular dementia. Am J Alzheimers Dis Other Dementias 2015; 30: 390–399.
Mori S, Crain BJ, Chacko VP, Van Zijl PC. Three-dimensional tracking of axonal projections in the brain by magnetic resonance imaging. Ann Neurol 1999; 45: 265–269.
Muhammed K, Manohar S, Ben Yehuda M, Chong TT-J, Tofaris G, Lennox G, et al. Reward sensitivity deficits modulated by dopamine are associated with apathy in Parkinson's disease. Brain 2016; 139: 2706–2721.
Mulin E, Leone E, Dujardin K, Delliaux M, Leentjens A, Nobili F, et al. Diagnostic criteria for apathy in clinical practice. Int J Geriatr Psychiatry 2011; 26: 158–165.
Nachev P, Kennard C, Husain M. Functional role of the supplementary and pre-supplementary motor areas. Nat Rev Neurosci 2008; 9: 856–869.
Nelder JA, Mead R. A simplex method for function minimization. Comput J 1965; 7: 308–313.
Ngandu T, Lehtisalo J, Solomon A, Levälahti E, Ahtiluoto S, Antikainen R, et al. A 2 year multidomain intervention of diet, exercise, cognitive training, and vascular risk monitoring

versus control to prevent cognitive decline in at-risk elderly people (FINGER): A randomised controlled trial. Lancet 2015; 385: 2255–2263.
Norris DG. Implications of bulk motion for diffusion-weighted imaging experiments: Effects, mechanisms, and solutions. J Magn Reson Imaging 2001; 13: 486–495.
Okada K, Kobayashi S, Yamagata S, Takahashi K, Yamaguchi S. Poststroke apathy and regional cerebral blood flow. Stroke 1997; 28: 2437–2441.
Onoda K, Kuroda Y, Yamamoto Y, Abe S, Oguro H, Nagai A, et al. Post-stroke apathy and hypoperfusion in basal ganglia: SPECT study. Cerebrovasc Dis 2011; 31: 6–11.
O'Sullivan M, Barrick T, Morris R, Clark C, Markus H. Damage within a network of white matter regions underlies executive dysfunction in CADASIL. Neurology 2005; 65: 1584–1590.
Padoa-Schioppa C, Assad JA. Neurons in the orbitofrontal cortex encode economic value. Nature 2006; 441: 223.
Pantoni L. Cerebral small vessel disease: From pathogenesis and clinical characteristics to therapeutic challenges. Lancet Neurol 2010; 9: 689–701.
Parks R, Crockett D, Manji H, Ammann W. Assessment of bromocriptine intervention for the treatment of frontal lobe syndrome: A case study. J Neuropsychiatry Clin Neurosci 1992; 4: 109–111.
Passingham RE, Bengtsson SL, Lau HC. Medial frontal cortex: From self-generated action to reflection on one's own performance. Trends Cogn Sci 2010; 14: 16–21.
Pauli P, Wiedemann G, Nickola M. Pain sensitivity, cerebral laterality, and negative affect. Pain 1999; 80: 359–364.
Paykel E, Priest R. Recognition and management of depression in general practice: Consensus statement. BMJ 1992; 305: 1198.
Pepys MB, Baltz ML. Acute phase proteins with special reference to C-reactive protein and related proteins (pentaxins) and serum amyloid A protein. In: Advances in immunology. Elsevier; 1983. pp. 141–212.
Pettigrew C, Soldan A, Sloane K, Cai Q, Wang J, Wang M-C, et al. Progressive medial temporal lobe atrophy during preclinical Alzheimer's disease. Neuroimage Clin 2017; 16: 439–446.
Piguet O, Hornberger M, Mioshi E, Hodges JR. Behavioural-variant frontotemporal dementia: Diagnosis, clinical staging, and management. Lancet Neurol 2011; 10: 162–172.

Polders DL, Leemans A, Hendrikse J, Donahue MJ, Luijten PR, Hoogduin JM. Signal to noise ratio and uncertainty in diffusion tensor imaging at 1.5, 3.0, and 7.0 Tesla. J Magn Reson Imaging 2011; 33: 1456–1463.
Powell JH, Al-Adawi S, Morgan J, Greenwood RJ. Motivational deficits after brain injury: Effects of bromocriptine in 11 patients. J Neurol Neurosur Psychiatry 1996; 60: 416–421.
Power MC, Mormino E, Soldan A, James BD, Yu L, Armstrong NM, et al. Combined neuropathological pathways account for age-related risk of dementia. Ann Neurol 2018; 84: 10–22.
Prange S, Pagonabarraga J, Krack P, Kulisevsky J, Sgambato V, Tremblay L, et al. Historical crossroads in the conceptual delineation of apathy in Parkinson's disease. Brain 2018; 141: 613–619.
Prince M, Guerchet M, Prina M, Alzheimer's Disease International. Policy brief for heads of government: The global impact of dementia 2013-2050. Alzheimer's Disease International; 2013.
Prins ND, van Dijk EJ, den Heijer T, Vermeer SE, Jolles J, Koudstaal PJ, et al. Cerebral small-vessel disease and decline in information processing speed, executive function and memory. Brain 2005; 128: 2034–2041.
Radakovic R, Harley C, Abrahams S, Starr JM. A systematic review of the validity and reliability of apathy scales in neurodegenerative conditions. Int Psychogeriatr 2015; 27: 903–923.
Radloff LS. The CES-D scale: A self-report depression scale for research in the general population. Appl Psychol Meas 1977; 1: 385–401.
Radloff LS. The use of the center for epidemiologic studies depression scale in adolescents and young adults. J Youth Adolesc 1991; 20: 149–166.
Raichle ME, Mintun MA. Brain work and brain imaging. Annu Rev Neurosci 2006; 29: 449–476.
R Core Team. R: A language and environment for statistical computing. Vienna, Austria: R Foundation for Statistical Computing; 2019.
Reitan RM. Validity of the Trail Making Test as an indicator of organic brain damage. Percept Mot Skills 1958; 8: 271–276.
Reuter M, Rosas HD, Fischl B. Highly accurate inverse consistent registration: A robust approach. Neuroimage 2010; 53: 1181–1196.
Reuter M, Schmansky NJ, Rosas HD, Fischl B. Within-subject template estimation for unbiased longitudinal image analysis. Neuroimage 2012; 61: 1402–1418.

Revelle W. psych: Procedures for Psychological, Psychometric, and Personality Research. Evanston, Illinois: Northwestern University; 2018.
Reyes S, Viswanathan A, Godin O, Dufouil C, Benisty S, Hernandez K, et al. Apathy: A major symptom in CADASIL. Neurology 2009; 72: 905–910.
Riesenfeld RF. Applications of B-spline approximation to geometric problems of computer-aided design. 1973.
Robert P, Lanctôt K, Agüera-Ortiz L, Aalten P, Bremond F, Defrancesco M, et al. Is it time to revise the diagnostic criteria for apathy in brain disorders? The 2018 international consensus group. Eur Psychiatry 2018; 54: 71–76.
Robert P, Onyike C, Leentjens A, Dujardin K, Aalten P, Starkstein S, et al. Proposed diagnostic criteria for apathy in Alzheimer's disease and other neuropsychiatric disorders. Eur Psychiatry 2009; 24: 98–104.
Robinson RG, Jorge RE, Clarence-Smith K, Starkstein S. Double-blind treatment of apathy in patients with poststroke depression using nefiracetam. J Neuropsychiatry Clin Neurosci 2009; 21: 144–151.
Rochat L, Van der Linden M, Renaud O, Epiney J-B, Michel P, Sztajzel R, et al. Poor reward sensitivity and apathy after stroke: Implication of basal ganglia. Neurology 2013; 81: 1674–1680.
Rosas H, Liu A, Hersch S, Glessner M, Ferrante R, Salat D, et al. Regional and progressive thinning of the cortical ribbon in Huntington's disease. Neurology 2002; 58: 695–701.
Rosseel Y. lavaan: An R package for structural equation modeling and more. J Stat Softw 2012; 48: 1–36.
Rubin DB. Inference and missing data. Biometrika 1976; 63: 581–592.
Rubin DB. Statistical matching using file concatenation with adjusted weights and multiple imputations. J Bus Econ Stat 1986; 4: 87–94.
Rubin DB. Multiple imputation for survey nonresponse. New York, NY: Wiley; 1987
Rubinov M, Sporns O. Complex network measures of brain connectivity: Uses and interpretations. Neuroimage 2010; 52: 1059–1069.
Sachdev PS, Blacker D, Blazer DG, Ganguli M, Jeste DV, Paulsen JS, et al. Classifying neurocognitive disorders: The DSM-5 approach. Nat Rev Neurol 2014; 10: 634–642.
Sagen U, Finset A, Moum T, Mørland T, Vik TG, Nagy T, et al. Early detection of patients at risk for anxiety, depression and apathy after stroke. Gen Hosp Psychiatry 2010; 32: 80–85.

Sagnier S, Munsch F, Bigourdan A, Debruxelles S, Poli M, Renou P, et al. The influence of stroke location on cognitive and mood impairment. A voxel-based lesion-symptom mapping study. J Stroke Cerebrovasc Dis 2019; 28: 1236–1242.
Salat DH, Buckner RL, Snyder AZ, Greve DN, Desikan RS, Busa E, et al. Thinning of the cerebral cortex in aging. Cereb Cortex 2004; 14: 721–730.
Santa N, Sugimori H, Kusuda K, Yamashita Y, Ibayashi S, Iida M. Apathy and functional recovery following first-ever stroke. Int J Rehabil Res 2008; 31: 321–326.
Sarubbo S, De Benedictis A, Maldonado IL, Basso G, Duffau H. Frontal terminations for the inferior fronto-occipital fascicle: Anatomical dissection, DTI study and functional considerations on a multi-component bundle. Brain Struct Funct 2013; 218: 21–37.
Sasaki N, Hara T, Yamada N, Niimi M, Kakuda W, Abo M. The efficacy of high-frequency repetitive transcranial magnetic stimulation for improving apathy in chronic stroke patients. Eur Neurol 2017; 78: 28–32.
Schaapsmeerders P, Tuladhar AM, Arntz RM, Franssen S, Maaijwee NA, Rutten-Jacobs LC, et al. Remote lower white matter integrity increases the risk of long-term cognitive impairment after ischemic stroke in young adults. Stroke 2016; 47: 2517–2525.
Schindlbeck KA, Eidelberg D. Network imaging biomarkers: Insights and clinical applications in Parkinson's disease. Lancet Neurol 2018; 17: 629–640.
Schmaal L, Veltman DJ, van Erp TG, Sämann P, Frodl T, Jahanshad N, et al. Subcortical brain alterations in major depressive disorder: Findings from the ENIGMA Major Depressive Disorder working group. Mol Psychiatry 2016; 21: 806.
Schmahmann JD, Smith EE, Eichler FS, Filley CM. Cerebral white matter: Neuroanatomy, clinical neurology, and neurobehavioral correlates. Ann New York Acad Sci 2008; 1142: 266.
Schwarz CG, Reid RI, Gunter JL, Senjem ML, Przybelski SA, Zuk SM, et al. Improved dti registration allows voxel-based analysis that outperforms tract-based spatial statistics. Neuroimage 2014; 94: 65–78.
Seeley WW, Crawford RK, Zhou J, Miller BL, Greicius MD. Neurodegenerative diseases target large-scale human brain networks. Neuron 2009; 62: 42–52.
Seeley WW, Menon V, Schatzberg AF, Keller J, Glover GH, Kenna H, et al. Dissociable intrinsic connectivity networks for salience processing and executive control. J Neurosci 2007; 27: 2349–2356.
Ségonne F, Dale AM, Busa E, Glessner M, Salat D, Hahn HK, et al. A hybrid approach to the skull stripping problem in MRI. Neuroimage 2004; 22: 1060–1075.

Ségonne F, Pacheco J, Fischl B. Geometrically accurate topology-correction of cortical surfaces using nonseparating loops. IEEE Trans Med Imaging 2007; 26: 518–529.
Shen J, Tozer DJ, Markus HS, Tay J. Network efficiency mediates the relationship between vascular burden and cognitive impairment: A DTI study in UK Biobank. Stroke 2020; 51: 1682–1689.
Shenhav A, Musslick S, Lieder F, Kool W, Griffiths TL, Cohen JD, et al. Toward a rational and mechanistic account of mental effort. Annu Rev Neurosci 2017; 40: 99–124.
Shibasaki H. Human brain mapping: Hemodynamic response and electrophysiology. Clin Neurophysiol 2008; 119: 731–743.
Shinar D, Gross CR, Price TR, Banko M, Bolduc PL, Robinson RG. Screening for depression in stroke patients: The reliability and validity of the center for epidemiologic studies depression scale. Stroke 1986; 17: 241–245.
Siegel J, Snyder A, Metcalf N, Fucetola R, Hacker C, Shimony J, et al. The circuitry of abulia: Insights from functional connectivity MRI. Neuroimage Clin 2014; 6: 320–326.
Silasi G, Murphy TH. Stroke and the connectome: How connectivity guides therapeutic intervention. Neuron 2014; 83: 1354–1368.
Silvetti M, Alexander W, Verguts T, Brown JW. From conflict management to reward-based decision making: Actors and critics in primate medial frontal cortex. Neurosci Biobehav Rev 2014; 46: 44–57.
Singer JD, Willett JB. Applied longitudinal data analysis: Modeling change and event occurrence. New York, NY: Oxford University Press; 2003.
Skidmore ER, Whyte EM, Butters MA, Terhorst L, Reynolds III CF. Strategy training during inpatient rehabilitation may prevent apathy symptoms after acute stroke. PMR 2015; 7: 562–570.
Skidmore F, Yang M, Baxter L, Von Deneen K, Collingwood J, He G, et al. Apathy, depression, and motor symptoms have distinct and separable resting activity patterns in idiopathic Parkinson disease. Neuroimage 2013; 81: 484–495.
Sled JG, Zijdenbos AP, Evans AC. A nonparametric method for automatic correction of intensity nonuniformity in MRI data. IEEE Trans Med Imaging 1998; 17: 87–97.
Smith SM. Fast robust automated brain extraction. Hum Brain Mapp 2002; 17: 143–155.
Smith SM, Jenkinson M, Johansen-Berg H, Rueckert D, Nichols TE, Mackay CE, et al. Tract-based spatial statistics: Voxelwise analysis of multi-subject diffusion data. Neuroimage 2006; 31: 1487–1505.

Smith SM, Jenkinson M, Woolrich MW, Beckmann CF, Behrens TE, Johansen-Berg H, et al. Advances in functional and structural MR image analysis and implementation as FSL. Neuroimage 2004; 23: S208–S219.
Smith SM, Nichols TE. Threshold-free cluster enhancement: Addressing problems of smoothing, threshold dependence and localisation in cluster inference. Neuroimage 2009; 44: 83–98.
Smith SM, Zhang Y, Jenkinson M, Chen J, Matthews P, Federico A, et al. Accurate, robust, and automated longitudinal and cross-sectional brain change analysis. Neuroimage 2002; 17: 479–489.
Spiegel DR, Chatterjee A. A case of abulia, status/post right middle cerebral artery territory infarct, treated successfully with olanzapine. Clin Neuropharmacol 2014; 37: 186–189.
Staekenborg SS, Su T, van Straaten EC, Lane R, Scheltens P, Barkhof F, et al. Behavioural and psychological symptoms in vascular dementia; differences between small-and large-vessel disease. J Neurol Neurosur Psychiatry 2010; 81: 547–551.
Starkstein SE, Brockman S, Hatch KK, Bruce DG, Almeida OP, Davis WA, et al. A randomized, placebo-controlled, double-blind efficacy study of nefiracetam to treat poststroke apathy. J Stroke Cerebrovasc Dis 2016; 25: 1119–1127.
Starkstein SE, Fedoroff JP, Price TR, Leiguarda R, Robinson RG. Apathy following cerebrovascular lesions. Stroke 1993; 24: 1625–1630.
Starkstein SE, Pahissa J. Apathy following traumatic brain injury. Psychiat Clin North Am 2014; 37: 103–112.
Starkstein SE, Sabe L, Vazquez S, Di Lorenzo G, Martinez A, Petracca G, et al. Neuropsychological, psychiatric, and cerebral perfusion correlates of leukoaraiosis in Alzheimer's disease. J Neurol Neurosur Psychiatry 1997; 63: 66–73.
Steinke W, Ley SC. Lacunar stroke is the major cause of progressive motor deficits. Stroke 2002; 33: 1510–1516.
Stuart AL, Pasco JA, Jacka FN, Brennan SL, Berk M, Williams LJ. Comparison of self-report and structured clinical interview in the identification of depression. Compr Psychiatry 2014; 55: 866–869.
Tamkin AS, Kunce JT. Construct validity of the Weigl Color-Form Sorting Test. Percept Mot Skills 1982; 55: 105–106.
Tang W, Chen Y, Liang H, Chu WC, Mok V, Ungvari GS, et al. Location of infarcts and apathy in ischemic stroke. Cerebrovasc Dis 2013; 35: 566–571.

Tang WK, Caeiro L, Lau CG, Liang H, Mok V, Ungvari GS, et al. Apathy and suicide-related ideation 3 months after stroke: A cross-sectional study. BMC Neurol 2015; 15: 60.
Tang W-K, Lau CG, Mok V, Ungvari GS, Wong K-S. Apathy and health-related quality of life in stroke. Arch Phys Med Rehabil 2014; 95: 857–861.
Tatemichi T, Desmond D, Cross D, Gropen T, Mohr J. Confusion and memory loss from capsular genu infarction: A thalamocortical disconnection syndrome? Neurology 1992; 42: 1966–1979.
Tay J, Lisiecka-Ford DM, Hollocks MJ, Tuladhar AM, Barrick TR, Forster A, et al. Network neuroscience of apathy in cerebrovascular disease. Prog Neurobiol 2020a; 188: 101785.
Tay J, Morris RG, Tuladhar AM, Husain M, de Leeuw FE, Markus HS. Apathy, but not depression, predicts all-cause dementia in cerebral small vessel disease. J Neurol Neurosurg Psychiatry 2020b; 91:953-959.
Tay J, Tuladhar AM, Hollocks MJ, Brookes RL, Tozer DJ, Barrick TR, et al. Apathy is associated with large-scale white matter network disruption in small vessel disease. Neurology 2019; 92: e1157–e1167.
Thal DR, Grinberg LT, Attems J. Vascular dementia: Different forms of vessel disorders contribute to the development of dementia in the elderly brain. Exp Gerontology 2012; 47: 816–824.
Therneau TM. A package for Survival Analysis in S. 2015.
Therneau TM, Crowson CS, Atkinson EJ. Adjusted survival curves. 2015.
Therneau TM, Grambsch PM. Modeling survival data: Extending the Cox model. New York, NY: Springer; 2000.
Thomas C, Frank QY, Irfanoglu MO, Modi P, Saleem KS, Leopold DA, et al. Anatomical accuracy of brain connections derived from diffusion MRI tractography is inherently limited. Proc Natl Acad Sci 2014; 111: 16574–16579.
Tombaugh TN, McIntyre NJ. The mini-mental state examination: A comprehensive review. J Am Geriatr Soc 1992; 40: 922–935.
Treadway MT, Zald DH. Reconsidering anhedonia in depression: Lessons from translational neuroscience. Neurosci Biobehav Rev 2011; 35: 537–555.
Tustison NJ, Avants BB, Cook PA, Zheng Y, Egan A, Yushkevich PA, et al. N4ITK: improved N3 bias correction. IEEE Trans Med Imaging 2010; 29: 1310.
Tzourio-Mazoyer N, Landeau B, Papathanassiou D, Crivello F, Etard O, Delcroix N, et al. Automated anatomical labeling of activations in SPM using a macroscopic anatomical parcellation of the MNI MRI single-subject brain. Neuroimage 2002; 15: 273–289.

van Almenkerk S, Smalbrugge M, Depla MF, Eefsting JA, Hertogh CM. Apathy among institutionalized stroke patients: Prevalence and clinical correlates. Am J Geriatr Psychiatry 2015; 23: 180–188.
van Buuren S, Brand JP, Groothuis-Oudshoorn CG, Rubin DB. Fully conditional specification in multivariate imputation. J Stat Comput Sim 2006; 76: 1049–1064.
van Buuren S, Groothuis-Oudshoorn K. Mice: Multivariate imputation by chained equations in R. J Stat Softw 2010: 1–68.
van Dalen JW, Moll van Charante EP, Nederkoorn PJ, van Gool WA, Richard E. Poststroke apathy. Stroke 2013; 44: 851–860.
van Dalen JW, van Wanrooij LL, Moll van Charante EP, Brayne C, van Gool WA, Richard E. Association of apathy with risk of incident dementia: A systematic review and meta-analysis. JAMA Psychiatry 2018a; 75: 1012–1021.
van Dalen JW, Wanrooij LL van, Moll van Charante EP, Richard E, van Gool WA. Apathy is associated with incident dementia in community-dwelling older people. Neurology 2018b; 90: e82–e89.
van den Heuvel MP, Sporns O. Network hubs in the human brain. Trends Cogn Sci 2013; 17: 683–696.
Van Der Elst W, Van Boxtel MP, Van Breukelen GJ, Jolles J. Assessment of information processing in working memory in applied settings: The paper & pencil memory scanning test. Psychol Med 2007; 37: 1335–1344.
Van der Elst W, Van Boxtel MP, Van Breukelen GJ, Jolles J. The Letter Digit Substitution Test: Normative data for 1,858 healthy participants aged 24–81 from the Maastricht Aging Study (MAAS): Influence of age, education, and sex. J Clin Exp Neuropsychol 2006; 28: 998–1009.
van Leijsen EM, Bergkamp MI, Van Uden IW, Ghafoorian M, Van Der Holst HM, Norris DG, et al. Progression of white matter hyperintensities preceded by heterogeneous decline of microstructural integrity. Stroke 2018; 49: 1386–1393.
van Leijsen EM, Tay J, van Uden IW, Kooijmans EC, Bergkamp MI, van der Holst HM, et al. Memory decline in elderly with cerebral small vessel disease explained by temporal interactions between white matter hyperintensities and hippocampal atrophy. Hippocampus 2019; 29: 500–510.
van Meer MP, van der Marel K, Wang K, Otte WM, el Bouazati S, Roeling TA, et al. Recovery of sensorimotor function after experimental stroke correlates with restoration of resting-state interhemispheric functional connectivity. J Neurosci 2010; 30: 3964–3972.

van Norden AG, de Laat KF, Gons RA, van Uden IW, van Dijk EJ, van Oudheusden LJ, et al. Causes and consequences of cerebral small vessel disease. The RUN DMC study: A prospective cohort study. Study rationale and protocol. BMC Neurol 2011; 11: 29.
van Reekum R, Stuss DT, Ostrander L. Apathy: Why care? J Neuropsychiatry Clin Neurosci 2005; 17: 7–19.
Vansteenkiste V, Lens W, De Witte H, Feather NT. Understanding unemployed people's job search behaviour, unemployment experience and well-being: A comparison of expectancy-value theory and self-determination theory. Br J Soc Psychol 2005; 44: 269–287.
van Uden IW, Van Der Holst HM, Schaapsmeerders P, Tuladhar AM, van Norden AG, de Laat KF, et al. Baseline white matter microstructural integrity is not related to cognitive decline after 5 years: The RUN DMC study. BBA Clin 2015; 4: 108–114.
Vergani F, Lacerda L, Martino J, Attems J, Morris C, Mitchell P, et al. White matter connections of the supplementary motor area in humans. J Neurol Neurosurg Psychiatry 2014; 85: 1377–1385.
Videbech P, Ravnkilde B. Hippocampal volume and depression: A meta-analysis of MRI studies. Am J Psychiatry 2004; 161: 1957–1966.
Viladrich C, Angulo-Brunet A, Doval E. A journey around alpha and omega to estimate internal consistency reliability. Ann Psychol 2017; 33: 755–782.
Wardlaw JM, Smith C, Dichgans M. Small vessel disease: Mechanisms and clinical implications. Lancet Neurol 2019; 18: 684–696.
Wardlaw JM, Smith EE, Biessels GJ, Cordonnier C, Fazekas F, Frayne R, et al. Neuroimaging standards for research into small vessel disease and its contribution to ageing and neurodegeneration. Lancet Neurol 2013; 12: 822–838.
Watanabe MD, Martin EM, DeLeon OA, Gaviria M, Pavel DG, Trepashko DW. Successful methylphenidate treatment of apathy after subcortical infarcts. J Neuropsychiatry Clin Neurosci 1995; 7: 502-504.
Watts DJ, Strogatz SH. Collective dynamics of 'small-world' networks. Nature 1998; 393: 440–442.
Wechsler D. Wechsler Adult Intelligence Scale - Third Edition (WAIS-III). 3rd ed. San Antonio, TX: The Psychological Corporation; 1997.
Whyte EM, Lenze EJ, Butters M, Skidmore E, Koenig K, Dew MA, et al. An open-label pilot study of acetylcholinesterase inhibitors to promote functional recovery in elderly cognitively impaired stroke patients. Cerebrovasc Dis 2008; 26: 317–321.

Widaman KF, Ferrer E, Conger RD. Factorial invariance within longitudinal structural equation models: Measuring the same construct across time. Child Devel Perspect 2010; 4: 10–18.
Widaman KF, Reise SP. Exploring the measurement invariance of psychological instruments: Applications in the substance use domain. In: Bryant K, Windle M, West S, editor(s). The science of prevention: Methodological advances from alcohol and substance abuse research. Washington, DC: American Psychological Association; 1997. pp. 281–324..
Winkler AM, Ridgway GR, Webster MA, Smith SM, Nichols TE. Permutation inference for the general linear model. Neuroimage 2014; 92: 381–397.
Withall A, Brodaty H, Altendorf A, Sachdev PS. A longitudinal study examining the independence of apathy and depression after stroke: The Sydney Stroke Study. Int Psychogeriatr 2011; 23: 264–273.
World Health Organization. Depression and other common mental disorders: Global health estimates. Geneva: World Health Organization; 2017.
Wothke W. Longitudinal and multigroup modeling with missing data. In: Little T, Schnabel K, Baumert J, editor(s). Modeling longitudinal and multilevel data: Practical issues, applied approaches, and specific examples. Mahwah, NJ: Lawrence Erlbaum Associates Publishers; 2000. pp. 219–240.
Yamagata S, Yamaguchi S, Kobayashi S. Impaired novelty processing in apathy after subcortical stroke. Stroke 2004; 35: 1935–1940.
Yang S-r, Hua P, Shang X, Cui Z, Zhong S, Gong G, et al. Deficiency of brain structural sub-network underlying post-ischaemic stroke apathy. Eur J Neurol 2015a; 22: 341–347.
Yang S-r, Shang X-y, Tao J, Liu J-y, Hua P. Voxel-based analysis of fractional anisotropy in post-stroke apathy. PLoS One 2015b; 10: e116168.
Yao H, Mizoguchi Y, Monji A, Yakushiji Y, Takashima Y, Uchino A, et al. Low-grade inflammation is associated with apathy indirectly via deep white matter lesions in community-dwelling older adults: The Sefuri Study. Int J Mol Sci 2019; 20: 1905.
Yao H, Takashima Y, Mori T, Uchino A, Hashimoto M, Yuzuriha T, et al. Hypertension and white matter lesions are independently associated with apathetic behavior in healthy elderly subjects: The Sefuri brain MRI study. Hypertens Res 2009; 32: 586–590.
Yesavage JA, Brink TL, Rose TL, Lum O, Huang V, Adey M, et al. Development and validation of a geriatric depression screening scale: A preliminary report. J Psychiat Res 1982; 17: 37–49.

Yoo W, Mayberry R, Bae S, Singh K, He QP, Lillard Jr JW. A study of effects of multicollinearity in the multivariable analysis. Int J Appl Sci Technol 2014; 4: 9.
Zalesky A, Fornito A, Bullmore ET. Network-based statistic: Identifying differences in brain networks. Neuroimage 2010; 53: 1197–1207.
Zawacki TM, Grace J, Paul R, Moser DJ, Ott BR, Gordon N, et al. Behavioral problems as predictors of functional abilities of vascular dementia patients. J Neuropsychiatry Clin Neurosci 2002; 14: 296–302.
Zénon A, Sidibé M, Olivier E. Disrupting the supplementary motor area makes physical effort appear less effortful. J Neurosci 2015; 35: 8737–8744.
Zhang Y, Brady M, Smith S. Segmentation of brain MR images through a hidden markov random field model and the expectation-maximization algorithm. IEEE Trans Med Imaging 2001; 20: 45–57.
Zhang Y, Wu J, Wu W, Liu R, Pang L, Guan D, et al. Reduction of white matter integrity correlates with apathy in Parkinson's disease. Int J Neurosci 2018; 128: 25–31.
Zhao Q-F, Tan L, Wang H-F, Jiang T, Tan M-S, Tan L, et al. The prevalence of neuropsychiatric symptoms in Alzheimer's disease: Systematic review and meta-analysis. J Affect Disord 2016; 190: 264–271.
Zwiers MP. Patching cardiac and head motion artefacts in diffusion-weighted images. Neuroimage 2010; 53: 565–575.